2018

# NUMERICAL SIMULATIONS OF PREMIXED FLAMES OF MULTI COMPONENT FUELS/AIR MIXTURES AND THEIR APPLICATIONS

Essa KH I J Salem
*University of Kentucky*, izzakhalil@gmail.com
Author ORCID Identifier:
https://orcid.org/0000-0002-5224-4707
Digital Object Identifier: https://doi.org/10.13023/etd.2019.113

STUDENT AGREEMENT:

I represent that my thesis or dissertation and abstract are my original work. Proper attribution has been given to all outside sources. I understand that I am solely responsible for obtaining any needed copyright permissions. I have obtained needed written permission statement(s) from the owner(s) of each third-party copyrighted matter to be included in my work, allowing electronic distribution (if such use is not permitted by the fair use doctrine) which will be submitted to UKnowledge as Additional File.

I hereby grant to The University of Kentucky and its agents the irrevocable, non-exclusive, and royalty-free license to archive and make accessible my work in whole or in part in all forms of media, now or hereafter known. I agree that the document mentioned above may be made available immediately for worldwide access unless an embargo applies.

I retain all other ownership rights to the copyright of my work. I also retain the right to use in future works (such as articles or books) all or part of my work. I understand that I am free to register the copyright to my work.

REVIEW, APPROVAL AND ACCEPTANCE

The document mentioned above has been reviewed and accepted by the student's advisor, on behalf of the advisory committee, and by the Director of Graduate Studies (DGS), on behalf of the program; we verify that this is the final, approved version of the student's thesis including all changes required by the advisory committee. The undersigned agree to abide by the statements above.

Essa KH I J Salem, Student

Dr. Kozo Saito, Major Professor

Dr. Alexandre Martin, Director of Graduate Studies

# NUMERICAL SIMULATIONS OF PREMIXED FLAMES OF MULTI COMPONENT FUELS/AIR MIXTURES AND THEIR APPLICATIONS

---

THESIS

---

A thesis submitted in partial fulfillment of the
requirements for the degree of Master of Science in Mechanical Engineering
in the College of Engineering
at the University of Kentucky


By

Essa KH I J Salem

Lexington, Kentucky

Director: Dr. Kozo Saito, Professor of Mechanical Engineering

Lexington, Kentucky


2019



https://orcid.org/0000-0002-5224-4707

ABSTRACT OF THESIS

NUMERICAL SIMULATIONS OF PREMIXED FLAMES OF MULTI COMPONENT FUELS/AIR MIXTURES AND THEIR APPLICATIONS

Combustion has been used for a long time as a means of energy extraction. However, in the recent years there has been further increase in air pollution, through pollutants such as nitrogen oxides, acid rain etc. To solve this problem, there is a need to reduce carbon and nitrogen oxides through lean burning, fuel dilution and usage of bi-product fuel gases. A numerical analysis has been carried out to investigate the effectiveness of several reduced mechanisms, in terms of computational time and accuracy. The cases were tested for the combustion of hydrocarbons diluted with hydrogen, syngas, and bi-product fuel in a cylindrical combustor. The simulations were carried out using the ANSYS Fluent 19.1. By solving the conservations equations, several global reduced mechanisms (2-5-10 steps) were obtained. The reduced mechanisms were used in the simulations for a 2D cylindrical tube with dimensions of 40 cm in length and 2.0 cm diameter.

The mesh of the model included a proper fine quad mesh, within the first 7 cm of the tube and around the walls.

By developing a proper boundary layer, several simulations were performed on hydrocarbon/air and syngas blends to visualize the flame characteristics. To validate the results "PREMIX and CHEMKIN" codes were used to calculate 1D premixed flame based on the temperature, composition of burned and unburned gas mixtures. Numerical calculations were carried for several hydrocarbons by changing the equivalence ratios (lean to rich) and adding small amounts of hydrogen into the fuel blends.

The changes in temperature, radical formation, burning velocities and the reduction in $NO_x$ and $CO_2$ emissions were observed. The results compared to experimental data to study the changes.

Once the results were within acceptable range, different fuels compositions were used for the premixed combustion through adding $H_2$/CO/$CO_2$ by volume and changing the equivalence ratios and preheat temperatures, in the fuel blends. The results on flame temperature, shape, burning velocity and concentrations of radicals and emissions were observed. The flame speed was calculated by finding the surface area of the flame, through the mass fractions of fuel components and products conversions that were simulated through the tube. The area method was applied to determine the flame speed. It was determined that the reduced mechanisms provided results within an acceptable range.

The variation of the inlet velocity had neglectable effects on the burning velocity. The highest temperatures were obtained in lean conditions (0.5-0.9) equivalence ratio and highest flame speed was obtained for Blast Furnace Gas (BFG) at elevated preheat temperature and methane-hydrogen fuels blends in the combustor.

The results included; reduction in $CO_2$ and $NO_x$ emissions, expansion of the flammable limit, under the condition of having the same laminar flow. The usage of diluted natural gases, syngas and bi-product gases provides a step in solving environmental problems and providing efficient energy.

KEYWORDS: Premixed Combustion, Reduced Mechanisms, Flame Speed, Flame Structures, Radical Formation

Essa KH I J Salem

4/12/2019

Date

# NUMERICAL SIMULATIONS OF PREMIXED FLAMES OF MULTI COMPONENT FUELS/AIR MIXTURES AND THEIR APPLICATIONS

By
Essa KH I J Salem

Kozo Saito
Director of Thesis

Alexandre Martin
Director of Graduate Studies

04/12/2019
Date

To my family

## ACKNOWLEDGMENTS

First, I would like to express my gratitude towards the College of Engineering at the University of Kentucky for having me as student for both my undergraduate and graduate years. It has been nearly 7 years, since I started my education, and the continued support from the faculty members of Mechanical Engineering department has been delightful. I would also like to give my sincere gratitude and thanks towards, my advisor Dr. Kozo Saito for accepting me as his student and a part of the IR4TD family. If it wasn't for his help and guidance during the most difficult times in my life, then I wouldn't have been able to complete my degree. I would also love to express, my sincere thanks towards, Dr. Li for helping me throughout this final to develop meaningful methods to obtain my results and properly validate my calculations based upon his experimental knowledge. I would also like to express my thanks towards Dr. Christoph Brehm, for teaching me the basics of CFD and coding knowledge that has helped along these years. Furthermore, I would like to thank the IR4TD family and my lab mates, Adnan Darwish, Mark Dorre, Masoud, and Ahmad for being great lab mates and friends who continually supported me throughout the years.

I would also like to thank Dr. Ahmad and Dr. Nelson for their guidance and support and making sure that I kept trying my best to create something that is unique, valid and beneficial to the IR4TD group. Finally, I would like to thank my family for always being there and standing by myside no matter how hard life got and also acknowledge the love and support from my Family back in Kuwait for being so patient with me, and believing that I could complete my program.

## TABLE OF CONTENTS

## LIST OF TABLES

## LIST OF FIGURES

## NOMENCLATURE

**Symbols**

| | | |
|---|---|---|
| n | Number of moles | - |
| H | Enthalpy | N.m |
| m | Mass flow rate | Kg/s |
| A | Air ratio | - |
| F | Fuel ratio | - |
| RR | Reaction rate | - |
| $S_l$ | Flame speed | m/s |
| D | Diameter | m |
| H | Height | m |
| L | Cone Slant Length | m |
| $A_f$ | Flame surface area | $m^2$ |
| $A_c$ | Model Cross section area | |
| $V_u$ | Average velocity | m/s |
| a | Angle of flame | degrees |
| u | Velocity component x | |
| v | Velocity component y | |
| w | Velocity component z | |
| P | Pressure | atm |
| $F_{mx}$ | Body force | Joules |

| | | |
|---|---|---|
| A | Pre-Exponential Factor | $s^{-1}$ |
| E | Activation Energy | Joules |
| R | Gas constant | J/mol K |
| $K_p(T)$ | Equilibrium Constant | - |
| K | Specific reaction rate | - |
| $X_i$ | Mole concentration | - |
| $k_f$ | Forward reaction rate | - |
| T | Temperature | - |
| $S(\phi)$ | Source term | - |
| $V_j'$ | Reactant stoichiometric coefficient | - |
| $V_j''$ | Product stoichiometric coefficien | - |
| c | Progress variable | - |
| $Y_i$ | Mass fraction | |
| $S_t$ | Turbulent velocity | m/s |
| $u'$ | Root mean velocity | |
| $l_f$ | Turbulent length | m |
| $T^o$ | Layer temperature | K |
| $Y_{f,u}^m$ | Unburnt fuel mass fraction | |
| $T_u$ | Unburnt temperature | K |
| $T_b$ | Burnt temperature | K |

**Greek**

| | | |
|---|---|---|
| φ | Equivalence ratio | - |

| | | |
|---|---|---|
| $\alpha$ | Thermal Diffusivity | $m^2/s$ |
| $\delta$ | Flame Thickness | mm |
| $\rho$ | Density | $kg/m^3$ |
| $\tau$ | Viscous Stress | - |
| $\mu$ | Viscosity | P |
| $\Delta$ | delta | |
| $\beta$ | Activation Energy temperature exponent | |

**Abbreviation**

| | | |
|---|---|---|
| RMS | Root Mean Square | - |
| COG | Coke Oven Gas | - |
| BFG | Blast Furnace Gas | - |

**Subscripts**

| | | |
|---|---|---|
| i | Reactants | - |
| j | Products | - |
| f | Final state | - |
| u | Average | - |

# Chapter 1 INTRODUCTION

## 1.1 Energy Consumption Through Combustion

The importance of combustion heavily relies on the fact that more than 85% of energy produced is mainly from the combustion of energy sources in the year of 2017.[1-5] However, with the recent technological developments these numbers have increased, based upon end user sectors. These sectors include residential, commercial, industrial, transportation and electric power sectors, where each has their own amount of energy consumption. Developed and industrialized countries use a large amount of energy, for example the United States as shown in Figure 1.1, where the total amount of energy consumed in primary 4 sectors is presented.

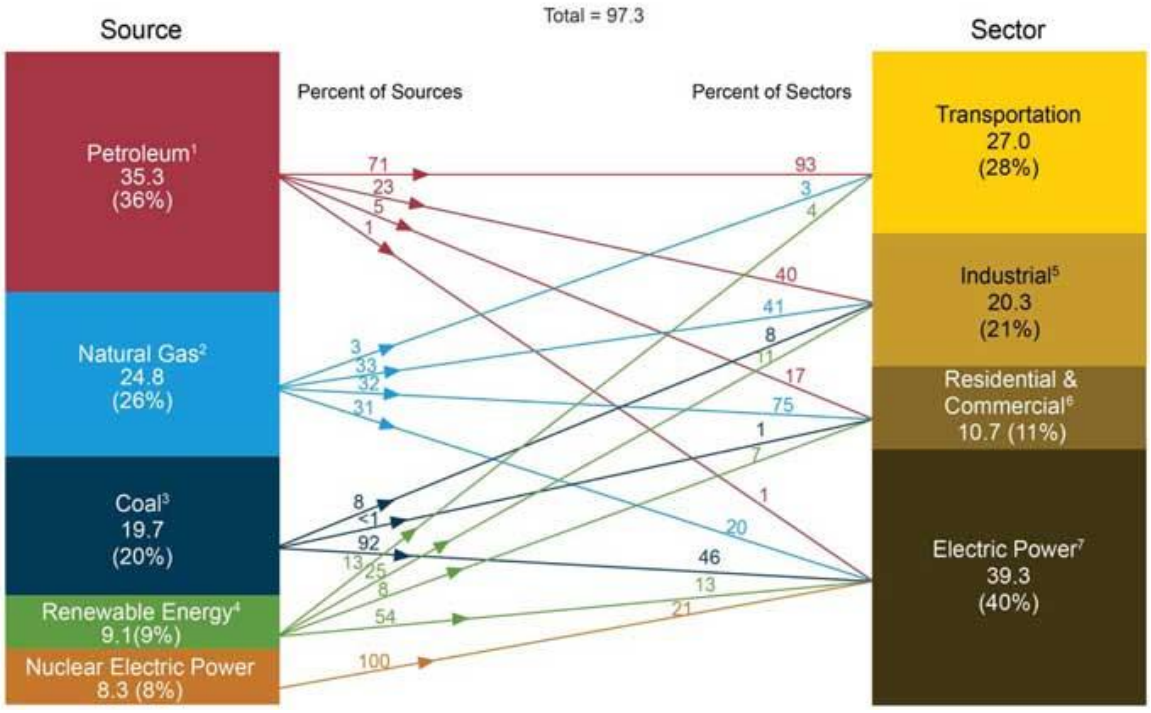


Figure 1-1 U.S energy consumption by end use sectors and sources [5]
(Courtesy of EIA)

It could be seen in Figure. 1.1 that the electric sector holds the highest energy consumption at about 39.3% for electric power and then is followed by transportation at 27%. The remaining 2 sectors share percentage at 11% and the industrial is at 20.3% an. In the recent

years, scientists have searched for renewable energy sources that could partly replace fossil fuels. Although these attempts are useful, it should be accepted that fossil fuels remain as the main energy contributor (gas, oil coal) for our daily lives' needs a representation can be shown in Figure. 1.2.

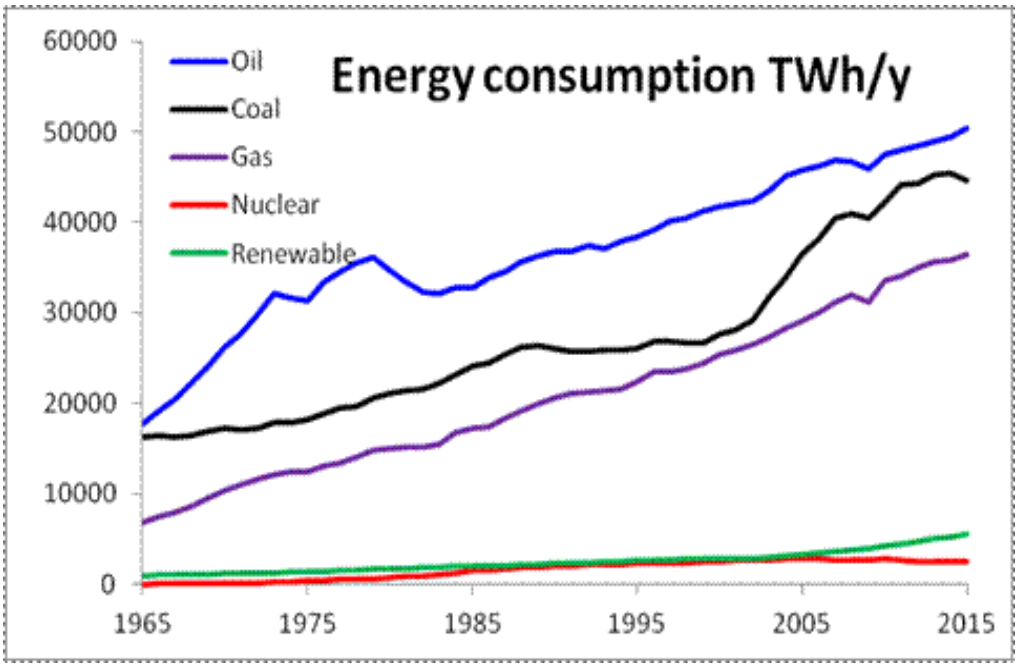


Figure 1-2 Comparison of fossil fuel, nuclear and renewable energy uses [5] (Courtesy of EIA)

It can be noted that the efforts of finding renewable energy sources are helpful, however, it is almost impossible to maintain life growth as it is by just relying on renewable energy sources. Furthermore, due to the scarcity of waste landfills, combustion process can be used as a way of toxic waste disposal and incineration, but it comes at the cost of environmental effects. Combustion has a disadvantage associated with its use, which is related to the generation of pollutants. This disadvantage is globally accepted as a problem, that affects both the environment and the daily lives in the world.

In the industrial sectors, during the combustion process of fossil fuels, large amounts of pollutants are generated. The main pollutants could be classified as unburned hydrocarbons, $NO_x$ , carbon monoxides, carbon dioxide and sulfur oxides [6] . These pollutants have a huge impact on health, acid rain, greenhouse gases formations and global

warming. it is also the main reason why government regulations have been placed. For example, within the years of 1976 to 2017, $CO_2$ emissions emitted through the exhaust of combustion equipment have almost doubled according to the U.S Energy Information Administration, and it is estimated to be increasing about 2-3% per year, and this needs to be addressed [7]

## 1.2 Fuel Dilution

Since the use of fossil fuel is dominant, researchers have been conducting experiments to find ways to make fuel combustion cleaner, while maintaining its usage. Many studies have been done to find alternative fuels that could help improve fossil fuel combustion. One method is the use of hydrogen addition to hydrocarbons [8]. This is usually referred to as Hydrogen Fuel Enhancement, in which hydrocarbons such as natural gases are blended with certain amount of hydrogen to form a gas mixture that is used in internal combustion engines and gas turbines. This is done as an attempt to reduce pollutant emissions and improve fuel economy. Hydrogen is a small element that is colorless. In industrial sectors sulfur-based odorant is added to natural gas so that it could be detected if there is a leak. However, it's hard to use the same technique for hydrogen because it is a light weight element that cannot be easily mixed with the odorant. It is difficult to store because of its small size and low energy density. In industry hydrogen can be compressed and liquified to be stored in tanks that contain pressure relief machinery to avoid sudden pressure increases [9, 10]. It was found that hydrogen is a notable energy source which has excellent combustion properties. These properties include; lower ignition energy, making it possible to be used for lean mixture combustion. One important trait of hydrogen is the short combustion time which can be used to enhance gas turbines to improve energy efficiency. Furthermore, hydrogen has a large flammability limits with the range of 4-75% in air compared to other fuels [9]

By comparing hydrogen with other fuels, it could be seen that the amount of energy required for its combustion is less than that for other fuels, making it a good candidate to be blended with other hydrocarbon-air mixtures. For internal combustion engines During the hydrogen combustion, the only product is water, which makes hydrogen an energy

source with no pollutant emissions, while all the other hydrocarbons combustion processes produce carbon dioxide. This enables the world to have zero, or reduced emission fuel [8]. However, an issue arises with hydrogen itself as a fuel due to its high combustibility which makes hydrogen explosive if it meets with air. For this reason, hydrogen is not used alone as an alternative fuel, but it is blended with other conventional fuels with high calorific values.

As part of this project hydrogen will be blended with methane at the ranges from 0% to 100% and simulated in both 1-D and 2-D cases. The results will be compared with experimental works to see hydrogens' flame speed, flame structure, and its ability to reduce $NO_x$ and $CO_2$ emissions. Many experiments have been done previously conducted which have proved that hydrogen behaves better than almost any fuels used for energy in terms of thermal efficiency and gas emissions tested in internal combustion (IC) engines [1, 2, 11].

### 1.3 Syngas

With fossil fuels being the dominant energy source, there is a need to understand that fossil fuels are finite energy, that will not last forever, and energy demands are continually increasing. This causes the amount of fossil fuels available in the world to decrease, and the cost of fuels to increase, which raises awareness to another issue- which is the search for alternative energy sources [12].

One of alternative energy sources is the synthetic gas from the products of biomass. Syngas is a gas mixture consisting of hydrogen, carbon monoxide and carbon dioxide, usually produced through gasification processes of hydrocarbons with certain amounts of heating values. The name itself describes its ability to synthesize chemical compounds and make them viable as fuels. The gasification process enables breaking the hydrocarbon chains in the biomass which contains large molecules of hydrocarbons. It is almost hard to burn it by itself unless specific biofuel is used. However, it can be blended with other conventional fuels specially in premixed combustion, to produce a viable source of energy.

Furthermore, the production of syngas relies on using petroleum materials that are left inside the combustion chamber. The produced syngas contains large amounts of carbon monoxide, hydrogen, carbon dioxide and left-over hydrocarbons which could be used to produce electricity for industrials sectors at lower operating costs. However, there are also some environmental concerns with nitric oxide formation from syngas, but recent studies have tried to dilute syngas with water vapor to reduce the formation of nitric oxides and increase the flame speed [13].Within the recent decades the use of low calorific-value fuels have increased in which new developments for gas-turbine power generation includes the use of Synthetic Gas, Coke Oven Gas (COG) and Blast Furnace Gas (BFG) [14]. it is important to note that (COG) used in industries usually contains similar species as Syngas but has methane percentages contained in its fuel. In gas turbines, the calorific values for natural gas is about 40 $MJ/M^3N$ and BFG has the lowest value and it is about 2.95 $MJ/M^3N$ [15, 16]. For that reason, it is important to develop models that are robust and contain detailed turbulence-chemistry interactions to further develop better gas-turbines by understanding the burning characteristics of syngas and by-product fuels.

### 1.4 Why premixed flames?

Flame propagation can vary based upon the medium it propagates through and the conditions that initiate the flames. Flames can either propagate through gases fuels or combustible dust cloud but vary depending on how the fuel and oxidizer are mixed, which results in classifying flames as premixed flames or diffusion flames [17]. In the premixed flames, the reactant gases are mixed before they are ignited. Premixed flames are the most dominant cases that researchers have studied. Experimental studies have been done to determine the flame structures, flame speed and flame characteristics. The results are then compared with CFD simulations. Often theoretical approaches that are applied for laminar premixed flames could extend to be applied for turbulent cases. By observing and understanding the behaviors of laminar premixed flames, researchers can develop basis for understanding the physical interpretation of combustion mechanics. Furthermore, studies of hydrocarbons mixed with hydrogen in premixed flames have helped to create better models for gas turbines that have higher energy efficiency [18].

A large amount of work has been implemented in CFD, such as using CHEMKIN software and PREMIX code, to simulate simple Bunsen burner flames. The simple studies of 1-D simulations proved to be very influential because of their ability to test several cases of diluting hydrocarbons and syngas to see the result in terms of efficiency and amount of emissions produced, offering substantial cost reduction for future development and minimize the impacts that pollutants have on the environment.

## 1.5 CFD Modeling

Computational Fluid Dynamics (CFD) has become an important numerical method which has emerged within the last 50 years. [19] It is a computational tool that focuses on the numerical solution of governing equations of mass, energy, and transport in fluid flows. The importance of CFD has recently increased with the technological development of computers, computing speed and affordability of computing resources. Its usage expands to reach areas of engineering equipment design, environmental and geological phenomena, power generation, automotive, oil and gas industry, and process engineering. Without the use of CFD several modern combustion problems would be impossible to solve or understand, especially in difficult geometries. In these cases, analytical solutions become very limited. One of the advantages of CFD modeling is that it provides flexibility in terms of creating prototypes without having the need to spend money on materials and labor, thus making it much easier to adjust models to create refined projects and view the points of interest where a certain model would fail. The contribution of CFD is apparent, where it is used alongside experimental work, and its ability is assessed through validation and verification.

The term verification refers to the ability of a certain model's solution and algorithm to be explained easily using mathematics, while validation is related to having the discrete solution of the model to be applicable with physical laws [19]. CFD in combustion can be applied in several engineering aspects such as aircraft engines, IC engines furnaces and power generation. However, due to the complexity of chemical kinetics and reacting flows, integrated models need to be incorporated so that it can be validated. The complexity of combustion revolves around, the process itself where researchers need to consider the

mixing, reaction time scales, and flame types. For example, in experiments the premixed combustion is easier to study and explain, however, in numerical simulations such as using ANSYS Fluent, premixed combustion modeling is far more difficult than non-premixed combustion [20]. Furthermore, detailed knowledge is required in understanding the flows and the kinetic complexity of reaction that goes through multiple steps but appears as a single simple reaction step in global steps. The transport equation, mass fractions and enthalpy of all species need to be considered to obtain meaningful results. Combustion problems become very complex, due to geometry, heat transfer, and number of iterations that must be repeated to get a converged solution. However, with proper knowledge and skills, CFD in combustion could be used to obtain satisfying performance results for combustion equipment, and reduce the time required to create products that are fuel efficient and cleaner for the environment.

## 1.6 Goals of Thesis

Understanding lean and rich premixed combustion fundamentals helps in developing better technology for industry. An in depth understanding of combustion processes such as methane-air and methane diluted with hydrogen provides an insight into the fundamentals behind the combustion of by-product fuel gas that is obtained from steel making processes. Usually these by-product gases can be mixed with air and exhaust gas and then burned in premixed conditions. However, compositions of these fuels vary based upon the methods that are used to produce them, where their initial preheat temperature conditions and enthalpy vary, leading to variation in flame speed. This enforces better understanding of the fundamentals of by-product gases such as methane, carbon dioxide, carbon monoxide and hydrogen to determine their flame speeds based upon the combustion of intermediate radicals. Better understanding of the fundamentals helps in improving the design of burners, combustors and the type of control methods to be used for by-product fuels in an efficient way that is safe and clean.

The focus of this research relies heavily upon the usage of CFD tools to simulate 2-D premixed flames with changes of equivalence ratio from lean to rich and preheat temperatures, and then determining the flame structures and flame speed based on changes

in the compositions of the mixtures. The results will be compared by using CHEMKIN PREMIX codes for 1-D cases, and ANSYS Fluent for 2-D, as well as with experimental results to validate the model. The goals of the research are listed as follows:

To develop a simple computational model to study the combustion process of two-dimensional laminar premixed flames with detailed chemical kinetics.

1. Lean and rich premixed combustion of methane-air and hydrogen-air;
2. Enhancing methane through hydrogen addition and obtaining the flame speed;
3. Comparing 1-D and 2-D results with experimental work and obtain agreement in results
4. Study radical concentrations and $NO_x$ formation with fuel dilution and different compositions.

To use reduced mechanisms that contain a smaller number of species with a decent level of accuracy, and then Gri-3.0 to obtain the characteristics of flames such as structure and flame speed.

1. Obtain results through usage of Gri-3.0;
2. Obtain results using 2 step, 5 step, and 10 step mechanisms and compare results with Gri-3.0;
3. Understanding the effect of radical formations on flame speed

To develop a model that is robust and contains detailed turbulence-chemistry interactions to further develop lower emission gas-turbines.

To be able to reduce computing time to study single, multiple hydrocarbons and syngas (COG, BFG) based upon their compositions and preheat temperatures., while generating results that are within accepted range of accuracy based upon simulations and experimental works previously done.

Implement the model to be served as guide into understanding experimental works with saving cost and time.

## 1.7 Structure of Thesis

The focus of this thesis is CFD analysis that is used to simulate and visualize premixed flames and develop the proper methods to find the flame speeds through temperature contours. Chapter 1 summarizes the usage of energy that is created through the process of combustion, the advantages, and comparison of energy sources and the pollutant emissions within the past 30 years. Fuel dilution and syngas usage are both introduced as a method of creating cleaner energy that is both efficient . CFD is also described as a method of understanding the process of combustion. Finally, the aims and goals of the research are outlined providing the importance of combustion modeling.

Chapter 2 lists the literature review of combustion mechanism, differences between premixed and diffusion flames in both laminar and turbulent conditions. A detailed explanation is provided of the ways researchers determined flame speed and previous works on hydrogen enrichment and by-product fuel usages in industry.

Chapter 3 summarizes the important conservation equations, chemical kinetics and reduced mechanism that are used to simulate combustion. Furthermore, the chapter goes over ANSYS components and their advantages with a detailed description of premixed combustion theory in fluent and the general models used in fluent to simulate premixed combustion.

Chapter 4 Goes over the problem statement, the process of generating the mesh and the assumptions made. The test cases for the whole project are presented, where the first couple cases compare the differences between the Transport and the Premixed Fluent model solutions. Furthermore, the flame speed is obtained via 1D CHEMKIN CODE then is compared with the flame speed obtained through Fluent in 2D. The effects of inlet velocity and hydrogen addition to hydrocarbons are tested through several reduced mechanisms. The chapter also goes over the properties of various syngases using reduced mechanism to obtain and study the effects of preheat temperature and radical formation on flame speed. Finally, two variants of syngas are tested which are BFG and COG where, their flame speeds and flame structures are obtained through different equivalence ratios and preheat temperature

# Chapter 2 LITERATURE REVIEW

## 2.1 Combustion Mechanism

During the fuel combustion, heat is released through exothermic chemical reactions with the mass and heat transfer. It is also well known that the rapid oxidation can generate heat and light depending on the rate of oxidation; in some cases, there are relatively small amounts of heat released without light [1, 20, 21]. Flames can be classified as premixed flames or diffusion flames based on the mixing process occurred before or during fuel burning. For premixed flames, both oxidizer and fuel are well mixed before the chemical reaction takes place. This type of flames usually occur in spark-ignition engines [17]. On the other hand, diffusion flames occur when reactants are initially separated, and mixing of reactants occur at the reaction region where fuels burn [17]. In some cases, both premixed and diffusion flames occur simultaneously when the reactants are not well mixed, and the diffusion is usually referred to the diffusion of chemical species from one side to the other. This flame is called partial premixed flame.

In combustion processes there is a thin layer in the reaction zone, referred to as the flame and behind which is the location where the fuels flow to the flame to sustain the reaction and the products diffuse out of the flames, and the heat is generated to raise temperature of the combustion products [17]. Sometimes autoignition can occur, which is basically a rapid oxidation reaction occurring within the unburned gas, leading to combustion happening in the entire volume. If this is happed in IC engines, it can create a loud noise referred to as knocks. It is always a challenging problem for the designers to eliminate or reduce knocks in engines. For the chemical reaction modeling one important aspect is to determine the stoichiometry, which is a quantity used to describe the nature of combustion to be fuel lean or fuel rich reactions. Stoichiometry quantifies the amount of oxidizer that is required to completely burn fuel so that the equivalent ratio (O/F or A/F) equals 1.In the case of having more oxidizer required than that for complete fuel burning, it is called fuel-lean combustion, and the equivalent ratio is less than the stichometry, while the opposite case of having less oxidizer for fuel is called fuel-rich combustion

$$\left(\frac{A}{F}\right)_{Stoich} = \left(\frac{m_{air}}{m_{fuel}}\right)_{Stoich} \tag{2.1}$$

To determine the equivalent ratio of air to fuel, first there is a need to write a reaction formula and balance the reaction. In an example of a hydrocarbon reacted with air, it can be expressed as follows [17].

$$C_xH_y + a(O_2 + 3.76N_2) \rightarrow xCO_2 + \left(\frac{y}{2}\right)H_2O + 3.76aN_2 \tag{2.2}$$

$$a = x + \frac{y}{4} \tag{2.3}$$

Throughout the project the oxidizer will be assumed as air consisting of 79% $N_2$and 21% $O_2$. Another indicator of the combustion condition is the equivalent ratio φ defined as following

$$\varphi = \frac{\left(\frac{n_{fuel}}{n_{air}}\right)_{actual}}{\left(\frac{n_{fuel}}{n_{air}}\right)_{stoich}} = \frac{\left(\frac{A}{F}\right)_{stoich}}{\left(\frac{A}{F}\right)_{actual}} \tag{2.4}$$

where n is the number of moles of the species. In the following formula a fuel rich mixture has an equivalence ratio greater than one, a lean mixture is the equivalence ratio <1 and stoichiometry occurs at 1. It is also important to note that equivalence ratio plays an important role in determining the performance of systems. In the case of methane, the overall stoichiometric combustion can be shown as follows

$$CH_4 + 2O_2 \rightarrow 2CO_2 + 2H_2O - \Delta H_c \tag{2.5}$$

where, $\Delta H_c$ represents the heat of combustion. Another important property of combustion is the adiabatic flame temperature. This temperature is achieved when the reaction of fuel and oxidizer is completed, and the only products are $CO_2$ and $H_2O$ for hydrocarbons react with air. It is well known that it is the highest temperature that a combustion process can

achive without a consideration of heat losses. The heat released during combustion is used to heat up the products of the combustion [22]. To obtain the adiabatic temperature, the final state of temperature is determined by summing up and equating the enthalpies of reactants and products shown in equation 2.5, then through multiple iteration and guessing, the final temperature could be achieved at the equality of enthalpies.

at constant pressure $\Delta H = 0$

$$\sum_{i} n_i \left[ H_T{}^{\circ}{}_1 - H_{298}{}^{\circ} + \left(\Delta H_f{}^{\circ}\right)_{298} \right]_i = \sum_{j} n_j \left[ H_T{}^{\circ}{}_2 - H_{298}{}^{\circ} + \left(\Delta H_f{}^{\circ}\right)_{298} \right]_j \quad (2.6)$$

Where $n_i$ and $n_j$ refer to number of moles for reactants and products respectively, in combustion system reaction for various species are required to be considered, because every reaction has an equilibrium, which can be determined through equating equations and solving for the unknown variables. However, in other combustion system with higher number of species softwares such as GASEQ are used to determine chemical equilibrium and adiabatic flame temperature [23].

## 2.2 Laminar/Turbulent Flames

The most common type of flame that is studied is the premixed flame configuration, where the flame travels in the form of a wave, when an explosive mixture is ignited. The flame could either be detonation or deflagration waves, depending on the mixing of the fuels, or how the wave travels through the apparatus. In premixed flames this wave is often called deflagration, which is a subsonic wave that propagates through a homogenous mixture, and it is usually slower than the detonation wave (diffusion flames) [22]. Both detonation and deflagration waves can be divided into either laminar or turbulent flames depending on the velocity of the gas that is supplied, slow fuel flowrate for laminar and fast for turbulent [22-24].

To develop better understanding of premixed flames, researchers study Bunsen burner flames. The Bunsen burner flame is the simplest form of premixed flames that is widely use in gas cookers, and heating unit's configuration as shown in Figure 2.1

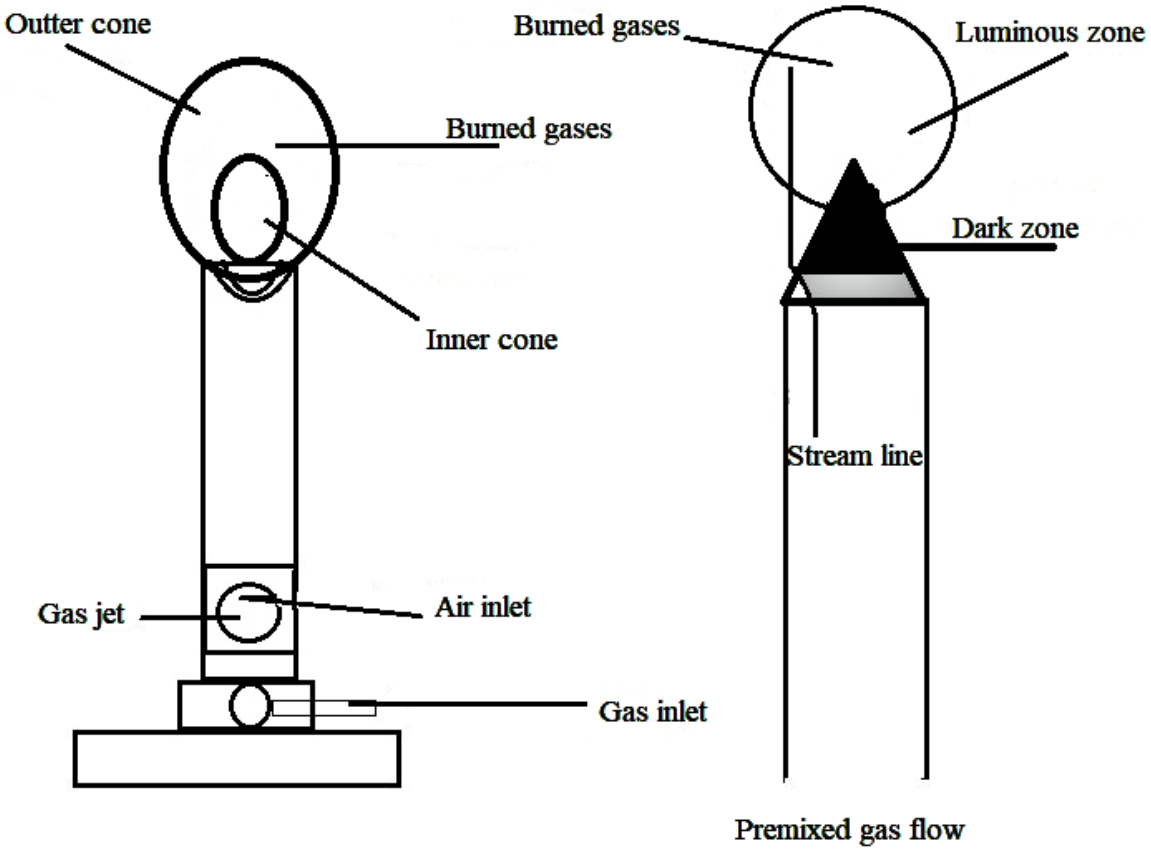


Figure 2-1 Bunsen burner configuration premixed flame zones [17]

The typical Bunsen burner displays both attributes of premixed and diffusion flames. The premixed flame is displayed in the inner core of the reaction zone, and in the case of fuel rich the outer cone displays diffusion flames due to incomplete combustion. As previously mentioned, the flame state could be represented by equation 2.1. As it enters the In the Bunsen burner, fuel and air are induced into the burner tube from the surrounding pipes and then are mixed to form a homogenous combustible mixture. The flow inside the tube is usually laminar if the Reynolds number is not large, with a parabolic profile, combined with the heat inside, it creates the parabolic flame that is stabled and anchored on top of the burner [22]. From Figure. 2.1 the dark area represents the unburned reactants and the

luminous zone is considered the flame where heat is released. The flame has a very thin layer about 1mm thickness. The flame color varies depending on equivalent ratio and type of fuel used. In the rich-fuel case, the luminous zone appears to be yellowish emitted from carbon particles, and purple in the fuel-rich flames is from CH radicals [24].

For hydrocarbon fuels laminar premixed flame front can be characterized as consisting of two zones, a preheat zone and a reaction zone. Sometimes a third zone is identified, known as the recombination zone, which occurs downstream of the flame front. In the natural gas combustion thermal pyrolysis usually occurs in the reaction zone, where the properties of reaction zone are determined by diffusion of H radicals against the convective flow of unburned gas into the preheat zone.

Thus, forming hydrogen peroxide, which does not get dissociated in the preheat zone, so it convects into reaction zone forming OH radicals that are formed at higher rate than the O and H radicals that appear in the reaction zone causing fuel decay [1, 25, 26] Further, this forms the intermediate zone where CO is converted into $CO_2$ and heat is released to increase temperature of combustion products. As CO is consumed, temperature decreases at the downstream. In the recombination zone reactions tend to be exothermic and radical concentrations are low. Recombination zone usually describes the aftermath of flame zone and it is not reflected in the temperature profiles. For methane-air flames, it has a short residence time which gives very small amount of pyrolysis. The components that leave the reaction zone are hydrogen and low hydrocarbons, in a normal setting the hydrocarbons have an average flame speed of 40 cm/s.

## 2.3 Fundamentals and measurements of Laminar flame speed

To describe premixed flames, three main properties are investigated: temperature, flame speed and flammability limits. Flame speed is a physicochemical property that depends on the thermodynamic properties of fuel used. Flame speed plays an important role in understanding flame characteristics, such as heat release and propagation rates [27, 28]. For Bunsen burners, the combustion tube, where fuel and air are well mixed, should be sufficiently long so that the velocity profile at the tube exit is parabolic The velocities of fuels and air can be well controlled by flowmeters. The stable flame sits on top of burners

with a conical shape. The flame speed is studied as the velocity that is normal to flame front as unburned mixture gases propagate through the combustion zone. There were three theoretical explanations that tried to determine the nature of flame speed: thermal, comprehensive, and diffusion theories [22].

The thermal theory analysis examined the flame speed through studying the energy equation. It was assumed that the propagation of heat through the gas layers is the main mechanism, where two zones exist and there is a point that separates the two zones into a next zone that ignites [16]. However, this theory falls short in being able to determine the ignition temperature. The Semenov theory contained the diffusion of molecules and heat without the study of radical diffusion. It initially contained an assumption of ignition temperature that was taken out from the final equation. Nowadays the final work of Semenov and Mallard is very similar to the activation energy asymptotic [29, 30]. Later Lewis proposed the diffusion of particles, which was later expanded to include that radical diffusion played more important role than the temperature gradient [31].

The comprehensive theory is based on the flame structure analysis that uses computational and numerical methods to acquire a solution for steady state mass, energy, species conservation equations based on a chemical reaction mechanism. These solutions can be obtained by using numerical simulation softwares such as CHEMKIN to simulate 1D premixed flame and its structure [32]. Effects of radical diffusion from the reaction zone to unburned reactants is the main factor in the propagation of flame wave in premixed flames. The concept of radical diffusion added an approximation [22] given by an inverse relationship between the flame thickness and laminar speed in relation to the overall reaction rate of the combustion which helps in determining the flame speed in some cases, but it is very limited, shown in equation 2.7 and 2.8

$$\delta_f = \frac{\alpha}{S_L} \tag{2.7}$$

$$S_L \cong (RR * \alpha)^{0.5} \tag{2.8}$$

Where α is the thermal diffusivity of unburned gases measured in $m^2/2$ and RR is the overall reaction rate, the flame thickness is represented by $\delta_f$ in (mm).

The common concept, between all the theories was the equations used to develop the concepts, where the exact solution of laminar flame propagation considers the basic equations of fluid dynamics to include the changes of heat and chemical species [1, 16, 25, 26, 29-31, 33].It is difficult to determine the flame speed for Bunsen burners, where initially researchers tried to observe the flames zones and determine which one was suitable for the measurements. Certain methods of observing the flame include shadowgraphs, schlieren pictures and direct method of observing the luminous part of flame, in which the side that is towards the unburned gases is measured. Each method defines a surface, and not all of them precisely defined a specific surface that could be used to measure the surface area of flames. The observations provided the measuring techniques for flame speed which include: stationary conical flames on cylinders, flames inside of cylinders, spherical expanding, soap bubble method, and flat flames. Each method has its own advantages and percentage of errors [34]

In the burner method ( Area Method ) the premixed flow goes through the tube that has a certain length to ensure the development of flows [34-36]where it displays the shape of a cone that is usually recorded, by modifying the nozzle it is possible to achieve a cone that has straight edges to be able to determine the surface area of the flame through simple cone surface area formula shown in Figure 2.2

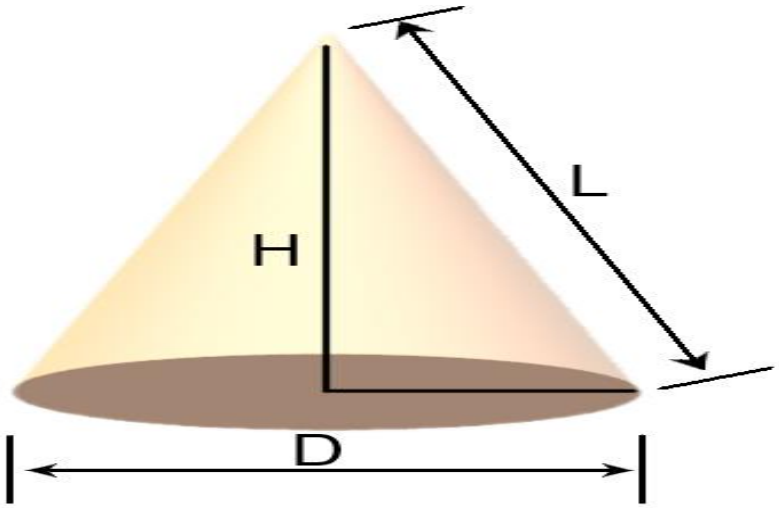


Figure 2-2 Surface area of a cone with straight edges [29]

To assure the flames is stable at the burner exit, the local flame speed must be the same as the flow velocity, then the measured average laminar flame speed $S_l$ can be determined by finding the area of the tube cross section in the following equation 2.9

$$A_f = \pi * \left(\frac{D}{2}\right) * \sqrt{H^2 + \left(\frac{D}{2}\right)^2} \tag{2.9}$$

Where D is the diameter, H is the height of the cone all measured in m then the flame speed is obtained through equation 2.10

$$S_l = \frac{V_u A_c}{A_f} \tag{2.10}$$

Where $V_u$ is measured in (m/s) and it represents the average velocity of the flow, $A_f\,(m^2)$ is the surface area obtained through the conic shape and $A_c\,(m^2)$ is the area of the cross section. It is important to note that during the measurement for area method, the velocity is not constant around the cone. Usually there are some heat losses that occur due to the walls, leading to lower temperature. That is because of low reaction rates that reduce the flame speed. Due to the variation of velocity vectors, it can be noticed that measuring flame

speed at each point yields a variable answer that is somewhat closely related, which could be considered as a disadvantage for this method. The results in this method have an accuracy of +/- 20% which led researchers to the use of schlieren cone because the streamlines remain constant all the way until the schlieren cone[34].The other method for stationary flame is the angle method, where the angle that is slant of the cone created alongside the axis burner is measured at the exact center of the cone to determine the flame speed through the following formula in equation 2.11 shown in Figure 2.3 [29]

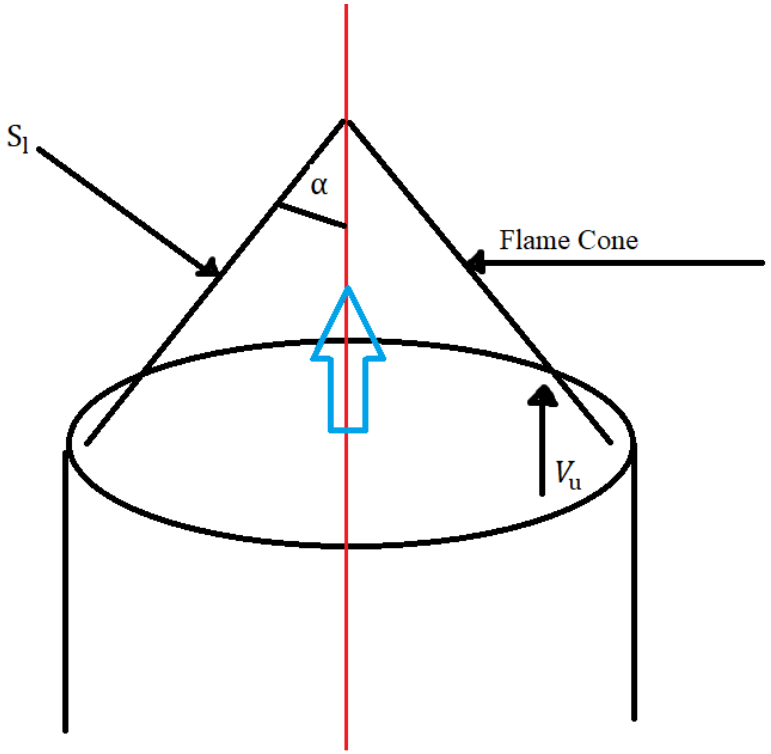


Figure 2-3 Estimation of the flame surface through the angle method [17]

$$S_l = U_u \sin \alpha \tag{2.11}$$

By maintaining a stable flame and uniform velocity profile, equation 2.11 could be used directly to find the flame speed. However, CHEMKIN software has a capability to determine flame speed for a mixture, with the known reaction kinetics [32, 33], and species concentrations referred to as the flame structure as shown in Figure. 2.4

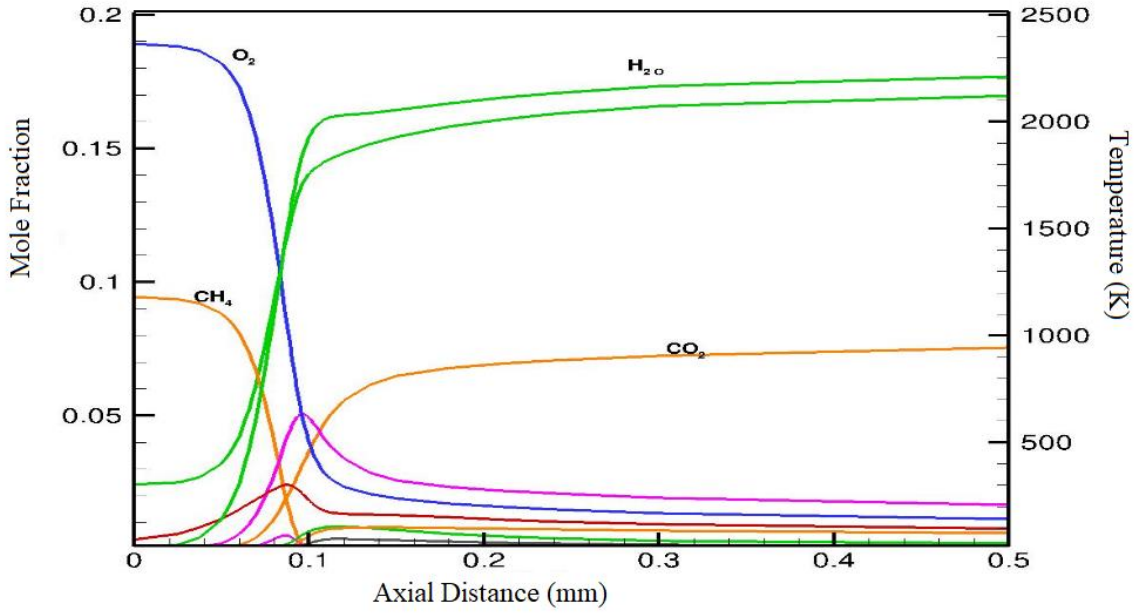


Figure 2-4 Methane-air flame structure displaying the reactants and products

The flame structure shown in Figure 2.4 could be used to understand the changes in reactants and products. However, these structures could also include that radical formation which are important in understanding the behavior of flame speed, where they will be used in this project to correlate the work done through simulation to experimental work [37, 38].

## 2.4 Reduced Mechanisms

To properly simulate combustion, there is a need for accurately predicting chemical properties of flames such as ignition delay, production and consumption of components, pollutants emissions and heat release. Further, with recent technological and computing development, several detailed chemical kinetics are available for the conventional hydrocarbons used in industry. However, even though these detailed chemical kinetic mechanisms provide very high accuracy for determining flame burning characteristics such as temperature, structures and speed. These mechanisms take longer periods of time and computing cost to get solutions. The increased amount of time required to run these

iterations, is because these models are designed to accurately depict fuel oxidation over large boundaries, that contain hundreds of species and chemical reaction steps [39].

The goal of mechanism reduction is to reduce the size of detailed mechanism by eliminating species and chemical reactions that have negligible influence on the phenomena of interest to obtain results that are within acceptable accuracy. To do so, the initial step, is understanding what type of fuel or hydrocarbon is being studied, then identify all the major species and reactions that play an important role in the flame characteristics that are being studied. It is identified by a reaction matrix where each element corresponds to the creation of species from all the reactions included in matrix as reactants [40].Once identified, the species and reaction with low importance are eliminated from the mechanism. This reduces the amount of differential equations that need to be solved. In addition, quasi-steady state assumption is applied to further reduce the differential equations into algebraic expressions that contain less amounts of species or assuming of species lumping [1, 39, 41].

Another technique used in mechanism reduction, is the sensitivity analysis which investigates the possibility of significant changes in reaction flow analysis due to having less amount of species. If there are changes, the species should not be taken of the skeletal mechanism due to its effects on temperatures, ignition timing for premixed flames. The important species in a mechanism are usually defined through knowing the reaction products, initial reactants, defining fuel and pollution components. In some cases, Directed Relation Graph Methodology is used to quantify the coupling between species and reactions by an indicator of error that shows how much error appears if certain species are eliminated [39]. Once a reduced mechanism is obtained it is tested with the skeletal mechanism, or with a mechanism that includes both the skeletal and reduced reactions and species, to visualize the differences in properties. Once an alignment is obtained the reduced mechanism can be used for further testing. In a comparison work done by Bendsten et all a 7-step mechanism was compared with Gri-3.0 and results for flame speed were within 4% error. However, in terms of saving computing time the 7-step excels due to having less amount of reaction and species whereas, the Gri-Mech 3.0 has about 53 species

325 reaction steps. The use of reduced mechanism can amplify the speed of prototype testing for future combustion use [40].

## 2.5 Previous Research on Hydrogen Enrichment and Syngas.

To study the laminar flame speed, a large amount of studies has been done through studying 1D freely propagating methane flames enriched with hydrogen. Researchers have experimentally determined the effects of hydrogen enrichment on methane by observation of laminar flame speed and then compared with simulations provided by CHEMKIN software. The set of experimental works was done by Yu et al [37, 42, 43] for a range of $0.5<\emptyset<1.25$ for the $H_2$ of 0% up to 75% volume concentration to determine the flame speed. Further work expanded by Lie et al [44, 45] in which the equivalence ratio was adjusted from 0.7- 2.2 with $H_2$ from 0 % up to 100% volume concentrations., With this experimental work Di Sarli et al. compared a numerical analysis using CHEMKIN [46] to study the detailed chemical kinetics and the effects of hydrogen dilution has on methane, in terms of flame structure, flame speed and important reaction steps. Through the sensitivity analysis they tried to study the enhancement of laminar flame speed with hydrogen addition and determined the following reaction steps to be of importance.

(R1) $H + O_2 + H_2O \Leftrightarrow HO_2 + H_2O$

(R2) $H + O_2 \Leftrightarrow O + OH$

(R3) $H + CH_4 \Leftrightarrow CH_3 + H_2$

(R4) $OH + CH_4 \Leftrightarrow CH_3 + H_2O$

(R5) $OH + CO \Leftrightarrow H + CO_2$

It was determined that in hybrid mixtures there are 2 regions. The first region is dominated by methane combustion and hydrogen can affect in few amounts of increased flame temperature and flame speed. That is due to hydrogen not being able to accelerate the combustion. In the second region the laminar flame speed is greatly enhanced by production of radicals. It increases as the fuel is at leaner conditions, which explain the overshoot of laminar flame speed after the values $0<H_2<0.70$ where a higher number of H

radicals presents [46]. In another study [18] the effect of hydrogen enrichment on $NO_x$and $CO_2$ formation was studied. The simulation showed that emissions are reduced when hydrogen was added into the fuel blends. Furthermore, there was a significant reduction in NO formation with the addition of hydrogen in fuel mixtures.

In the recent decades the use of low calorific value fuels has increased, which use Synthetic Gas, Coke Oven Gas (COG) and Blast Furnace Gas (BFG) in gas-turbine power generation. [47]. During steel process of turning coal into steel, there are a large amount of fuel gases remaining in the chamber that could be reused to produce energy. Coke oven gas is the by-products of the process remaining in the coke oven battery after pit coal has been processed. During the dry distilling of coals, the gas is produced at high temperatures without the presence of oxygen. The components of coke gas are mainly about 10-50% methane, 50% hydrogen with the remaining carbon monoxide and nitrogen. With the high calorific value, the use of coke gas could be promising for generating gas engines. The advantages of these gases come from its stable compositions with high contents of hydrogen. However, the large amount of hydrogen makes the combustion to be quick and may cause engine knock and backfire. In previous studies [47] it is suggested to use a lean mixture and vary the engine load and gas converter by increasing carbon monoxide content to reduce the speed of the combustion through safe handling of the gases. The resultant products can generate steam that is fed into boilers, and then reused for steel processes. The other by product gas is the Blast Furnace Gas which a product of iron ore reduction with coke into pic iron. Its heating value is very low which makes it difficult to sustain a continuous combustion so that BFG need to mix with other combustible gases to improve its efficiency. Clarke-energy have been using BFG and COG gas in Jenbacher gas engines by varying compositions and calorific quantities [47].

# Chapter 3 MODELING COMBUSTION WITH ANSYS FLUENT

This chapter includes description of CFD capabilities and the advantages, governing equations, and chemical kinetics used for combustion. A comparison between the transport and premixed combustion models will be made to determine which is applicable in studying simulation of premixed flames. In addition, assumptions, boundary conditions were set up for convergence and stability of the model. At the end Fluent capabilities of determining the laminar flame speed will be presented

## 3.1 ANSYS Fluent Description and Advantages

Computational Fluid Dynamics has become an important aspect of visualizing and studying the process of combustion through its vast algorithms, and pre and post processing capabilities. It has become a reliable tool in the design of prototypes and industrial equipment. It is believed with advanced technology, CFD solutions will continue to have an increased accuracy with low cost of computing units [48]. For this project, ANSYS 19.1 software is used that can create simulations to study disciplines of chemistry, fluid dynamics, heat transfer and other engineering applications. Building into ANSYS, ANSYS Fluent software is designed to simulate flows, turbulence, military equipment, and applications used in industry to produce energy. The important aspect for this research is the ability of Fluent to simulate combustion inside of cylinders, through high performance computing that solves large and complex fluid dynamics problems.

ANSYS Fluent provides the capabilities to generate the desired geometry with selected materials and to model it into a mesh. During the meshing process, it is possible to generate a mesh containing small elements, which allow the transfer of heat and the flow to be modeled with Fluent using specific shapes to create a single volume. However, the volume needs to be meshed into even smaller elements for increased accuracy. However, increasing the number of elements and nodes increases the computing time. Once the mesh and boundary conditions on the geometry are defined, Fluent contains the fluid solver, which allows the user to operate the parameters, refine the boundary conditions and select

the type of solution model such as premixed combustion model, non-premixed model and transport model which will be selected based upon the problem that is being studied. The final model of the project contained about 42000 elements that were analyzed. Although selecting even smaller size, say maximum 160000 elements, can provide results that were about 3.5% more accuracy, running simulations with current 42000 elements saved at least 4 hours per run.

Some of the advantages provided by ANSYS tools are the ability to investigate systems that are difficult to test experimentally due to their hazardous nature. ANSYS provides detailed results for the model for which, each section or part could be selected, visualized and investigated for errors and deformations. In a short time period it can predict results at designed conditions of heat, temperature and deformation through the usage of simulations. This enables the vast range of testing conditions until an optimal result is obtained before a physical prototype is tested which results in better efficiency, better costs and fast computing time [48, 49].

### 3.2 ANSYS Code Components.

To obtain a solution for the designed problems, the software requires several steps for the CFD code to work. The code contains numerical solutions and algorithms that are embedded in the User Interface to provide flexibility and friendly use. The main elements of every coding software; are the pre-processor, post-processor and solver. Every engineering problem has an input or an initial condition. The pre-processor serves as the input of the problem that is studied. This step includes defining the geometry of the system, creating the grids and the mesh. This reduces the model into small elements. Furthermore, the specification of boundary conditions of the wall, inlet, outlet domain and type of symmetry is part of the preprocessor [49].

The pre-processor also controls the definition of the material, fluid properties and the chemical phenomena that is required to test the model. The solver describes the techniques that are used to solve the problem through discretization, algebraic solution and approximation methods used for the flow variables [50, 51]. For the current research, one common method used in CFD is the Finite Element Method (FEM). It relies on the use of

simple linear and quadratic equations to determine the unknown variables in the flow. The governing equations are solved by finding the exact solution, but sometimes it is difficult to obtain exact solution for systems. For this reason, indicators of errors are defined. These indicators are known as residuals which are defined for every variable and must be within a certain defined limit for the solution to converge. However, to minimize the error the CFD code has built in tools to multiply the residuals with weight functions to obtain algebraic equations that could be integrated to obtain solutions for each coefficient of interest. The post-processor is the final step. Once a solution is obtained, the software can provide the data for every variable in terms of XY plots or visual contours. For combustion problems users can investigate the temperature, velocity, species molar concentrations and mass fractions, NO formations, particle tracking, vector plots, and streamlines through the flow.

## 3.3 Conservation Laws

### 3.3.1 Mass Conservation

To attain mass balance in fluids based upon the continuity equation, where it describes the mass balance; as the rate that mass of fluid that is increased which is equal to net flow of mass into the fluid or the change in mass is equal to mass inflow minus the mass outflow. and it is shown as following.

$$\frac{\partial \rho}{\partial t} + \frac{\partial (\rho u)}{\partial x} + \frac{\partial (\rho v)}{\partial y} + \frac{\partial (\rho w)}{\partial z} = 0 \qquad (3.1)$$

Where ρ is the fluid density measured in $(\frac{kg}{m^3})$, t is time (s), u,v,w are the componenets of velocity in x,y,z.,If ρ is constant the notation changes to match equation 3.2 and mass conservation could be written in vector notation as following

$$\frac{\partial (u)}{\partial x} + \frac{\partial (v)}{\partial y} + \frac{\partial (w)}{\partial z} = 0 \qquad (3.2)$$

$$\frac{\partial \rho}{\partial t} + \mathrm{div}(\rho U) = 0 \tag{3.3}$$

Where U is the velocity vector, where equation 3.3 describes the 3D continuum for mass conversation in a compressible flow where the term on left describes the time rate of change and the second term is the convective term that describes the net flow out of the element through the boundary

### 3.3.2 Momentum Conservation

From Newton's 2nd law of motion, momentum conservation is explained as the rate of change in momentum with addition of the surface forces such as pressure, viscous force and volume forces as shown for x,y,z components

$$\rho \frac{Du}{Dt} = + \frac{\partial(-p + \tau_{xx})}{\partial x} + \frac{\partial \tau_{yx}}{\partial y} + \frac{\partial \tau_{zx}}{\partial z} + F_{mx} = 0 \tag{3.4}$$

$$\rho \frac{Dv}{Dt} = + \frac{\partial(-p + \tau_{yy})}{\partial y} + \frac{\partial \tau_{xy}}{\partial x} + \frac{\partial \tau_{zy}}{\partial z} + F_{my} = 0 \tag{3.5}$$

$$\rho \frac{Dw}{Dt} = \frac{\partial(-P + \tau_{zz})}{\partial z} + \frac{\partial \tau_{xz}}{\partial x} + \frac{\partial \tau_{yz}}{\partial y} + F_{mz} = 0 \tag{3.6}$$

where P is the pressure, $\tau$ is the viscous stress tensor, $\tau_{ij}$ represents the viscous stress of i component on the surface which along the direction of the surface normal to j direction, and $F_{mx}$ is the body force of x component .It is possible to modify these Navier-Stokes equations of momentum through understanding that viscous stresses are proportional to deformation rates and these terms involve 2 constants which are dynamic viscosity $\mu$ related to linear deformation and $\lambda$ stresses related to volumetric deformations by substituting in previous equation $\mu$

$$\rho \frac{Du}{Dt} = \frac{-\partial \rho}{\partial x} + \mathrm{div}(\mu \Delta v) + F_{mx} = 0 \tag{3.7}$$

$$\rho \frac{Dv}{Dt} = \frac{-\partial \rho}{\partial y} + \text{div}(\mu \Delta v) + F_{my} = 0 \tag{3.8}$$

$$\rho \frac{Dw}{Dt} = \frac{-\partial \rho}{\partial z} + \text{div}(\mu \Delta v) + F_{mz} = 0 \tag{3.9}$$

### 3.3.3 Energy Equation

The energy equation is derived from the first law of thermodynamics which describes that the rate of change of energy or a particle is equal to rate of heat added to that same particle with the addition of the work done. The rate of energy increase and the net heat transfer rate to the particle can be defined as

$$\rho \frac{DE}{Dt} \tag{3.10}$$

$$-\text{div}\, q = \text{div}(k \Delta T) \tag{3.11}$$

The total work done by a surface force on a particle can be described as

$$-\text{div}(\rho U) + \left[\frac{\partial(u\tau_{xx})}{\partial x} + \frac{\partial(u\tau_{yx})}{\partial y} + \frac{\partial(u\tau_{zx})}{\partial z} + \frac{\partial(v\tau_{xy})}{\partial x} + \frac{\partial(v\tau_{yy})}{\partial y} + \frac{\partial(v\tau_{zy})}{\partial z} + \frac{\partial(w\tau_{xz})}{\partial x} + \frac{\partial(w\tau_{yz})}{\partial y} + \frac{\partial(w\tau_{zz})}{\partial z}\right] \tag{3.12}$$

With the addition of energy source per unit time and volume, the rate of increase of energy can be written

$$\rho\frac{DE}{Dt} = -\mathrm{div}(\rho U) + \left[\frac{\partial(u\tau_{xx})}{\partial x} + \frac{\partial(u\tau_{yx})}{\partial y} + \frac{\partial(u\tau_{zx})}{\partial z} + \frac{\partial(v\tau_{xy})}{\partial x} + \frac{\partial(v\tau_{yy})}{\partial y} + \frac{\partial(v\tau_{zy})}{\partial z} + \frac{\partial(w\tau_{xz})}{\partial x} + \frac{\partial(w\tau_{yz})}{\partial y} + \frac{\partial(w\tau_{zz})}{\partial z}\right] + \mathrm{div}(k\Delta T) + E = 0 \quad (3.13)$$

### 3.3.4 Transport Equation

The transport equation can be to describe how a quantity is transported in space, for example transport of chemical concentration inside a flow. It is also referred to as the modeling pollutant formation, dispersion flow, and mathematically it represents convection and diffusion equation which is used in many CFD models [51]. The transport equation shares similarities between the other conservation equations, and if a variable is introduced for example $\phi$ that transport equation can be written as

$$\frac{\partial\rho(\phi)}{\partial t} + \mathrm{div}(\rho\phi U) = \mathrm{div}(\alpha\Delta\phi) + S_\phi \quad (3.14)$$

Equation (3.14) represent the transport equation given the property $\phi$ which describes the process of transport through rate of change term and convection terms on the left-hand side then the diffusion coefficient and source term $S_\phi$ on the right-hand side [50, 52, 53]

## 3.4 Chemical Kinetics

Combustion process contains many elementary reactions or reaction steps that are usually studied through the consumption of reactants and production generation with heat releases that flow into the process. That concept has forced researchers into trying to determine the reaction rate at which the combustion occurs in. One such condition relies on knowing the temperature and concentration of the reactants [22].

A chemical reaction can be written as following

$$\sum_{j=1}^{N_r} V_j'(X_j) \Leftrightarrow \sum_{j=1}^{N_p} V_j''(X_j) \tag{3.15}$$

where $X_j$ the molecular formula of species j in the system. The $V_j'$ and $V_j''$ represent the stoichiometric coefficient of species j where single prime represents for the reactant and double prime represents the products, respectively. $N_r$ and $N_p$ represent the number of species for reactants and products for the species another important property to identify is the rate of change (consumption or production) for each species due to reaction process The rate of change of the species is defined as the reaction rate (RR) and it is proportional to the product of concentrations of reactant species [22, 24] as shown following

$$RR \sim \prod_{j=1}^{n} (X_j)^{V_j'} \tag{3.16}$$

$$RR = k \prod_{j=1}^{n} (X_j)^{V_j'} \tag{3.17}$$

where k is defined as the specific reaction rate constant and $V_j'$ is the reaction order based on the species. To determine the net rate of change of concentration of species i in the reaction, considering the equation in equation 3.18, could be explained in the following

$$\frac{d(X_i)}{dt} = [V_i'' - V_i']RR = [V_i'' - V_i']k_f \prod_{j=1}^{n} (X_j)^{V_j'} \tag{3.18}$$

Where $(X_i)$ represents the molar concentration of species i. $k_f$ is the forward reaction rate. Using the above equation provides less error in sign determination and applies for stoichiometric coefficients that are less or greater than one.

The reaction rate constant of an elementary reaction can be described through the Arrhenius reaction rate expression from

$$k_f = A \exp\left(\frac{E}{RT}\right) \tag{3.19}$$

Where A is called the pre-exponential factor or frequency factor, E is the activation energy, R is universal gas rate constant and T is the temperature in K.

The pre-exponential factor may depend weakly on the temperature and becomes $AT^{\beta}$ so that Arrhenius rate could be changed as following

$$k_f = AT^{\beta} \exp\left(-\frac{E}{RT}\right) \tag{3.20}$$

β is the exponential temperature of the reaction and the other properties are usually determined experimentally. For a reverse reaction, the rate constant cab be expressed based on the forward reaction rate constant and equilibrium constant as obtained bellow,

$$k_r = \left(\frac{k_r}{K_p}\right) \tag{3.21}$$

$K_p$ (T) is the equilibrium constant of the reaction aA+bB =cC+dD can be written as

$$K_p = \left([C]^c[D]^d/[A]^a[B]^b\right) \tag{3.22}$$

Where each letter corresponds to the concentrations of reactants and products

### 3.5 Chemical Kinetic Mechanisms(10-step and 5-step)

The reaction mechanism (reaction pathways) can be divided into two categories, comprehensive mechanism and reduced mechanism. The comprehensive mechanism describes all species and reactions that occur in the system. An example given is the Gri Mech 3.0 which contains 325 reaction and 53 species, while the reduced mechanism only describes the major and important species and reactions for a specific species and reactions of interest [54].

The current project relies heavily on the use of reduced mechanism that could simulate hydrocarbon fuels, including methane, hydrogen, syngas, BFG and COG. The current Fluent version has certain limitation to the amount of species and steps used, which is also one of the reasons why reduced mechanism are implemented. Using reduced mechanism, one can obtain results at an accuracy within desired limits in timely manner to predict the flame structures, characteristics and emissions produced. Furthermore, these reduced mechanisms make simulations feasible, and it takes only a few chemical reactions to simulate combustion of hydrocarbons over certain range of conditions. One of the tested reduced mechanism in this project was implemented by Belcadi et al. which has 15 species and 10 reaction steps. It determines the characteristics of $CH_4$ CO and $NO_x$ based on the singular perturbation method (CSP) using a procedure created in the S-Step algorithm based on steady state species [55]. The reason for implanting this mechanism into ANSYS was because its numerical results for $0.6 \leq \phi \leq 1.5$ were already previously tested and validated [18, 55-59] with the 1-D Premixed Code, GRI-3.0 and experimental data. The same range of equivalence ratio is used within this project to determine the flame characteristics for lean/rich fuel conditions

(R1) $H_2 \Leftrightarrow 2H$

(R2) $H_2 + O_2 \Leftrightarrow 2OH$

(R3) $2H_2 + O_2 \Leftrightarrow 2H_2O$

(R4) $2CO + O_2 \Leftrightarrow 2CO_2$

(R5) $2CH_4 + O_2 \Leftrightarrow 2CO + 4H_2$

(R6) $2CH_4 \Leftrightarrow 2CH_3 + H_2$

(R7) $2CH_4 + 3O_2 \Leftrightarrow C_2H_2 + 6OH$

(R8) $2HCN + O_2 \Leftrightarrow 2CO + H_2 + N_2$

(R9) $O_2 + N_2 \Leftrightarrow 2NO$

(R10) $H_2 + 2N_2 \Leftrightarrow 2N_2O$

In this reduced mechanism, the first two reactions are the chain initiation reactions of the radicals H and OH from $H_2$ and $O_2$. Furthermore, the reaction R3 to R5 are the global reactions for carbon monoxide and water generations. The reactions R6 and R7 are the steps for the conversion of $CH_4$ to generate radicals $CH_3$ and OH. The last three reaction describe the $NO_x$ formation that will is studied in this project. they include prompt and reburning reactions, thermal NO and Nitrous oxide formations. Upon comparisons within a seven-step mechanism and GRI-Mech 3.0 there was a pretty good agreement in the flame structure of major and minor species and the flame speed for flame propagating [54-57].

Reduced mechanisms are introduced by sensitivity analyses to get a skeletal mechanism from a set of reactions, then the steady-state assumptions are used in reactions and species to get reduced mechanisms [58]. Mechanism reductions have widely been used specially in single component fuels or syngas [59-63]. However, researches carried on the syngas variants such; as BFG and COG are few, and recent research was conducted by Nikolaou et al. [64] in which the skeletal mechanism with 49 reactions was used to validate CO, $H_2$, $H_2O$, $CO_2$ and $CH_4$ with both low and high mole fractions of hydrogen and methane. To produce a 5-step mechanism, that can validate the results for laminar flame speed and flame structures

(R1) $O_2 + H_2O + 3CO \Leftrightarrow 2H + 3CO_2$

(R2) $H_2 + CO_2 \Leftrightarrow H_2O + CO$

(R3) $2H + CO_2 \Leftrightarrow H_2O + CO$

(R4) $2H_2O + O_2 + 2CO \Leftrightarrow 2H + 2CO_2 + H_2O_2$

(R5) $CH_4 + 2H + 4CO_2 \Leftrightarrow 5CO + 3H_2O$

During the development of the 5-step mechanism it was noticed that there would be a slight overestimation due to the introduction of steady-state assumptions that could result in overestimated values of reaction rates [64]. For the radical, OH if the reaction rate is overestimated for CO+OH= $CO_2$+H it leads an increased consumption of CO which causes the increased estimated values of flame speed through increased activation energy of the

chain branching reaction O+$H_2$= H+OH.Both mechanisms will be used for simulating the flame structure of the gas and determining the flame speed that is close to experimental work.

### 3.6 Premixed Combustion Theory in Fluent

Simulations of a premixed combustion in Fluent are far more difficult to model than a non-premixed combustion, because of how the reaction occurs within a thin flame that propagates and is affected by turbulence. To determine the rate of propagation of the flame for subsonic flows, the laminar flame speed and turbulent eddies needs to be found. As mentioned in Chapter 2 different methods could be applied to find the laminar flame speed or simply using 1-D CHEMKIN PREMIX Code. The turbulent model proposed by Zimont et al [27, 28] applies the solutions of transport equation to determine the progress variable which is the summation of the products species, through turbulent flame speed. The progress variable could be defined in equation 3.23 as

$$c = \sum_{i=1}^{n} Y_i / \sum_{i=1}^{n} Y_i, eq \tag{3.23}$$

$Y_i$ and $Y_i, eq$ represent the mass fraction of species and the total mass fraction of species i and n is the number of products. It is required to define the value of c as a boundary term in the inlets of CFD model where c=0 refers to unburnt and c=1 refers to burned

The propagation of flame front for reaction progress variable could be defined as

$$\frac{\partial}{\partial t}(pc) + \nabla.(p\bar{v}c) = \nabla.\left(\frac{\mu_t}{Sc_t}\nabla c\right) + pS_c \tag{3.24}$$

$$pS_c = p_u S_T |\nabla c| \tag{3.25}$$

$$S_T = A(u')^{\frac{3}{4}} S_l^{0.5} \propto^{-0.25} l_t^{0.25} = Au' \left(\frac{\tau_t}{\tau_c}\right)^{0.25} \quad (3.26)$$

where $S_T$ (m/s) is the turbulent flame speed which is based upon the assumption of wrinkled and thick flame fronts. A is the model constant, $u'$ is RMS of velocity, $S_l$ is laminar flame speed (m/s), $\propto$ is the thermal diffusivity of unburned mixture ($m^2/s$), $l_t$ is turbulent length scale (m), $\tau_t$ and $\tau_c$ turbulent time scale and chemical time scale both measured in s , $p_u$is density of burnt mixture. The premixed model assumes small scale equilibrium in the laminar flame, which is expressed by turbulent flame speed expression [19].

### 3.7 Premixed Combustion and Transport Models in Fluent and Limitations

Fluent assumes that premixed combustion occurs when fuel and oxidizer are properly mixed before a spark or ignition occurs, and then flame front will propagate into the unburned reactants. As mentioned before a laminar flame speed could be determined by the rate of species diffusion. That reason internal flame structures, chemical kinetics at a molecular level are studied and resolved to find the laminar speed of flame [65]. The thickness of the flames is usually very small, in the order of millimeters, so detailed resolution is required to view and measure them.

The premixed combustion simulates flame in a zone where reactions take place and there is a distinct separation between burnt product and unburned reactions. Fluent uses the finite-rate formulation to model premixed flames [65]. However, there are certain limitations for the premixed model in fluent, including not being able to use coupled solvers for the premixed combustion model, because it requires the segregated solver. The model is only valid for sub-sonic flows and cannot be used for detonations or diffusion flame where mixture is ignited by shock wave heat. Furthermore, the premixed combustion model cannot be used with the models for pollutant formations such as NO and discrete-phase particles. The current work uses premixed combustion model to determine the adiabatic flame temperatures of each fuel composition and then a transport model is used to demonstrate the mixing of chemical species.To simulate the combustion process, each

reaction in transport model will be defined in terms of stoichiometric coefficients, formation enthalpies, mole fractions and other parameters that control the reaction rate where turbulence chemistry interaction will be analyzed through the eddy-dissipation model.

### 3.8 Stability and Convergence

CFD simulations can be difficult to understand due to having difficulties in obtaining a converged solution. It is important to note that stability depends heavily on the quality of the grid, and mesh refinement. The convergence can be affected by several factors including complex geometry, little number of cells or having large number of elements, and conservative under-relaxation factors [53]. One method to understand the convergence is to define the residuals. During the simulation, the CFD solver runs several iterations, at the end of each iteration, each quantity is summed to record the convergence history from first time step, until the last iteration. In Fluent, the solver investigates different coefficients that play contribution in the solution discretization where the residuals are computed by the segregated solver through the following equation 3.28

$$R^x = \sum_{\text{cells}} \left| \sum_{ab} a_{ab} x_{ab} + b - a_p x_p \right| \tag{3.27}$$

where x is a variable at certain cell p, a is the center coefficient, b is the contribution of the constant part of source term. This equation is for the unscaled residual where Fluent applies a scaling to the residual called scaling factor which represents the flow of certain variable x. In terms of continuity the $a_p x_p$ is replaced by $a_p v_p$ where $v_p$ is the magnitude of the velocity at a certain cell. The residuals help to describe the solution convergence, through normalization for both unscaled and scaled factors. The default criteria for convergence are the order of $10^{-3}$ for all conversation equation except for energy which is at the order of $10^{-6}$.Another important criterion for this project is the relaxation factor, a factor that slows down the changes from one iteration to another. It is used throughout the simulation for species in the mixture. Its values range between 0 and 1. If it is greater than 1 it is over-relaxation. The optimum value is determined through trial and error.

### 3.9 Determining the Flame Speed in Fluent.

The goal of this project is to determine the flame speed of different fuels at various conditions. However, Fluent requires the laminar flame speed as a property or an input at beginning of run which depends on combustion temperature and pressure. Usually laminar flame speed is measured through previous experiments or in 1-D CHEMKIN simulations, However, to find the flame speed the present studies use fitted curves during the analytical process at the end of rum. The mass fractions of fuels and radicals' compositions will be observed, and the surface area of the flame is determined as the region between the initial and final of a flame. This area will be fitted into piecewise-linear polynomials to determine the actual surface area of the flame, and the surface area alongside the area of the cylinder will be used to determine flame speed through the area method, and then compared with experimental data. The results will be validated for the fuels of hydrogen, methane, methane-hydrogen, syngas, blast furnace gas and coke oven gas as the inlet compositions at the range from fuel lean to rich at temperatures from 298 to 898 K. More detailed explanation will be presented in chapter 4

# Chapter 4 COMPUTATIONAL MODEL SET UP AND VALIDATION

This chapter will go over the computational model used in the project. This model simulates a combustor, that is analyzed by ANSYS Fluent, using both the premixed combustion model and the species transport model. The premixed combustion model is used to calculate the adiabatic flame temperatures for the tested cases, while the species transport model is used to determine the flame structure, flame speed and other properties of interest for this study. The chapter begins with the model's geometry and mesh generation. Fluent transport solver uses the K-ε turbulence model to solve methane air mixture combustion and obtain the flame properties.

## 4.1 Problem Statement and Model Design

The model consists of a 2.0 cm by 40 cm rectangle domain. The left side in Figure 4.1 is the inlet where air and fuel mixture combustible flows in, and the right side is the outlet., The line through the x axis represents the symmetry line, allowing the simulations to be conducted only at half of the domain. Another boundary of the domain is the solid non-slide wall.

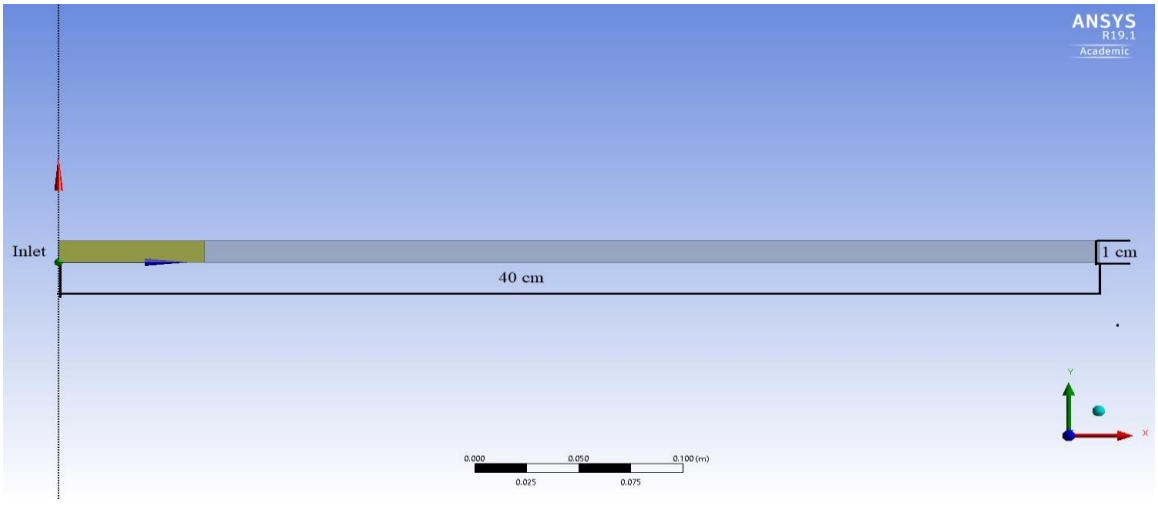


Figure 4-1 Model of the domain used for premixed combustion simulations.

For the preliminary study of methane-air combustion, the premixed combustion model and the transport model are used to solve conservation and transport equations. To properly define the boundary conditions and meshing refinement, the model is divided into 2 main parts, a preheat zone and a reaction zone. In the preheat zone heat and mass diffusion process. As the premixed combustible approaches the reaction zone, it is gradually heated up by heat conduction from reaction zone, resulting in continuously increasing temperature until a minimum ignition temperature is reached. Continuous heating of premixed combustible eventually leads to its ignition in the reaction zone, and chemical reaction rate rapidly increases due to activation of the reaction, and then rapidly decreases due to consumption of reactants. In this process, combustion products are generated, and heat is released. The reaction zone can be further divided into 2 zones, a slim zone and a reaction zone. The slim zone has a fast kinetics speeds, including fractions of fuel molecules and the intermediate species. The molecular reactions are dominant in this zone. The gradient of temperature and species concentrations are high. At atmospheric pressure the thickness of this zone is less than 1 mm. The reaction zone is the broad area with slow kinetics speed, where the reactions of radicals, for example in methane air $CO + OH \Leftrightarrow CO_2 + OH$ , are dominant and the thickness of this zone is up to 3 mm or higher based on the tested conditions.

The flow will vary based upon on the fuel mixture tested in the domain. The flow is normal to the inlet with a constant velocity throughout most of the project to develop a conical flame shape for all the tested cases. The fuel mixture inlet velocity is considered to 0.8 m/s. The outlet is defined as a pressure outlet. The wall boundary is assumed to be adiabatic temperature for the premixed combustion model, and to be ambient temperature for species transport model.

The project studies detailed combustion properties so that it needs to create a reference slice as shown in Figure. 4.1. The element sizes near the inlet and wall are smaller than these in the remainder of the domain. The 7 cm length from the inlet is resemble the area where combustion occurs. The other part of 33 cm will resemble the flame propagation to the outlet.

### 4.1.1 The meshing processes.

When simulating any problem, there is a need to construct the grid of the model that could solved at every point. One such method is the Finite Element Method which is used to approximate the geometry by discretizing the model into smaller shape functions. Using ANSYS built in meshing pre-processor, it is capable to identify the boundaries and generate the mesh. The meshing process helps to dictate the location, where the numerical equations are applied and solved on the model. Acceptable discretization elements include quadrilaterals and triangular cells for 2D models to obtain continuous distributions on each element, with the use of shape functions. The current project uses quadrilateral cells, which are generated with the face meshing tool. The values for the element size are defined to be 0.08 mm near the walls. Near the axis the element size is defined to be 0.16 mm. To get these small meshes for the element size, a bias factor is applied of 2. The bias factor determines the ratios between large and small edges and provides the ability of mesh edges to be within the designed values for element sizing. The edge of the 7 cm of the combustion region has 470 divisions, and the products region of the last 33 cm has about 60 divisions with an application smooth transition of 1.095. Smoothness is used for better accuracy and provide smooth change in size and reduce the number of sudden jumps in the size of cells, for better accuracy. This is done by adjusting the element shapes and quality, by changing the vertices of the mesh [66]. The meshing process is shown in Figure 4.2 where the difference in sizing for each edge is represented to include a finer mesh within the first 7 cm of the domain and less refinement was applied to the remaining parts of the domain. The final mesh is shown in Figure 4.3

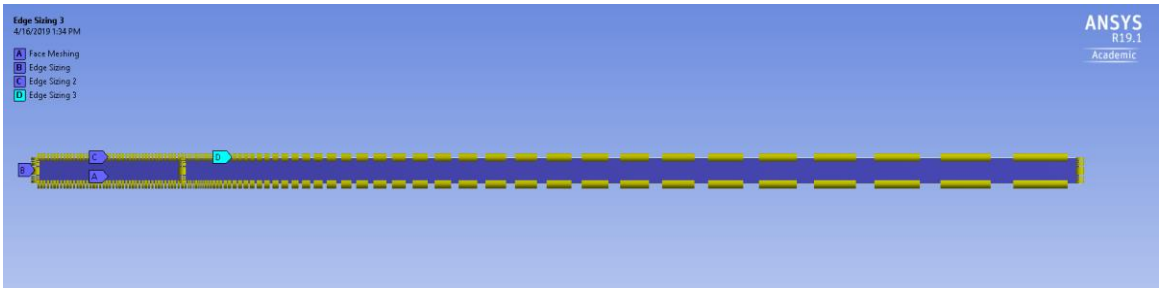


Figure 4-2 The different sizing used for the reaction location and products parts

The meshing is finer within the first 7 cm of the tube, and less refining was applied to the remainder of the tube shown in Figure 4.2

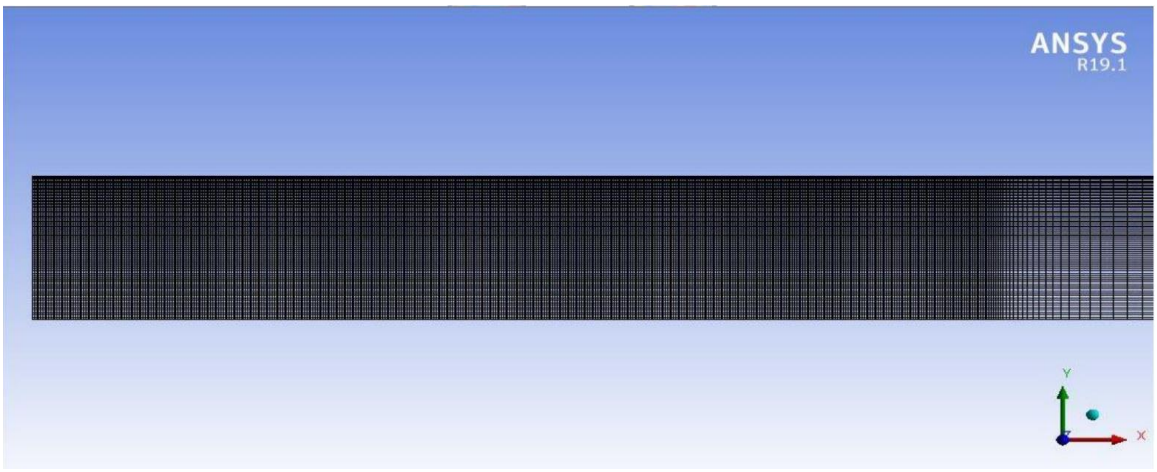


Figure 4-3 The final mesh for simulating premixed combustion test conditions

Table 4-1 The total number of elements and nodes within the tube model

| Domain. | Nodes | Elements |
|---|---|---|
| Combustion Region 7 cm | 37130 | 37680 |
| Product Region 33 cm | 4740 | 4880 |
| Total | 41870 | 42560 |

The first 7 cm of the tube contain higher number of elements and nodes, due to its being the main subject of interest, in studying the flame shape and flame speed. The remaining 33 cm describe the flow of products to the outlet and they contain less elements and nodes. Once the mesh is generated the boundary conditions are defined, by creating named selections on each edge, to define the velocity inlet, pressure outlet and axis of symmetry shown in Figure 4.4.

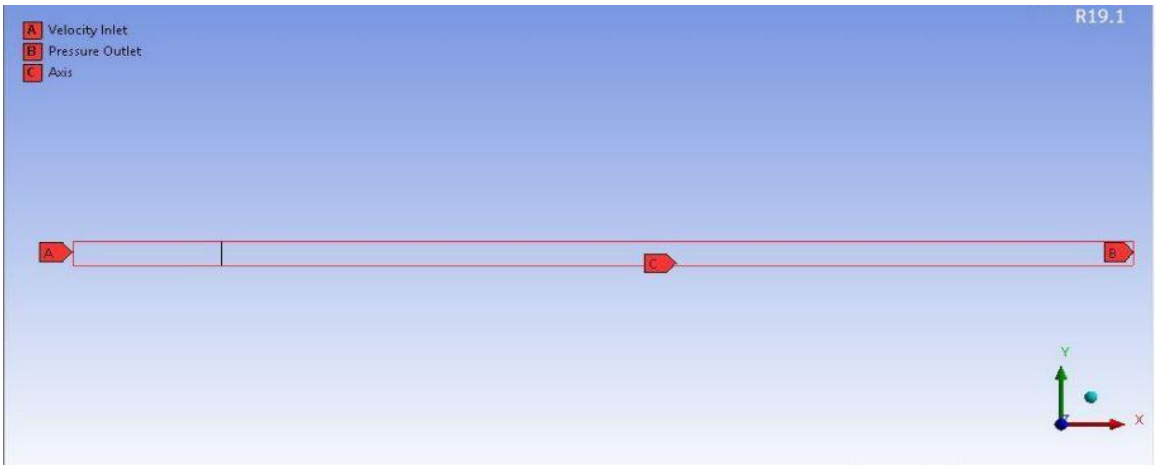


Figure 4-4 The boundary conditions defined in Fluent for model used in 2D

The next step is to define the solution process, but before that the mesh must be checked by ANSYS Fluent, where the domains are defined, and the face area volume statistics are checked, for convergence and for better simulations the minimum volume is required to be a positive number.

## 4.2 Test Cases

To provide proper validation, comparisons are made between 1D premixed flames using CHEMKIN PRO, a PREMIX code and Fluent 2D simulation of premixed flames using the geometry mentioned before in ANSYS Fluent. The current project is broken into 4 testing phases which are listed as following

Table 4-2 Methane and Hydrogen Tested Cases

| Fuel | Oxidizer | $V_{in}$ (m/s) | Equivalence Ratio | Mechanism/Step |
|---|---|---|---|---|
| Methane | Air | 0.2 | 1 | 2,5,10, Gri-3.0 |
| Methane | Air | 0.6 | 1 | 2,5,10, Gri-3.0 |
| Methane | Air | 0.8 | 1 | 2,5,10, Gri-3.0 |
| Methane | Air | 1 | 1 | 2,5,10, Gri-3.0 |
| Methane | Air | 0.8 | 0.6 | 2,5,10, Gri-3.0 |
| Methane | Air | 0.8 | 0.8 | 2,5,10, Gri-3.0 |
| Methane | Air | 0.8 | 1 | 2,5,10, Gri-3.0 |
| Methane | Air | 0.8 | 1.5 | 2,5,10, Gri-3.0 |
| Hydrogen | Air | 0.8 | 1 | 2,5,10, Gri-3.0 |
| Hydrogen | Air | 0.8 | 1.5 | 2,5,10, Gri-3.0 |
| Hydrogen | Air | 0.8 | 2 | 2,5,10, Gri-3.0 |
| Hydrogen | Air | 0.8 | 2.5 | 2,5,10, Gri-3.0 |

The first test cases were tested for methane and hydrogen air at different velocities at stichometry, to understand the effect of inlet velocity on the shape of flame, and if there are any effects on the flame speed. Methane-air was simulated using the 2-5-10 step mechanism then it was compared with the GRI-Mech 3.0 to determine the reliability of the reduced mechanisms used as shown in Table 4.2. Each test case for methane air was tested for fuel lean to rich conditions and the flame speed was determined. The second part of the project was to understand the effect that hydrogen had on methane flame characteristics;

such as flame structure, $NO_x$,$CO_2$ emissions and flame speed. The results were compared side by side by the results obtained from CHEMKIN shown in Table 4.3

Table 4-3 Hydrocarbon dilution with hydrogen tested cases

| Fuel | Oxidizer | $V_{in}$ (m/s) | Equivalence Ratio | Mechanism Step |
|---|---|---|---|---|
| Methane-Hydrogen (0-50% $H_2$) | Air | 0.8 | 0.6 | 5,10 |
| Methane-Hydrogen (0-50% $H_2$) | Air | 0.8 | 0.8 | 5,10 |
| Methane-Hydrogen(0-100% $H_2$) | Air | 0.8 | 1 | 5,10 |
| Methane-Hydrogen(0-50%$H_2$) | Air | 0.8 | 1.5 | 5,10 |
| Methane-Hydrogen(0-50% $H_2$) | Air | 0.8 | 0.6 | 5,10 |
| Propane-$H_2$ (0-30% $H_2$) | Air | 0.8 | 0.6 | 5,10 |
| Propane-$H_2$ (0-30% $H_2$) | Air | 0.8 | 0.8 | 5,10 |
| Propane-$H_2$ (0-30% $H_2$) | Air | 0.8 | 1 | 5,10 |

Once the results were within an acceptable range of accuracy, the 10-step and 5-step mechanisms were used for the next phase of the project, which included testing syngas. Syngas simulations using the GRI-Mech 3.0 became time consuming and tedious, so there was a need for using reduced mechanisms to save time. While using the 5 step mechanism tests were done on syngas composing of 50% CO 50% $H_2$ and %5 $H_2$ and 95% CO to determine their flame speed and understand the effects of preheat temperature on fuel mixtures and flame speeds.

Table 4-4 Tested Conditions for syngas at different composition and equi-ratios

| Fuel | Oxidizer | Vin (m/s) | Equivalence Ratio | Mechanism Step |
|---|---|---|---|---|
| $H_2$-CO (50/50) | Air | 0.8 | 0.6 | 5,10 |
| $H_2$-CO (50/50) | Air | 0.8 | 0.8 | 5,10 |
| $H_2$-CO (50/50) | Air | 0.8 | 1 | 5,10 |
| $H_2$-CO (50/50) | Air | 0.8 | 1.5 | 5,10 |
| $H_2$-CO (5/95) | Air | 0.8 | 0.6 | 5,10 |
| $H_2$-CO (5/95) | Air | 0.8 | 0.8 | 5,10 |
| $H_2$-CO (5/95) | Air | 0.8 | 1 | 5,10 |
| $H_2$-CO (5/95) | Air | 0.8 | 1.5 | 5 |

The final phase of the project included; testing 2 modifications of syngas which were the Blast Furnace (BFG) Gas and Coke Oven Gas (COG) shown in Table 4.4.

Table 4-5 Tested Conditions for BFG and COG.

| Fuel | Oxidizer | Vin (m/s) | Equivalence Ratio | Mechanism Step |
|---|---|---|---|---|
| COG (298,598,898) K | Air | 0.8 | 0.6 | 5 |
| COG (298,598,898) K | Air | 0.8 | 0.8 | 5 |
| COG (298,598,898) K | Air | 0.8 | 1 | 5 |
| COG (298,598,898) K | Air | 0.8 | 1.5 | 5 |
| BFG (298,598,898)K | Air | 0.8 | 0.6 | 5 |
| BFG (298,598,898)K | Air | 0.8 | 0.8 | 5 |
| BFG (298,598,898)K | Air | 0.8 | 1 | 5 |
| BFG (298,598,898)K | Air | 0.8 | 1.5 | 5 |

Only the 5-step mechanism was used, because it contained the important reactions steps for BFG and COG to obtain proper flame structures and flame speed that is tested at 3 different preheat temperatures 298 K 598 K and 898 K. All the tested fuels were simulated

in fuel lean and fuel rich conditions. Detailed explanation for each case will be given throughout Chapter 4

## 4.3 Methane-Air and Methane-Hydrogen Air 1D-2D Detailed Study

To simulate the cases for this project, 2 models are used and they include; the premixed combustion model and transport model. The premixed model was used to compute the adiabatic flame temperature, while transport model was used to simulate the changes in temperature, velocity, emissions and fuel components

### 4.3.1 Premixed Model/Transport solution set up and Adiabatic Temperature

To calculate the adiabatic temperature using the premixed model, several steps are required to be taken before running simulation. When the model is set on premixed combustion, the energy equation needs to be set off because the assumption of adiabatic setting in Fluent and application of a spark inside the tube. The use of premixed model is very limited, because the user must specify methane- air properties such as the flame speed, viscosity, unburnt temperatures and thermal diffusivity. The properties have been extracted from GASEQ [23] which is a software used to determine chemical equilibrium and adiabatic flame temperatures. for different equivalence ratios from 0.6 to1.5 an example of property input is shown in Figure 4.5

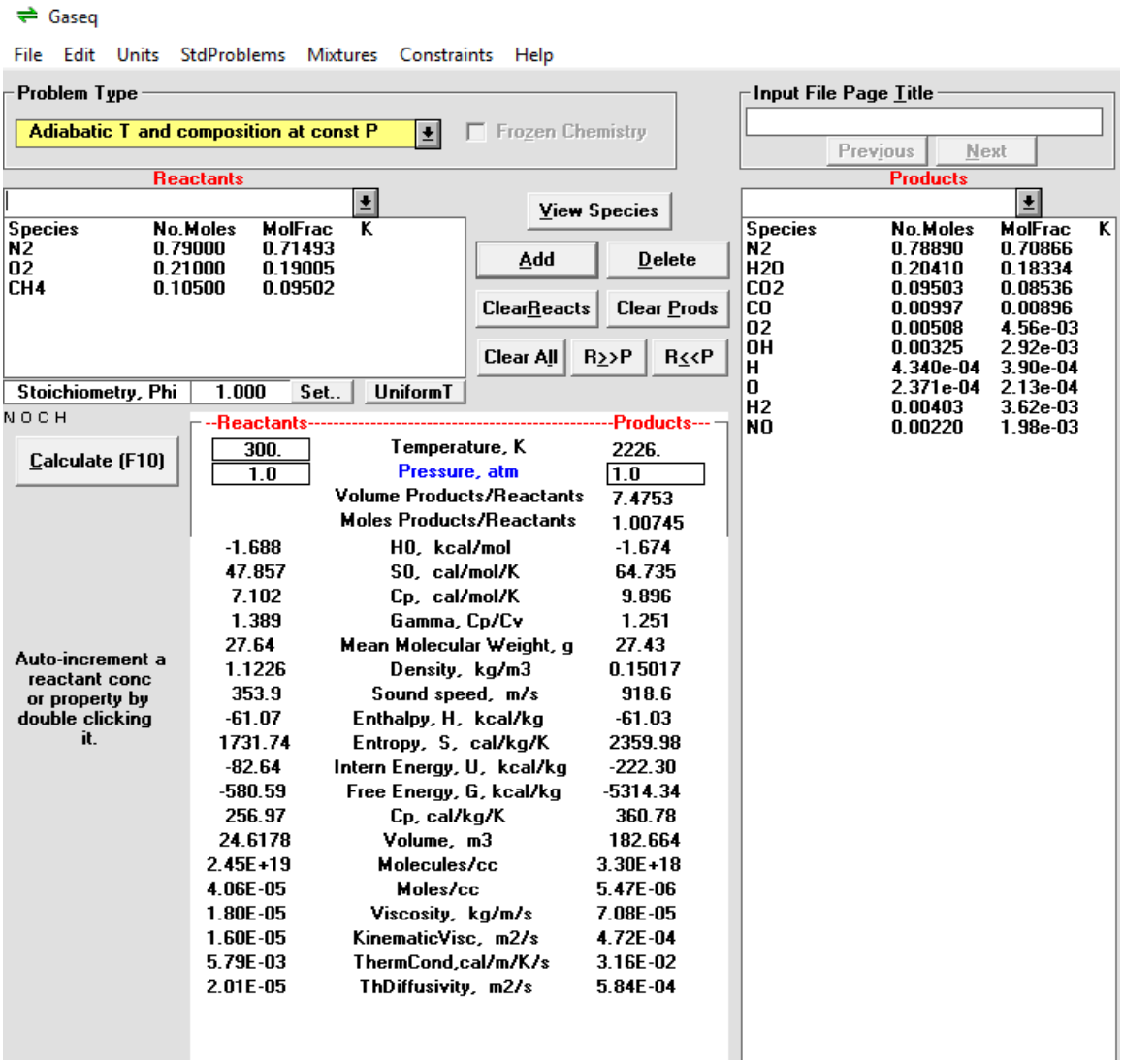


Figure 4-5 A sample calculations of equilibrium properties for methane obtained through GASEQ

After the properties are set up, the next step is to define inlet velocity of fuel mixture which is 0.8 m/s in this study. In the premixed model the simulation, is run in a steady-state condition, to ensure that the domain is full of fuel mixture, requiring about 1000-2000 iterations. Once the tube is full, the premixed model it is switched to transient, to be able to define a spark inside of the mixture. In this study the spark is defined at the location of 1 mm from the x-axis and radius of 1.5mm with the duration of 0.003 s and an energy of 0.006 j. Since the combustion process occurs quickly the time step is set to 0.001s to visualize the flame. The solution method configuration for Premixed Model is shown in Table 4.6.

Table 4-6 Solution setting for the premixed model

| Solution Method | Pressure-Velocity Coupling |
|---|---|
| Scheme | SIMPLE |
| Gradient | Least Square Cell Based |
| Pressure | Second Order |
| Momentum | Second Order Upwind |
| Turbulent Kinetic Energy | Second Order Upwind |
| Turbulent Dissipation Rate | Second Order Upwind |
| Progress Variable | Second Order Upwind |

SIMPLE scheme is one of the four segregated algorithms provided by Fluent. for steady-state calculations SIMPLE scheme is often used, while PISO is used for transient problems containing laminar flows, to obtain convergence that is limited by velocity coupling. SIMPLE advantages appear in the ability of the scheme to converge solutions very quickly. Schemes are usually changed depending on the complexity of the problem. The Least Square Cell Based is a solution method, in which the cell gradient is determined by solving a problem relating to minimizations. To obtain a solution for a problem that has a non-square matrix, the least square through multiplication of weight factors cell gradients is used. The second order upwind setting is used, for the conservation equations to increase the accuracy, where the solutions are determined through solving multidimensional linear reconstruction to compute values at each cell to receive high accuracy [49]

Once a simulation is converged, the result of the adiabatic flame temperature can be viewed through the contour graph and plotted in Excel through the data points shown in Figure 4.6

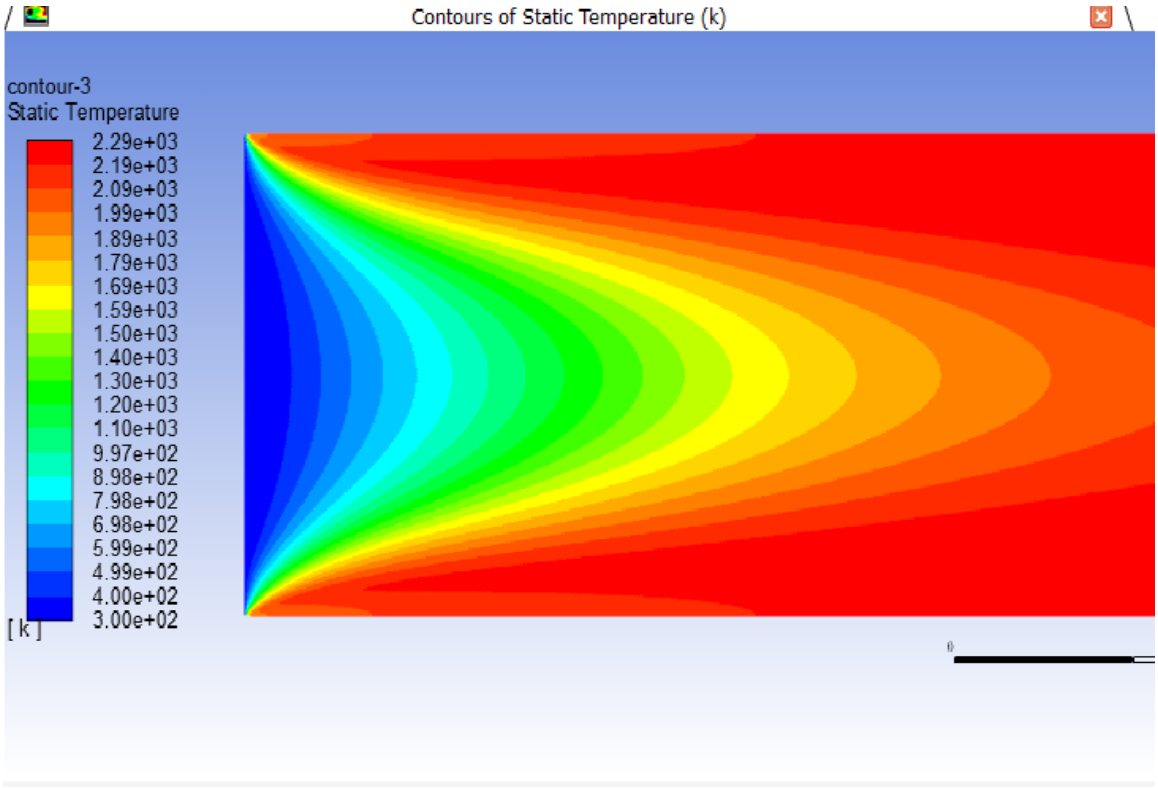


Figure 4-6 Adiabatic flame temperature contour using Premixed Model

The adiabatic flame temperature calculated through the premixed model is about 2290 K, with the assumption made, that the wall is assumed to adiabatic in the premixed model case, so the heat of combustion is contained in domain and carried all the way to the outlet. The difference of adiabatic flame temperature using premixed model is within 2% error of the GASEQ adiabatic temperature of methane combustion of 2230 K. A comparison can be made between the premixed model and transport and the results are shown in Figure 4.7

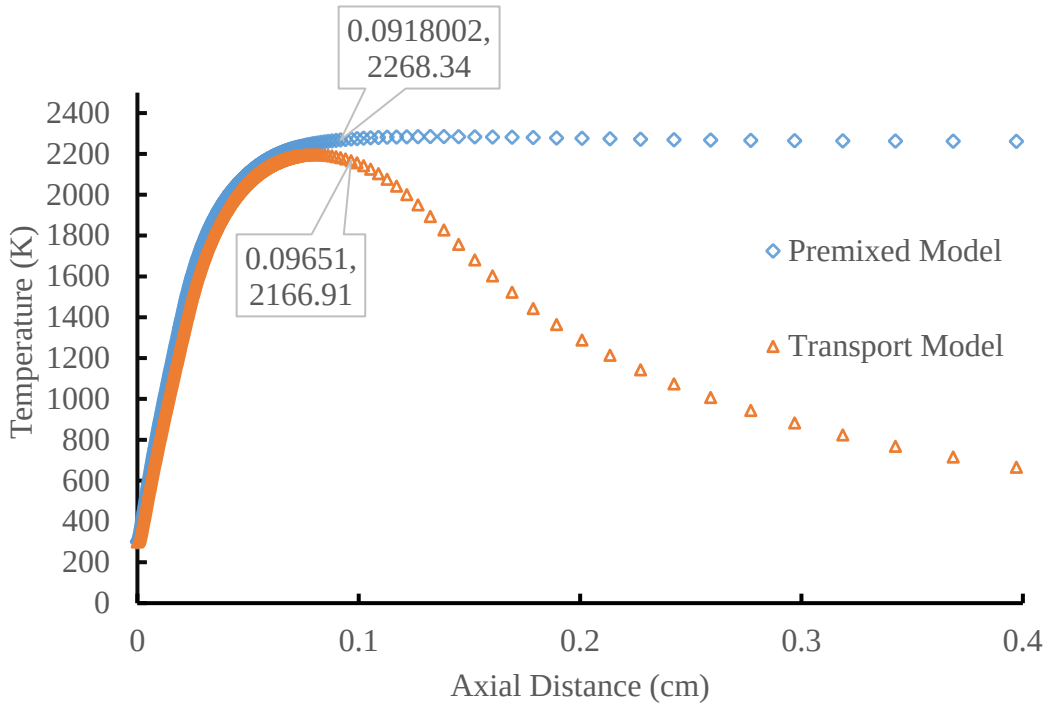


Figure 4-7 Represents the temperature with premixed and transport model

It is clear in Figure 4.7. The premixed model provided better accuracy in determining the adiabatic flame temperature of the combustion. The transport model has about 3% error. The premixed model has disadvantages such as; the need to specify all fuel characteristics including flame speed, which is the main property studied in this project. for that reason, this model will only be used to compute the adiabatic flame temperature while the transport model will be used to model and calculate all the flame properties. The comparison of the calculated adiabatic flame temperature between the GASEQ adiabatic flame temperature calculation and Fluent simulations is shown in Figure 4.8

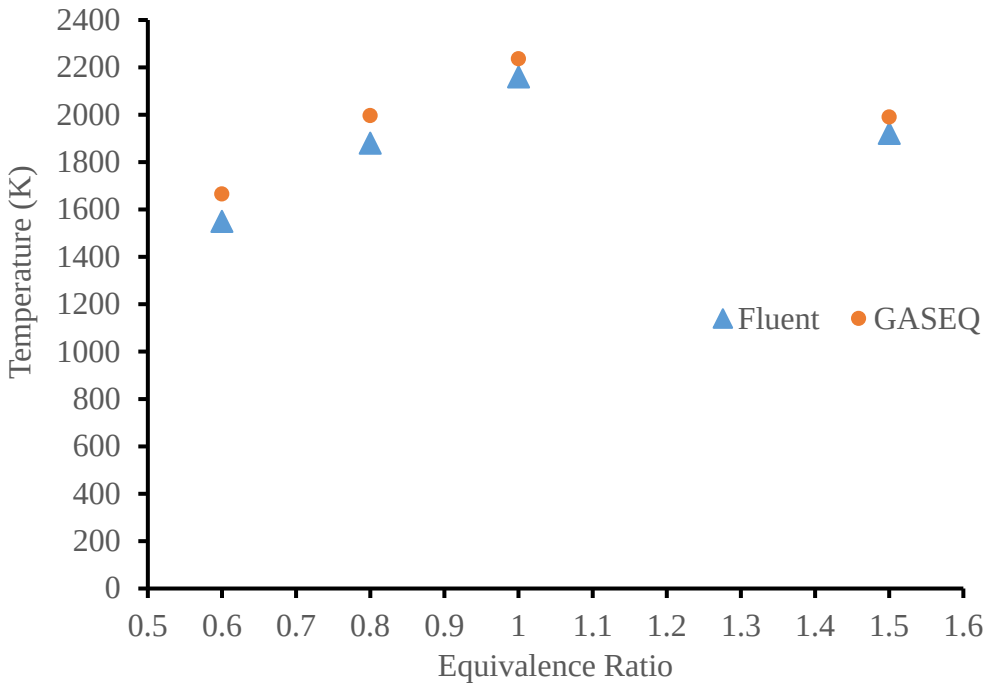


Figure 4-8 Represents adiabatic temperature with Fluent and GASEQ.

The adiabatic flame temperature for methane-air combustion is within 3-7% error of the values calculated through GASEQ at the equivalence ratios of 0.6 to1.5 which is within the acceptable range that could be used as the first step to validate the model.

### 4.3.2 Determinations of the Flame Speed of Methane with the Transport Model

It is experimentally difficult to produce laminar velocity of a premixed fuel that has a defined velocity inlet, for an undisturbed flame without including the heat loss that always occurs in experiments and buoyancy effects during work in space shuttles. However, in numerical simulations it is possible to obtain constant flame speed with certain conditions of initial pressure and temperature. The solution procedure is very similar when the transport model is used; however, the user must specify the mole or mass fraction of the reactants, to determine results. Furthermore, there is no spark that needs to be activated to force combustion so the energy equation in this model is activated. Furthermore, the properties will be determined throughout the combustion, and there is no need to initially specific the flame speed or properties prior to the combustion. If a new fluid is being introduced into the reaction, then the user must specify the properties of the fluid/material.

The combustion occurs via the balance of chemical reactions and concentrations. The solution method through Fluent is summarized in Table 4.7

Table 4-7 Solution methods used for the transport model

| Solution Method | Pressure-Velocity Coupling |
|---|---|
| Scheme | Coupled |
| Gradient | Least Square Cell Based |
| Pressure | Second Order |
| Momentum | Second Order Upwind |
| Energy | Second Order Upwind |
| Turbulent Kinetic Energy | Second Order Upwind |
| Turbulent Dissipation Rate | Second Order Upwind |
| Fuel Components | Second Order Upwind |
| Pseudo Transient | |

The solution method in the transport mode differs in the scheme used, which applies the coupled scheme that is used in the present study to increase the CFD solver robustness. The method relies on the solving the conservation equations of momentum, species mass and energy for the coupled system of fluid dynamics. The transport model includes the energy equations and all the fuel components which are determined through second order upwind algorithms. The finite volume method is used to discretize the model. The momentum equations are solved and then followed by the continuity equation. The pressure and mass flowrate are updated for each point until convergence is achieved for all residuals at 0.001 except for energy equations at $10^{-6}$

Upon completing a test case with the transport model, it is possible to view the changes in temperature, reactants and products throughout the domain before and after the combustion

takes place an example of methane air at equivalence ratio, temperature, velocity magnitude and mass fraction contours for $CO_2$ are shown in Figure 4.9-4.11

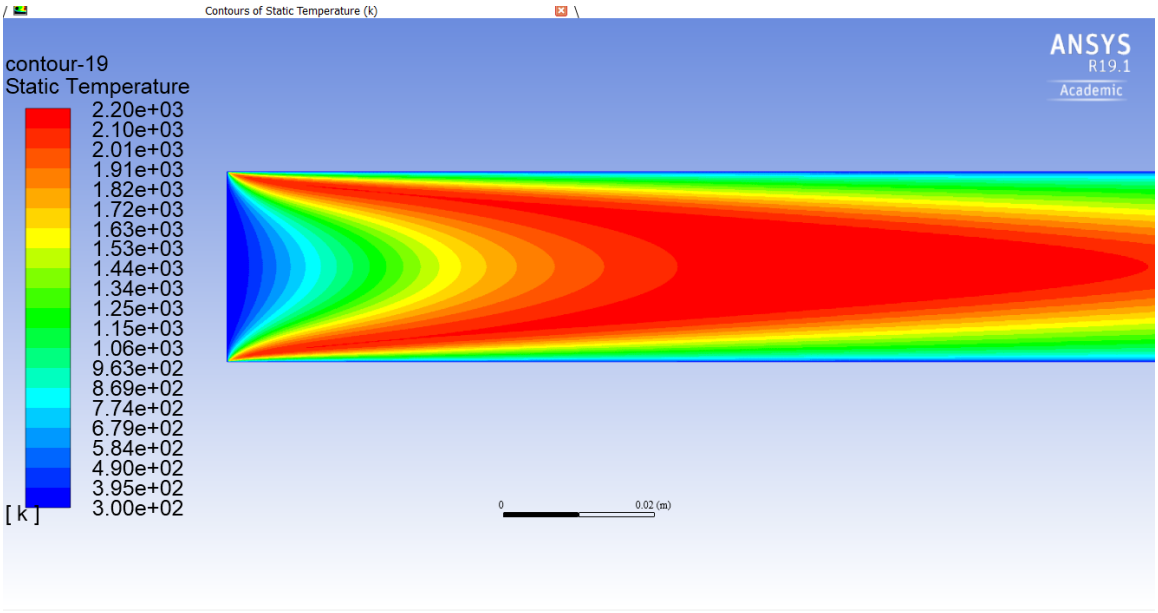


Figure 4-9 Temperature contour for premixed combustion at stoichiometry

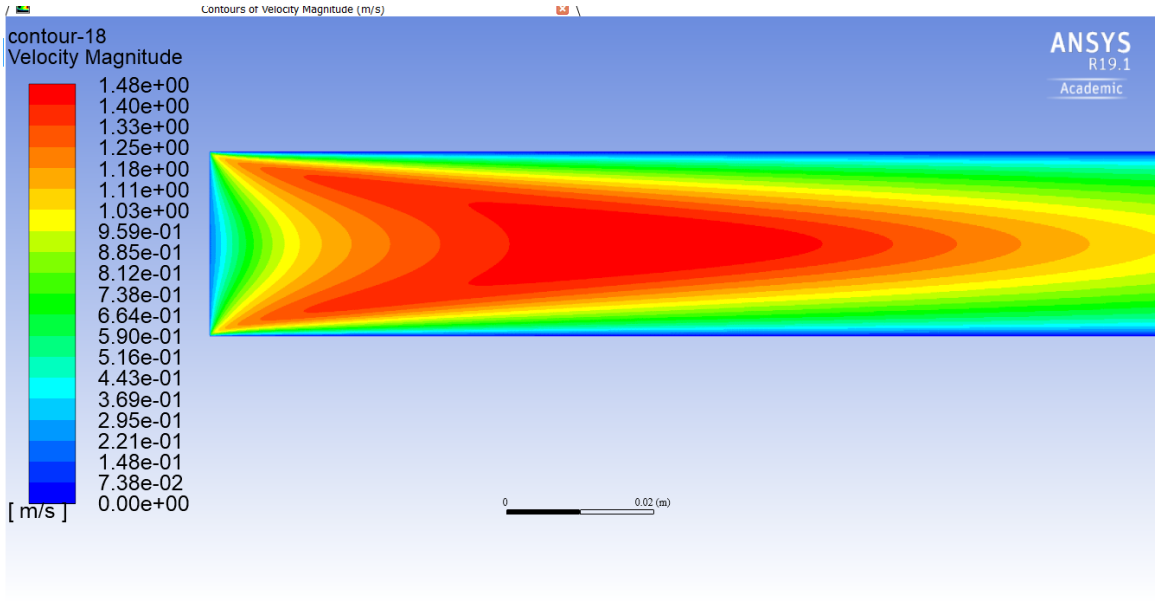


Figure 4-10 Velocity magnitude of the flow during the combustion

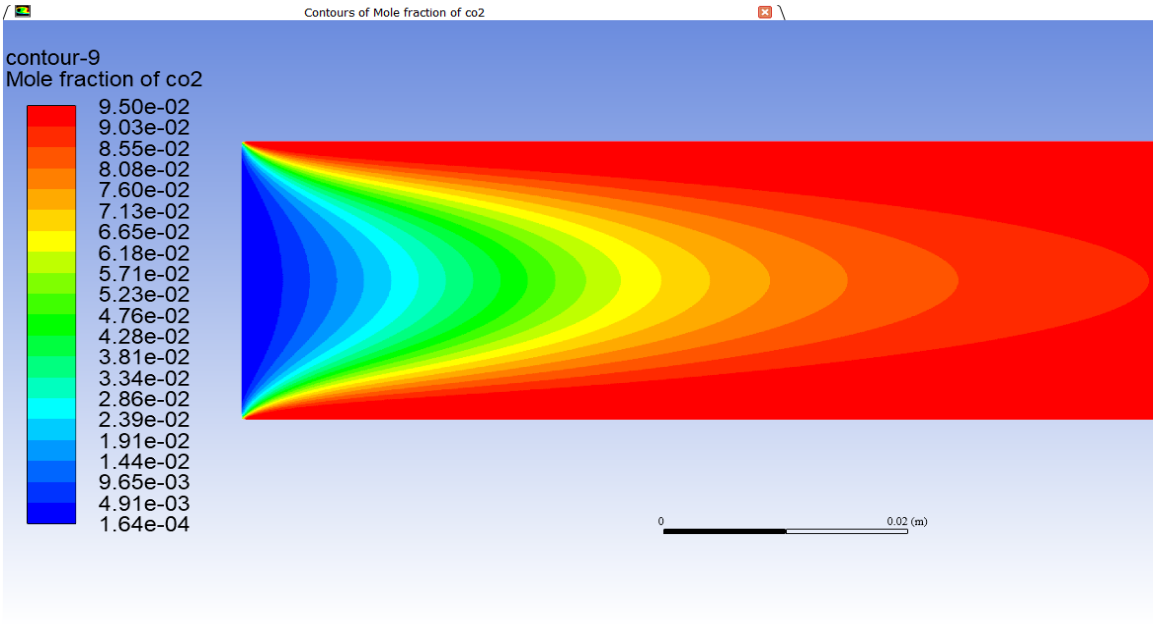


Figure 4-11 Contour representing the conversion of CO into $CO_2$

It is important to know that the wall is not the adiabatic in the case of using the transport model, instead it is at ambient temperature and atmospheric pressure. During the combustion process, temperature reaches a peak value then is reduced towards the outlet, to be able to determine velocity, according to the work done by Langan [54] the major heat release occurs during the conversion of CO to $CO_2$. The consumption of CO occurs at the same location, where the heat of the release, and reaction rate start rapidly decrease, thus, representing the end of the flame wave. Furthermore, the area where the temperature increases is the location of deflagration wave where the flames is in conic shape as shown in Figure 4.12. To determine the surface area of the flame, it is important to define the boundaries of the flame. The beginning of the flame wave occurs at the first spot, where reactant decay occurs. This can be determined by the mass fraction of methane contour. Upon closer examination of the stream lines of the flame front between those regions, it can be noticed that the stream lines are in an axial direction in the domain, until they cross a surface usually where the H radicals are formed, then the direction becomes normal to flame front. The middle of the surface between both boundaries is determined to be the surface area of the flame

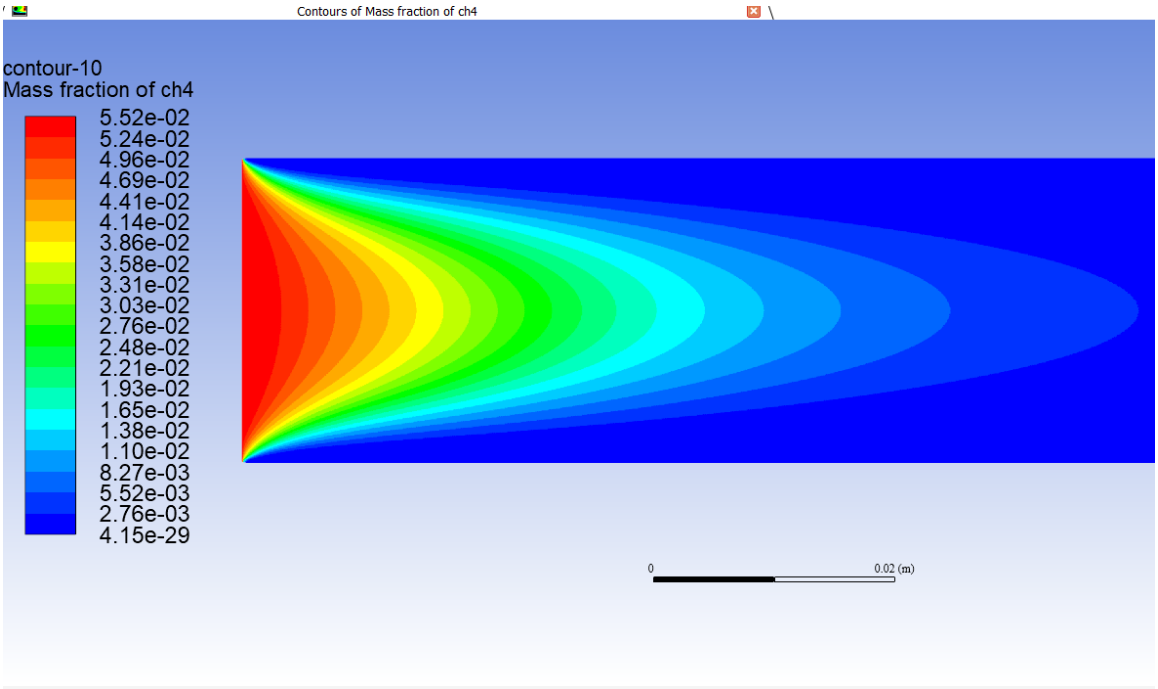


Figure 4-12 The mass fraction of Methane representing fuel decay.

By extracting the data points for the boundaries of the flame front and plotting them in Excel, the classification of the zones is as follows; the beginning of the flame was the fuel decay, the middle is completion of mass fraction the fuel species and end zone was the full completion of CO converting into $CO_2$,shown as following in Figure 4.13

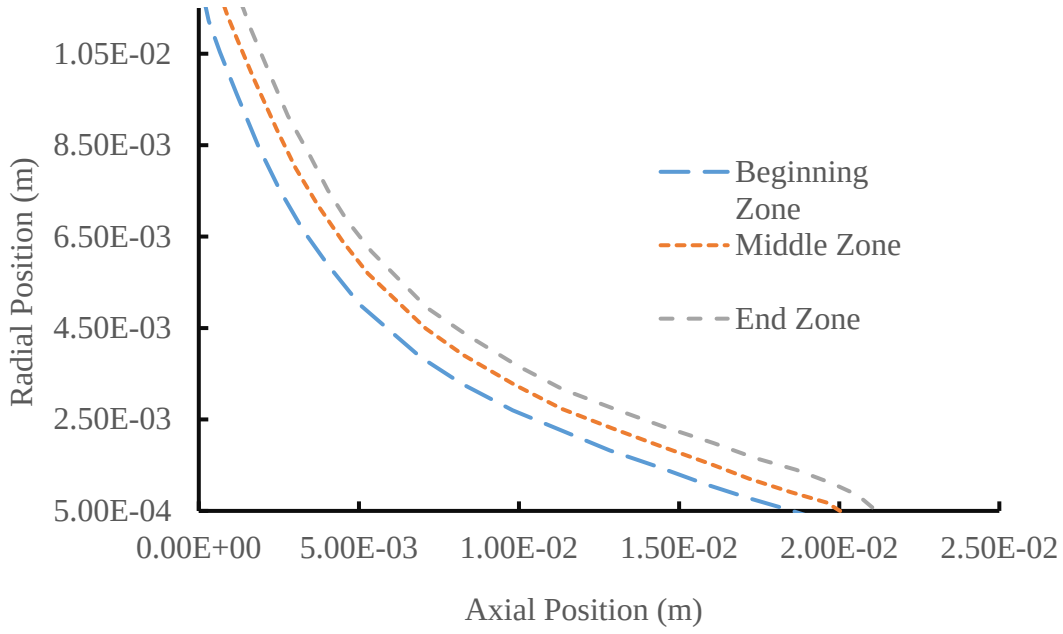


Figure 4-13 Represents the boundaries of the flame where the middle zone is where surface area is calculated

For stoichiometric methane air reaction, the flame thickness could be calculated by plotting the 3 flame areas shown in Figure 4.13. Due to symmetry only half of the domain was plotted. By using piece-wise polynomial integration the surface area could be calculated which is then plugged in equation 2.10 to determine the total flame surface area which was $571.3mm^2$ in the present study which was used to determine the flame speed to be ~ 0.36 m/s.

The experimental value of methane-air flame speed at stochiometric ratio is 0.38 m/s [22] which is within 5% of error of the actual value. Second method to determine the burning velocity, is by using the area method however, the error with using this method is usually 15%-20%. If a temperature contour for methane was created using Fluent it is possible to select specific parts temperatures in the contour, then measure the distances to apply the area method to determine flame speed of the wave as shown in Figure 4.14

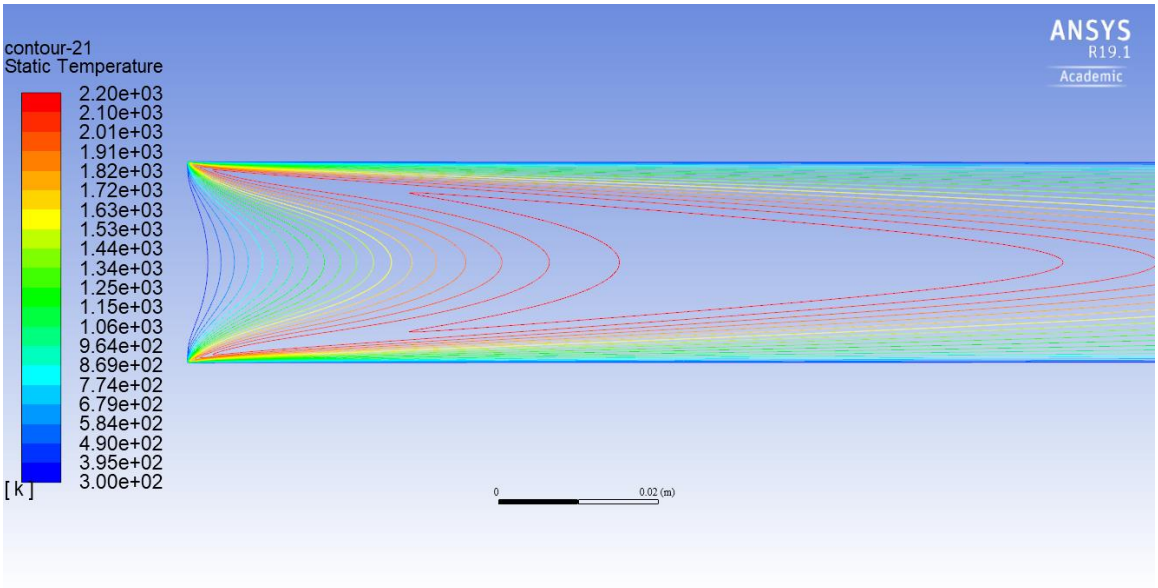


Figure 4-14 Temperature contour of methane to determine surface area of flame.

### 4.3.3 Effect of Fuel Inlet Velocity on The Flame Shape and Speed

By changing the inlet velocity of methane mixture, the peak flame temperature on the axis of the domain shifts to downstream direction and the flame becomes longer. This results in small increases of the flame temperature when the inlet velocity is increased from 0.2 to 0.8 m/s. Further increasing in inlet velocity changes the flame length, but doesn't increase flame temperature anymore, instead temperature remains constant and is independent of the inlet velocity. This occurs partially due to weak convective heat transfer from flame to the wall. As the inlet velocity increases, the total amount of energy in the fuel increases, while the heat loss is increased, resulting in the peak flame temperature to be slight increased. The only observed phenomena by inlet velocity increase is the flame prolong because the flame front needs to be adjusted at the one point on the flame segment where its flow velocity equals the local flame speed, providing anchoring of the entire flame.

However, if the inlet velocity is further increased the mixture flow becomes turbulent and the flame is unstable and wrinkled. Further increasing inlet velocity will cause the flow velocity to be higher than the flame speed at all flame front and the flame blow off occurs. The comparison of flame shapes at different inlet velocities is shown in Figure 4.15

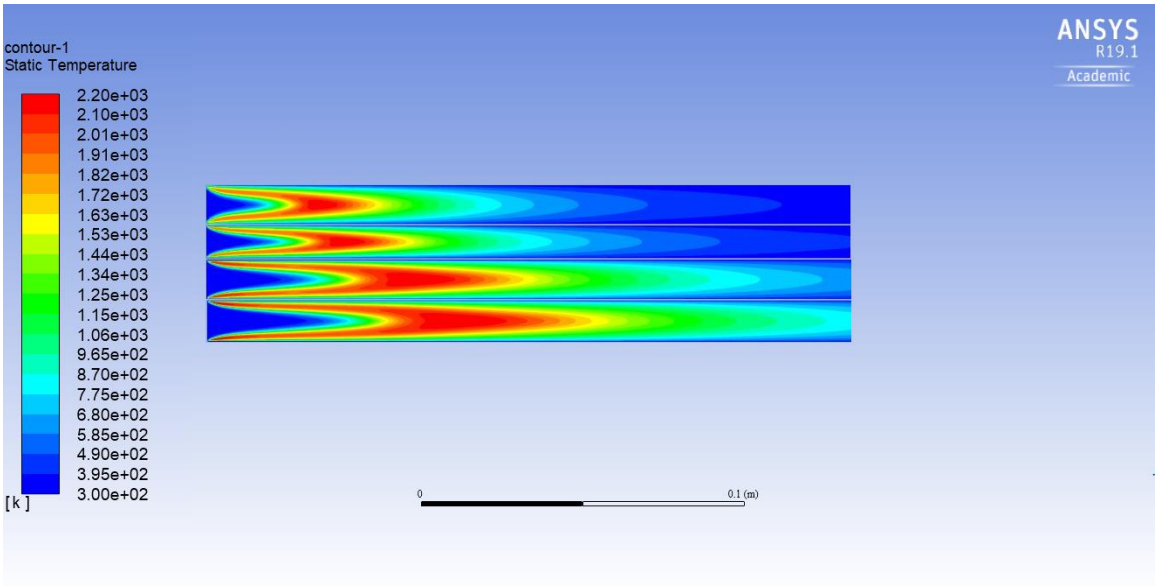


Figure 4-15 Effect of inlet velocity on flame shape through elongating the flame

In figure 4.16 the plots of flame shapes as the inlet velocity changes. The flame becomes thicker along the axis than near the wall due to higher velocities at the axis which elongate the flames. A closer look of flame elongation could represent by plotting only half symmetry of the flows shown in Figure 4.16

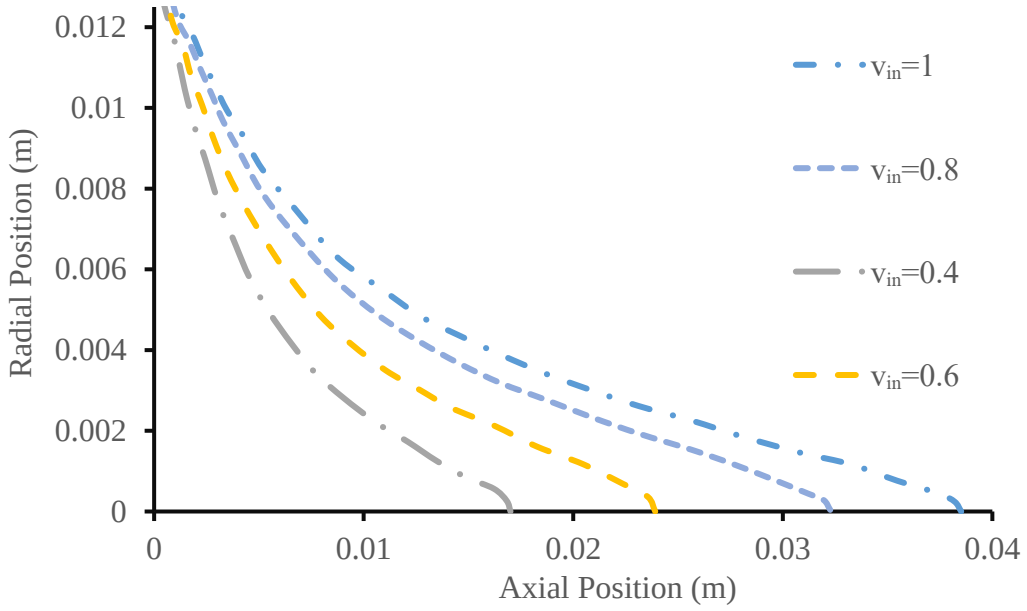


Figure 4-16 Half symmetry of flame wave shape at different fuel inlet velocities.

By computing the surface area of the flames at different fuel inlet velocity, the flame speeds were determined. It was found that the flame speed remains unchanged at ~ 0.36 m/s for methane-air mixture at stoichiometric ratio same as presented in Glassman and Yetter [1, 22, 54]. This is because the flame speed is a fuel property related to its activation energy and is independent to the operational conditions including the flame speed.

### 4.3.4 Reduced Mechanism Comparison

In Chapter 3 two reduced mechanism discussed by Belcaidi and Nikolau [55, 56, 64], that were used in simulations of this project. To save computational time, not only half of the volume was considered due to symmetry, but also the use of reduced mechanisms was implemented. Their usage was found to yield reasonable results based upon the governing equations and assumptions, that were used to obtain them. Given a detailed reaction mechanism such as GRI-3.0, it is possible to produce mechanisms with fewer species, less linear algebra calculations and accurate results. GRI-3.0 with its 325 reactions and 53 species has been an accurate numerical tool that is used to describe methane and $NO_x$ reactions [54]. However, for complex mixtures each simulation becomes tedious due to having all the reactions steps that the solver must calculate. The 10-step mechanism was used in this project for simulating, methane-air, methane-hydrogen and syngas reaction for the cases of fuel lean to fuel rich equivalence ratios. The determined flame speed using this mechanism was within 10% error at different conditions, upon comparison with GRI-3.0 mech, there was a good agreement on flame speed for different fuel mixtures. The agreement is also seen to be good for major and minor species when comparing the flame structures.

Due to the complexity of combustion requirements for BFG and COG gas a 5-step mechanism was used to predict the results within an acceptable range. Based on their testing ,and experimental work there was a good agreement, on the major species concentrations, heat release rates, and flame speeds were presented, between experiments conducted by Li et al. and their simulations using GRI-Mech 3.0 at different conditions of different initial temperature, pressure and fuel compositions[1, 64, 67] a comparison is made for methane air reaction using 2 step, 5 step, 10 step and GRI-3.0 Mech shown below in Figure 4.17

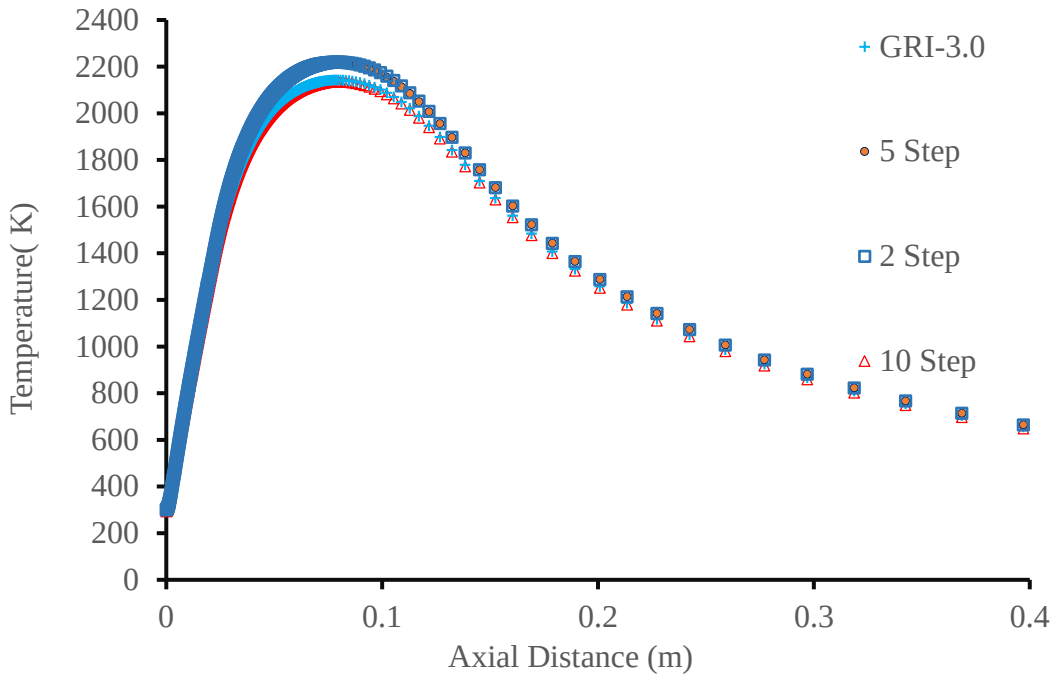


Figure 4-17 Comparison of different reduced mechanism and GRI-3.0 for stoichiometric methane-air.

It can be seen that using 4 different mechanisms the peak temperature of stoichiometric methane-air combustion is similar. However, results by using 10-step mechanism and GRI-3.0 mechanism are close to each other with only 15 K difference. Using 2 step and 5 steps produces higher adiabatic flame temperatures. The reason for high temperature may be due to combustion completement. It is well known that one-step overall reaction generates the highest adiabatic flame temperature because all hydrocarbon fuel is converted to $CO_2$ and $H_2O$which have the highest heat of formation as compared with other hydrocarbons and radicals. With reduced such as 2 or 5 steps mechanism, less unburned hydrocarbons are present in the system, leading to the higher temperature than these using 10 steps or GRI-3.0 full mechanisms. In the simulation below when the $NO_x$ formation is required to be implemented the 10-step mechanism will selected. In others, the 5-step mechanism will be used.

## 4.4 1D-2D Simulations for Flame Speed of Hydrogen-Enriched Fuels by CHEMKIN and Fluent.

### 4.4.1 CHEMKIN and PREMIX 1D Simulations

During the simulations there is a need to visualize the flame structure and verify the results obtained with Fluent within an acceptable accuracy. The results will be simulated using a chemical kinetics software CHEMKIN-PRO that performs a detailed 1D simulation with PREMIX code and GRI-3.0 Mechanism. CHEMKIN-PRO contains a set of different models that can determine the flame structures, and laminar flame speed for 1D propagating flame [1, 32, 33, 68]. The GRI-3.0 has been validated for all hydrocarbon fuels at ambient pressure, but discrepancies occur between simulations and experimental results at high pressure [44, 45, 69-72]

The numerical analysis for the given problem was carried out by PREMIX which simulates steady-state laminar 1D flames. The method applied in this code depends on the time integrating and Newtonian iteration method to solve the conservation of energy, mass and species. The method used to solve 1D problem is defined as TWOPNT, included in the CHEMKIN-Pro which is a boundary layer problem solver, that specifies the temperature for a single point, then the GRI-Mech 3.0 is used to over write the original CHEMKIN reactions and transport properties into the mechanism file to be interpreted by CHEMKIN interpreter [73]. The structure of the program can be summarized as following; the input file is supplied by the user, where the input file contains the species, and chemical reactions which are processed through a library that contains all thermodynamic properties. The properties are stored in linking file that will be used as an input for the transport property program which estimates the polynomial solution of temperature dependent, species and other properties through PREMIX. The CHEMKIN and Transport libraries are called to specify the reaction and species properties to set up the calculations that will be read, through PREMIX as an input file to provide the iterations. That will compute the final solution. The final solution will come out as output file that could be exported or re-used again for new simulations [33]

Note that, there are uncertainties in parameterizing the combustion model, usually happening due to Input propagating input uncertainties through models. The uncertainties lead to discrepancies in the prediction of combustion properties. To set up PREMIX, the

input file was modified by setting the curvature to 0.2 and 0.7 for grid control, the calculation domain was set from 0 to 4 cm to maintain adiabatic equilibrium. The mass flowrate is set to $0.04 g/cm^2$ at initial temperature of 298k and 1 atm for pressure.

It is possible to obtain the major and minor species mole fraction, and plot them to obtain the flame structure, a simple simulation is shown in Figure 4.18 to show the radical formation for case of stoichiometric methane

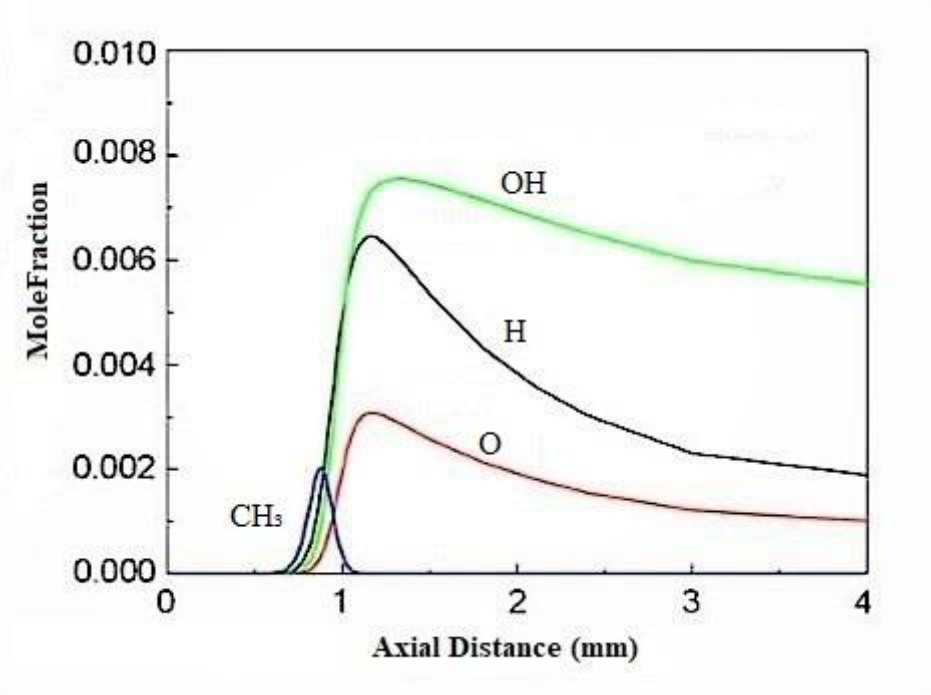


Figure 4-18 Methane air flame structure showing minor species.

In Figure 4-18 the minor species and radicals for methane air combustion are shown where the comparison will vary based upon the composition of the fuel, for each cases the radicals will calculated and compared using Fluent.

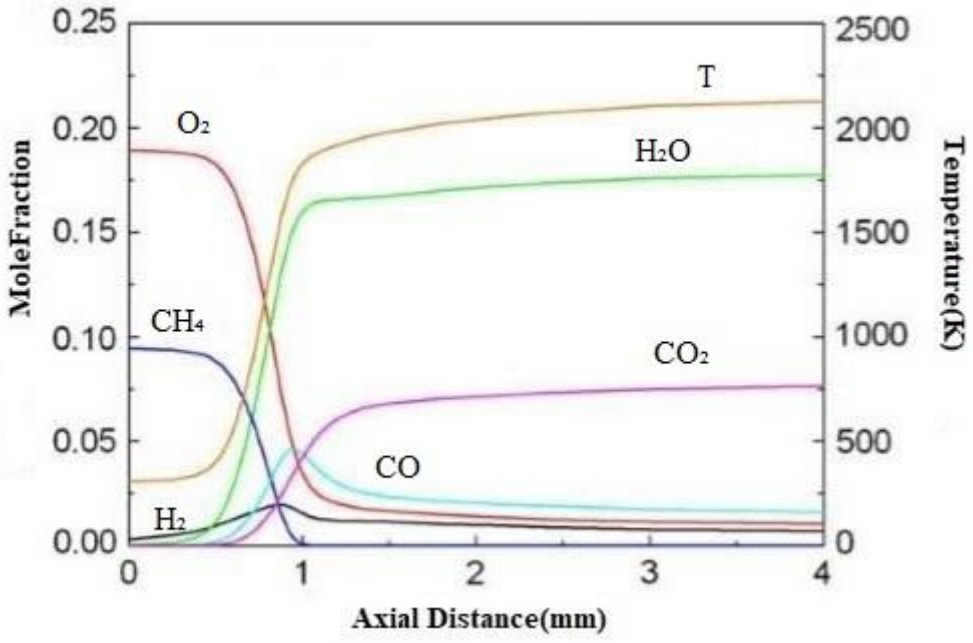


Figure 4-19 Methane air flame structure containing major species, radicals and adiabatic temperature.

The reaction fuel decomposition starts to form radicals and intermediates species, where they play an important role in sustaining and accelerating the combustion processes. It can be seen in Figure 4.19, in the thin reaction zone, the mole fractions of $CH_4$ and $O_2$ rapidly decrease due to chemical reaction and convert to the combustion products, and heat is suddenly released, leading the temperature to be quickly increased.

It is realized from Figure. 4.18 and 4.19 the concentrations of methane and oxygen are suddenly decreased at 1 mm downstream where at the exact location radicals and intermediate species are generated and reach relatively high concentrations. hydrogen molecules diffuse upstream where there is initially no $H_2$presence. This is because hydrogen is a light molecule and it tends to diffuse to upstream region. On the other hand, CO is first generated in the reaction zone, and then reacts with $O_2$ to form $CO_2$. At the downstream the concentrations of radicals and intermediate molecules are reduce and remain at low concentrations.

To understand and study methane-hydrogen blending it is important to know the chemical formula of hydrogen-air and methane-air reactions can be expresses as,

$$H_2 + 0.5(O_2 + 3.76N_2) \rightarrow +H_2O + \frac{3.76}{2}N_2 \tag{4.1}$$

$$CH_4 + 2(O_2 + 3.76N_2) \rightarrow +CO_2 + 2H_2O + 3.76(2)N_2 \tag{4.2}$$

When methane and hydrogen are mixed general chemical formula can be written as,

$$\begin{aligned}(1-\gamma)C_xH_y + \gamma H_2 + \left[(1-\gamma)\left(x+\frac{y}{4}\right)+\frac{1}{2}\gamma\right](O_2 + 3.76N_2) \\ \rightarrow (1-\gamma)xCO_2 + [(1-\gamma)\left(\frac{y}{2}\right)+\gamma]H_2O \\ + 3.76[(1-\gamma)\left(x+\frac{y}{4}\right)+0.5\gamma]N_2\end{aligned} \tag{4.3}$$

where γ represents the mole fraction of hydrogen in hydrogen-methane mixtures defined as

$$\gamma = \frac{X_{H_2}}{X_{CH_4} + X_{H_2}} \tag{4.4}$$

By applying the previous equation, it is possible to determine the different composition for the reactants as shown in Table 4.8 where determination of each input is required in to provide the values of mole fractions for each fuel component

Table 4-8 Shows the mole fractions at 0-40% hydrogen content in methane.

| $H_2$ volume | $CH_4$ Fraction | $H_2$ Fraction | $O_2$ Fraction | $N_2$ Fraction |
|---|---|---|---|---|
| 0 | 0.095 | 0 | 0.19 | 0.715 |
| 0.1 | 0.0918 | 0.0102 | 0.1887 | 0.7093 |
| 0.2 | 0.088 | 0.022 | 0.187 | 0.703 |
| 0.3 | 0.0838 | 0.0358 | 0.185 | 0.6956 |
| 0.4 | 0.078 | 0.052 | 0.183 | 0.6870 |

The current project simulates hydrogen methane blends from 0 to 100% for fuel lean-rich.

The flame structure of methane-hydrogen at 0% is shown in Figure 4.20

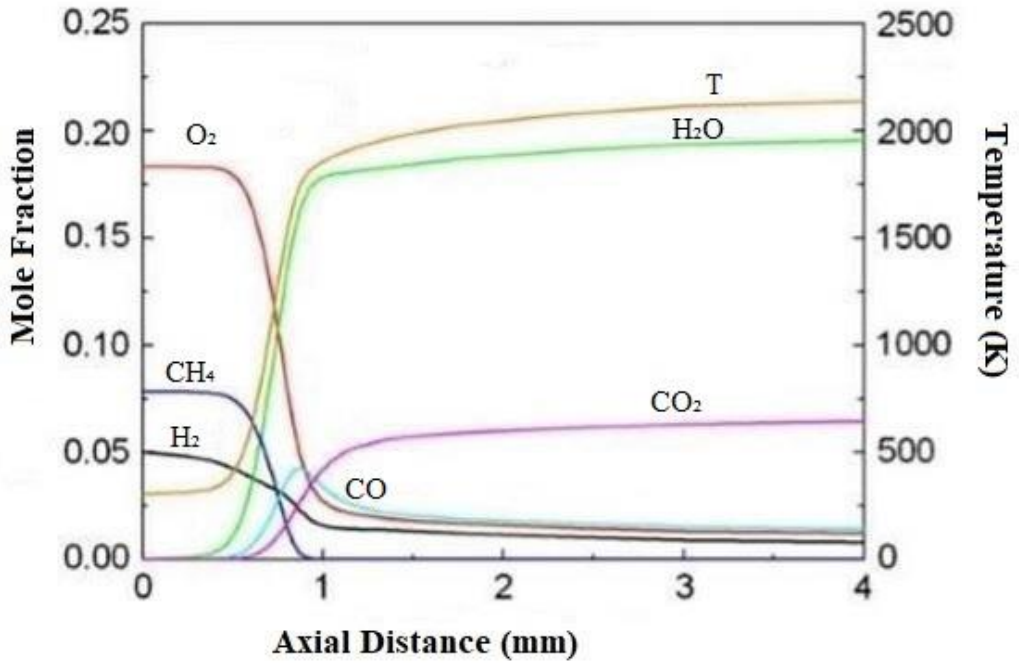


Figure 4-20 Represents flame structure for 40% hydrogen-methane blend

When fully enriching methane with hydrogen the result is shown in Figure 4.21

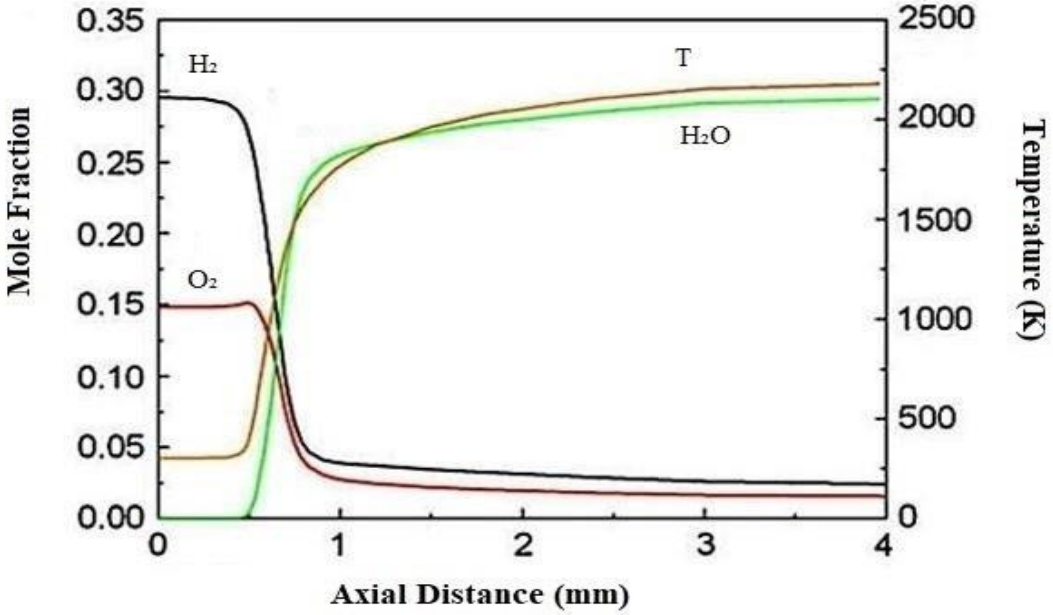


Figure 4-21 Represent flame structure for 100% hydrogen-methane blend

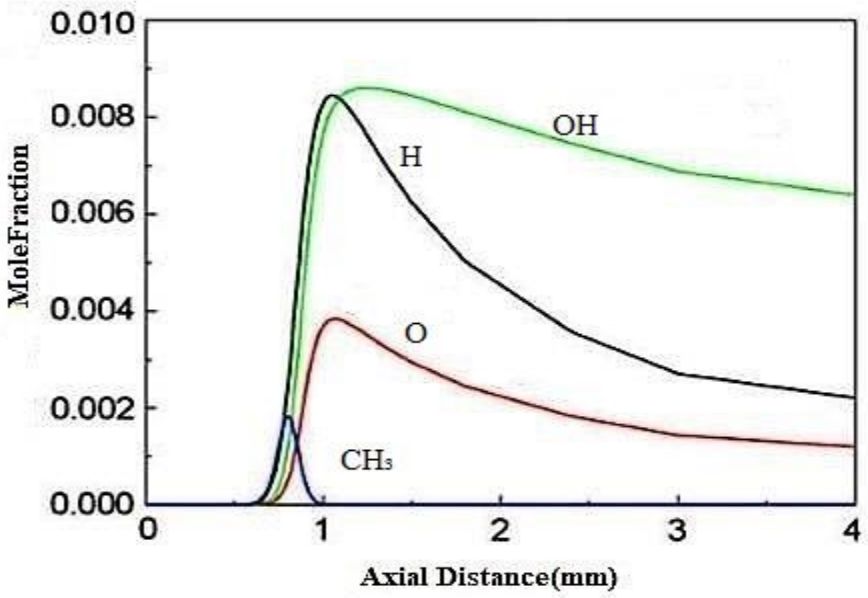


Figure 4-22 Represents the radical formation at 40% hydrogen dilution

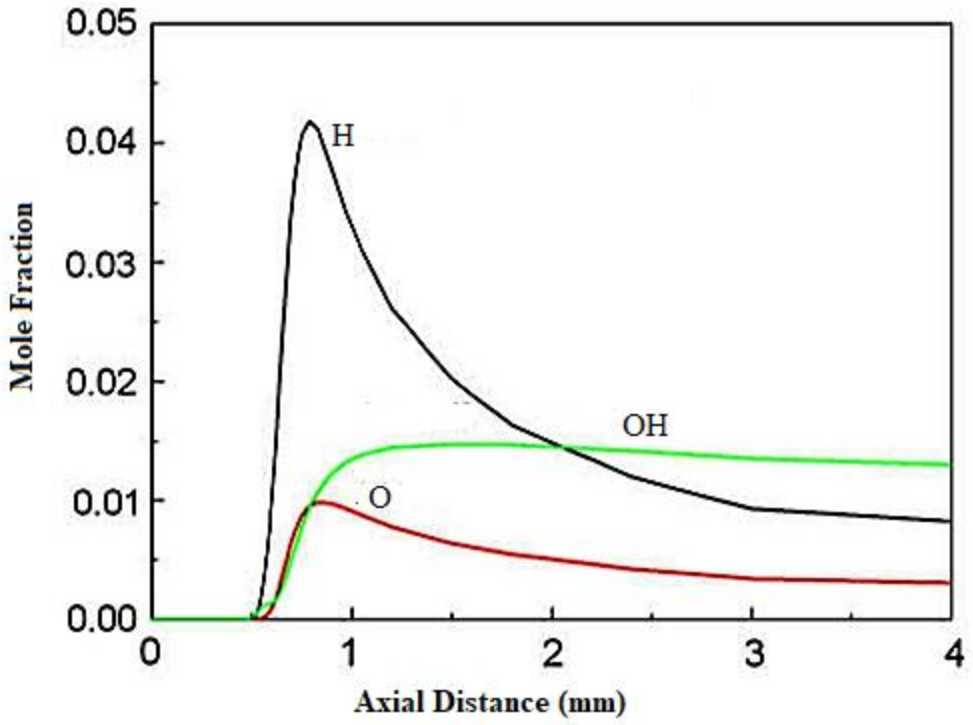


Figure 4-23 Represents the radical formation at 100% hydrogen dilution

To determine the flame speed in CHEMKIN an approximation method is used as in the equation below.

$$S_l = A(T^o)(Y_{f,u}^m)\frac{T_u}{T^o}\left(\frac{T_b - T^o}{T_b - T_u}\right)^n \tag{4.5}$$

where $T^o$ is the layer temperature, $Y_{f,u}^m$ is the mass fraction of unburned fuel, and $T_b$and $T_u$ represent burned and unburned temperatures. For the hydrogen blends, the flame speed can be written as the function of individual flame speed of each fuel in the mixture.

$$S_l = (\varphi, \gamma) = \gamma . S_{L_{h_2}}(\varphi) + (1 - \gamma) . S_{L_{CH_4}}(\varphi) \tag{4.6}$$

Where $S_{L_{h_2}}$ and $S_{L_{CH_4}}$ are the flame speeds for methane and hydrogen in cm/s that are calculated for certain equivalence ratio φ. the flame speed for methane, hydrogen, and hydrogen methane-hydrogen blends are shown in Figure 4.24 and 4.25

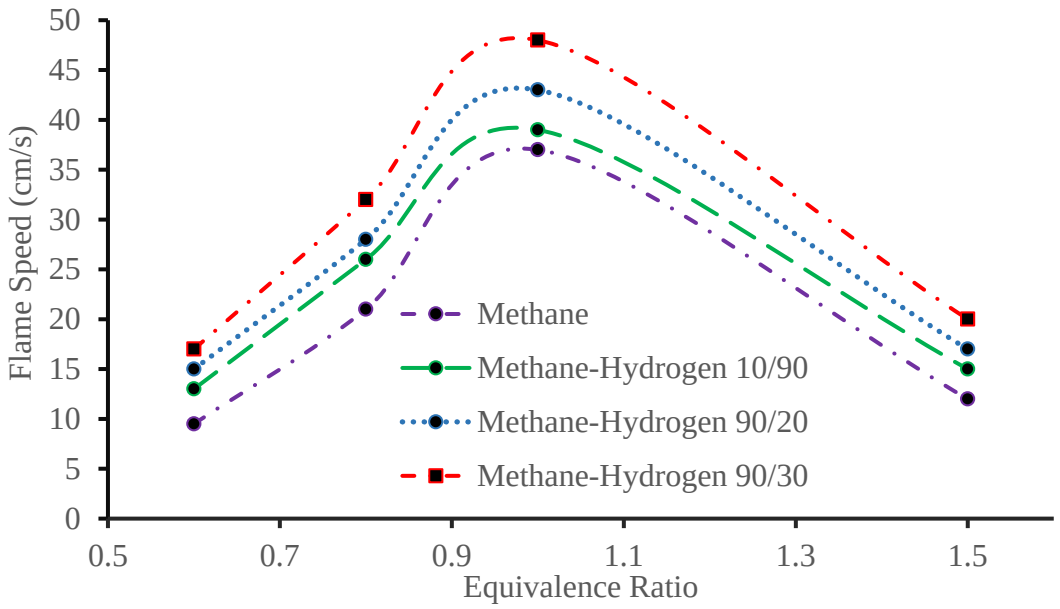


Figure 4-24 Flame speed for lean-rich methane-hydrogen 0-30%

It can be noticed from Figure 4.24 as hydrogen is added into methane the flame speed increasing with more hydrogen dilution.

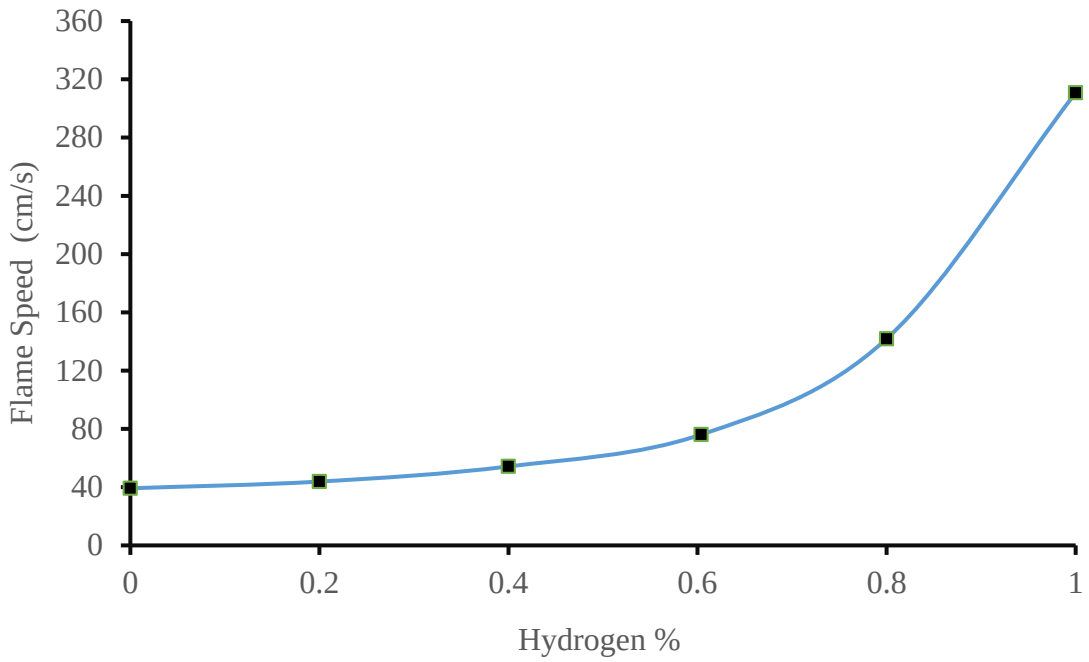


Figure 4-25 The flame speed measured at hydrogen blending from 0% to 100% in methane-air at stoichiometry

The addition of hydrogen to methane enhances the combustion and increases the flame speed. The increases of the flame speed are small, only a few percentages until hydrogen content increases to 70%, and after that it quickly increases because the fuel becomes fully enriched with hydrogen. The non-linear relation of flame speed of $CH_4$-$H_2$ mixture with the $H_2$ content affects the kinetics., At lean conditions hydrogen addition enhances the chemical reaction rate because the $H_2$ molecule is more reactive than methane. The results obtained through PREMIX and CHEMKIN can be used as the method to justify simulation in Fluent model.

### 4.4.2 Methane-Hydrogen Enrichment Fluent Results

In the Fluent simulation it requires to input mole fractions of each species. A prepared formula will make the input much easier for the simulations.

for stichometry $\phi$=1

$$(1-m-n)CH_4 + mH_2 + nCO + [2-1.5(m+n)](O_2 + 3.76N_2) \rightarrow$$
$$(1\text{-}m)\,CO_2 + (2-m-2n)H_2O + 3.76[2-1.5(m+n)N_2 \quad (4.7)$$

When $\phi$<1

$$\phi(xCH_4 + mH_2 + nCO) + y(O_2 + 3.76N_2) \rightarrow aCO_2 + bH_2O + cO_2 + 3.76yN_2 \quad (4.8)$$

When $\phi$>1

$$\phi(xCH_4 + mH_2 + nCO) + y(O_2 + 3.76N_2) \rightarrow aCO_2 + bH_2O + cO_2 + dCO + 3.76yN_2 \quad (4.9)$$

where m and n are the mole fraction for hydrogen and carbon monoxide.

By establishing a balance of atoms in the species, the unknow species coefficients can be expressed as,

$$x = 1 - m - n \quad (4.10)$$

$$y = 2 - 1.5(m + n)$$

$$a = \phi(1 - m)$$

$$b = \phi(2 - m - 2n)$$

$$c = (1 - \phi)[2 - 1.5(m + n)]$$

In the case of fuel-rich condition, the values of a,b,c are not determined, because the number of species coefficient exceeds the number equations. They depend on the chemical equilibrium at adiabatic flame temperature which will be found using GASEQ. The following Table 4.9 summarizes the mole fraction value for each component at equivalence ratios of 0.6, 0.8 and 1

Table 4-9 Mole Fraction of each component of methane-hydrogen combustion

| Equivalence Ratio | Hydrogen Fraction | Methane | Hydrogen | Oxygen | Nitrogen |
|---|---|---|---|---|---|
| 0.6 | 0.0 | 0.0593 | 0.0 | 0.1976 | 0.7431 |
| 0.6 | 0.1 | 0.0574 | 0.0064 | 0.1967 | 0.7395 |
| 0.6 | 0.2 | 0.0552 | 0.0138 | 0.1956 | 0.7354 |
| 0.6 | 0.3 | 0.0526 | 0.0226 | 0.1943 | 0.7305 |
| 0.8 | 0.0 | 0.0775 | 0.0 | 0.1938 | 0.7287 |
| 0.8 | 0.1 | 0.075 | 0.0083 | 0.1926 | 0.7241 |
| 0.8 | 0.2 | 0.072 | 0.018 | 0.1912 | 0.718 |
| 0.8 | 0.3 | 0.0685 | 0.0293 | 0.01895 | 0.7126 |
| 1 | 0.0 | 0.0951 | 0.0 | 0.1901 | 0.7148 |
| 1 | 0.1 | 0.0918 | 0.0102 | 0.1887 | 0.7094 |
| 1 | 0.2 | 0.088 | 0.022 | 0.1870 | 0.703 |
| 1 | 0.3 | 0.0836 | 0.0358 | 0.1850 | 0.6956 |

Figure 4.26 displays the adiabatic temperature of methane-air at stoichiometry with 0% hydrogen added, as a function of distance from the inlet for methane-air at equivalence ratios from lean to rich fuel conditions using Fluent.

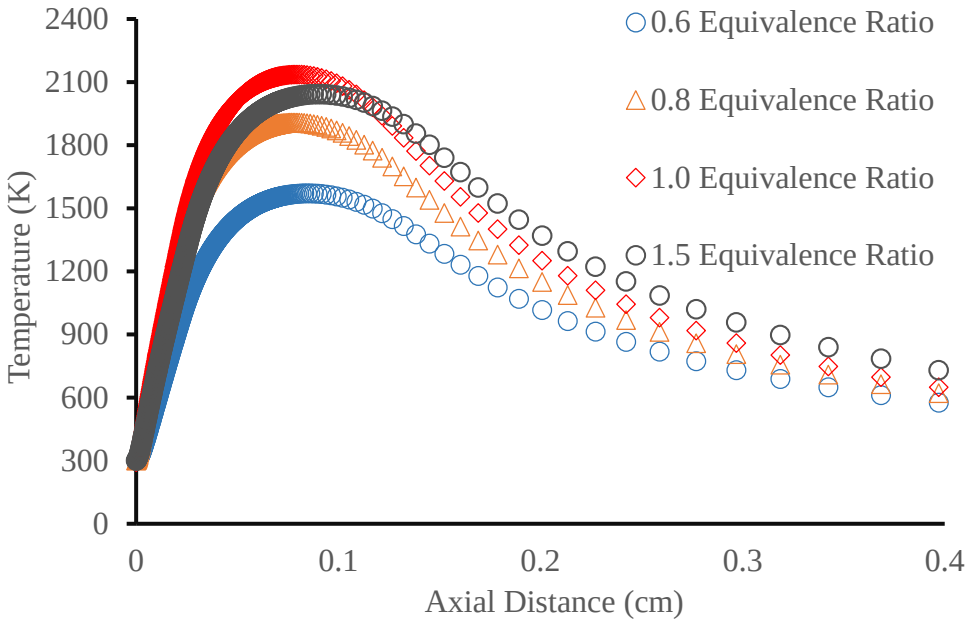


Figure 4-26 Temperature contour for lean-rich methane air combustion

Upon comparing the flame speed at different equivalence ratios between Experimental [74] work done by, 1D and 2D simulations shown in Figure 4.27, it is important in terms of making sure the work done between 1D , 2D and experimental are within an acceptable range of accuracy.

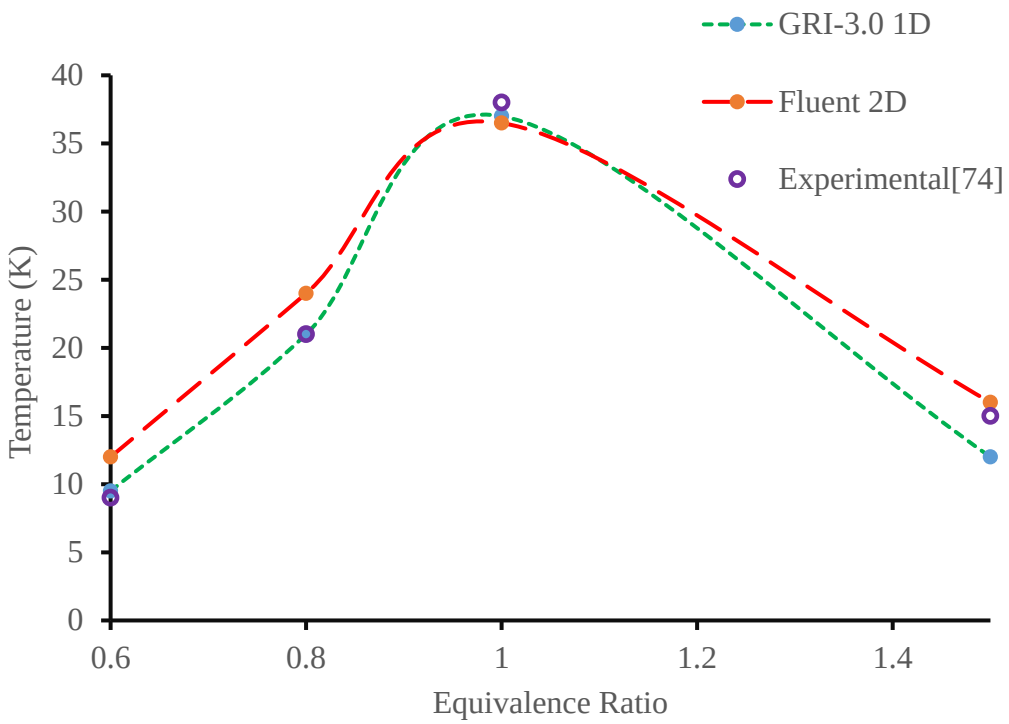


Figure 4-27 Flame speed for 1D-2D and experimental work comparison[74]

Figure 4.27 shows the calculated flame speeds of methane-air combustion using 1D CHEMKIN PREMIX code with GRI-3.0 mechanism and 2D model in Fluent and compared with the experimental results conducted by Hermanns et al [74] ]. In the Fluent simulation the flame speed was obtained using the surface area method. . Results from Fluent provide a slight overestimation, about 5% error, but it is still within an acceptable accuracy. Figure 4.28 displays the calculated flame speeds for different $CH_4$-ratios and plotted as the function equivalent ratio using Fluent simulations

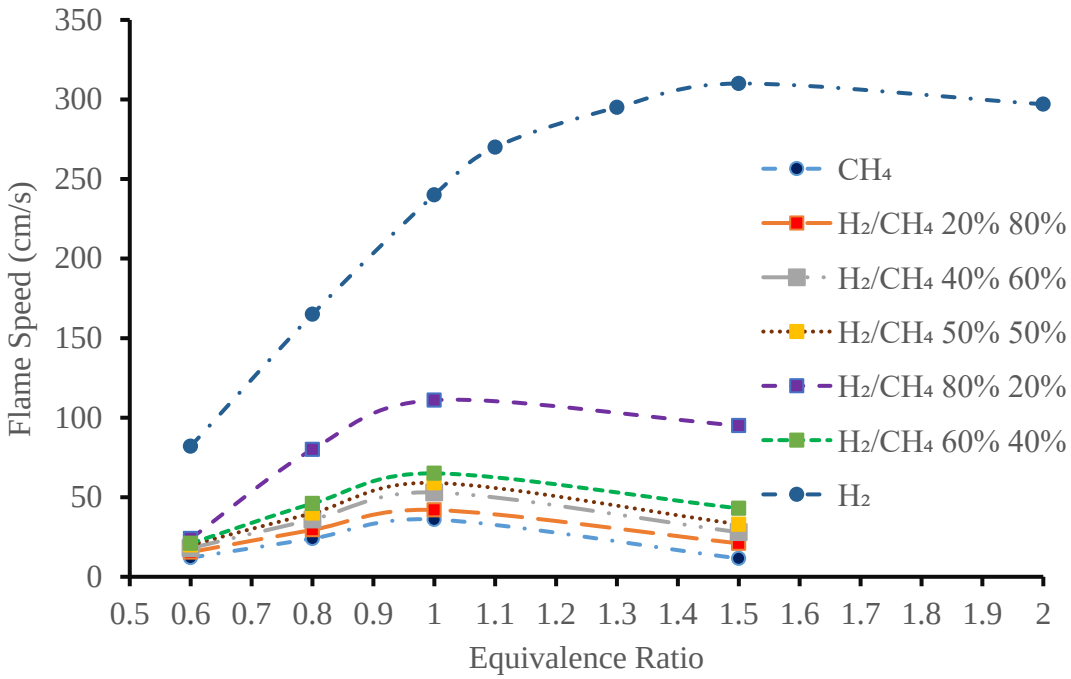


Figure 4-28 Flame speed of $H_2$-$CH_4$ air mixture at ambient conditions

It can be seen in Figure 4.28 the peak flame speed for pure $CH_4$-air combustion flame is about 40 cm/s, and peaks on the rich side around 1.05. With the $H_2$ content in the $CH_4$-$H_2$ mixture is increased, the flame speeds continuously increase. However, their flame speeds still peak at the rich side around 1.05, following the trend of pure methane, even for the high $H_2$ concentration, for example 20 % $CH_4$ – 80 % $H_2$. The above correspondence is sufficiently offset for the $H_2$-air flame, for which the flame speed peaks at about 1.75 as shown in Figure 4.26. This sufficiently offset to rich peaking is a consequence of high diffusivity of $H_2$ molecules. The Lewis number for lean and rich $H_2$-air mixtures are far from unity (0.33 and 2.3). The effect of Lewis number reduces the flame speed on the lean side but increases the flame speed in rich side. As a result, the peak flame speed shifts to the far rich side. It also indicates that there is a slight increase of flame speed with 10-60% hydrogen content. However, when hydrogen content reaches 70%, the flame speed increases more quick as shown in Sarli et al. work [46]. This can be explained by presenting the flame structure shown in Figure 4.29

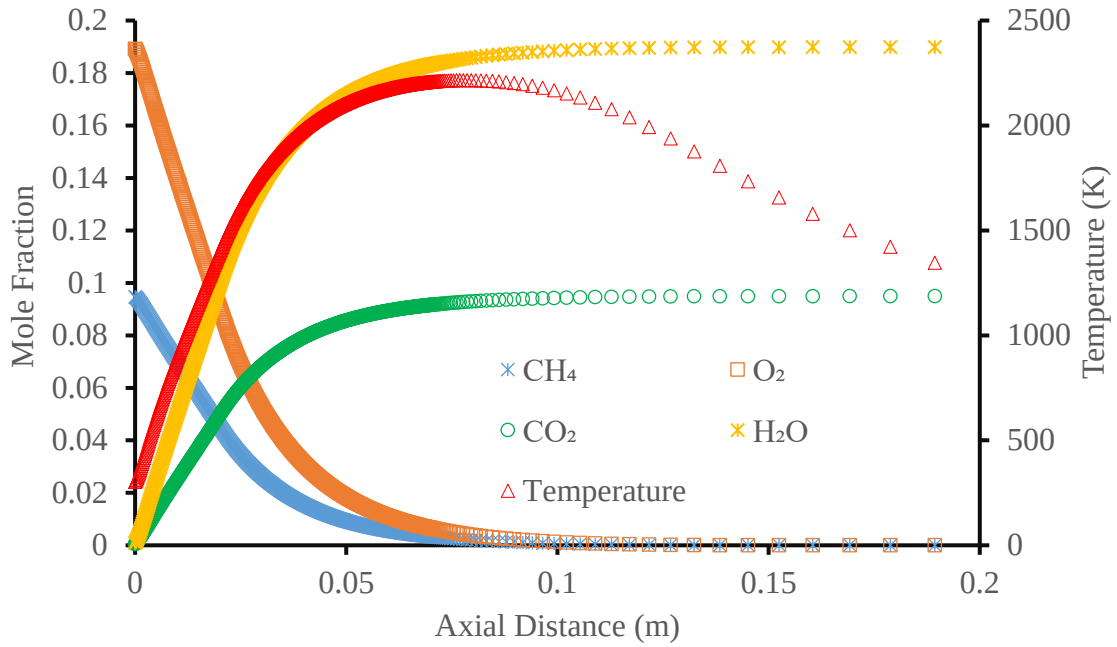


Figure 4-29 Methane-air flame structure obtained through fluent

Intermediate species and radicals play an important role in the hydrocarbon reactions because they are highly reactive. They participate in the sequence of reactions and serve as the chain carriers. Chain reactions can further classify into straight chain and branched-chain reactions. Branched reactions will lead to chemical explosion which is not studied in this project. The straight chain reaction sustains the reactions. Below several reaction steps discuss the H and OH radicals in a simple $H_2$ reactions. The reactions (R1) – (R4) are the major elementary reactions, In which H and OH radicals are created. In reaction (R1), a radical is consumed, and another radical is created know as chain propagation. In (R2) and (R3) one radical is consumed but more than one radical is generated; it is called chain-branching reaction. (R4) is the chain termination in which two H radicals combine to convert to a molecule.

(R1) $H_2 + OH \Leftrightarrow H_2O + H$

(R2) $O_2 + H \Leftrightarrow OH + O$

(R3) $O + H_2 \Leftrightarrow OH + H$

(R4) $H + H + M \Leftrightarrow M + H_2$

The results obtained with Fluent correspond to these with 1D PREMIX code which can further confirm the model used in the project.

With the hydrogen addition the $H_2$ concentration increases so that the forward reaction rate in (R1) is increased that promotes more H and OH radical formation which can be shown in Figures 4.30 and 4.31. This is essential because the flame speed is controlled by the diffusion of radicals and transport processes specially in premixed flames.

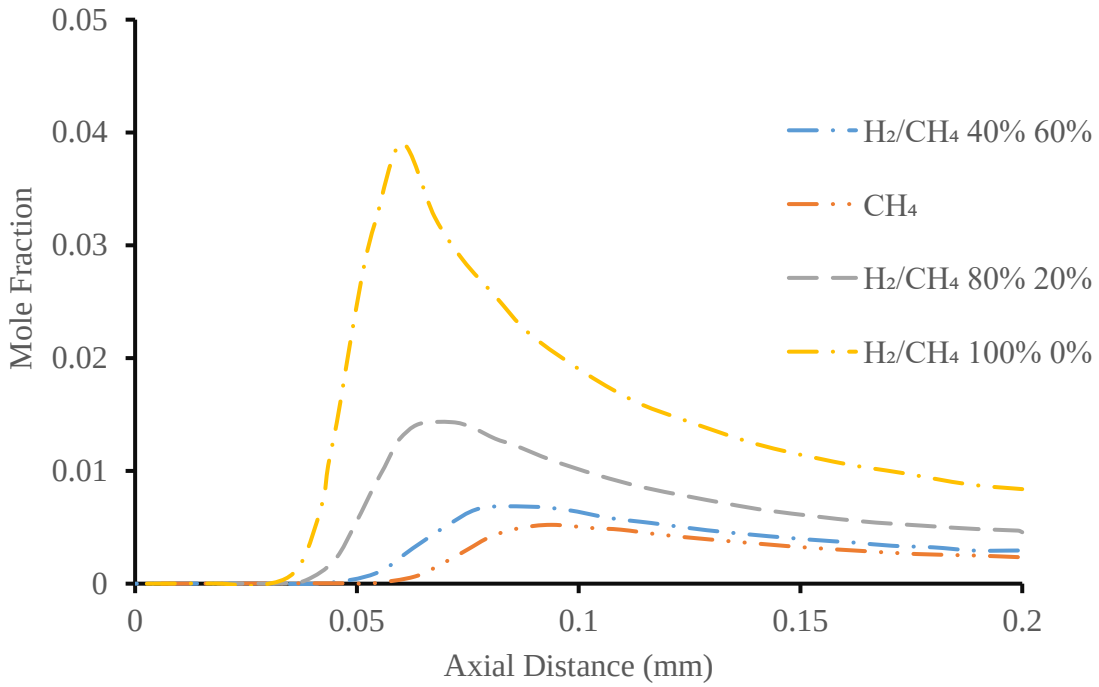


Figure 4-30 Represents changes in H radical as methane is diluted with hydrogen.

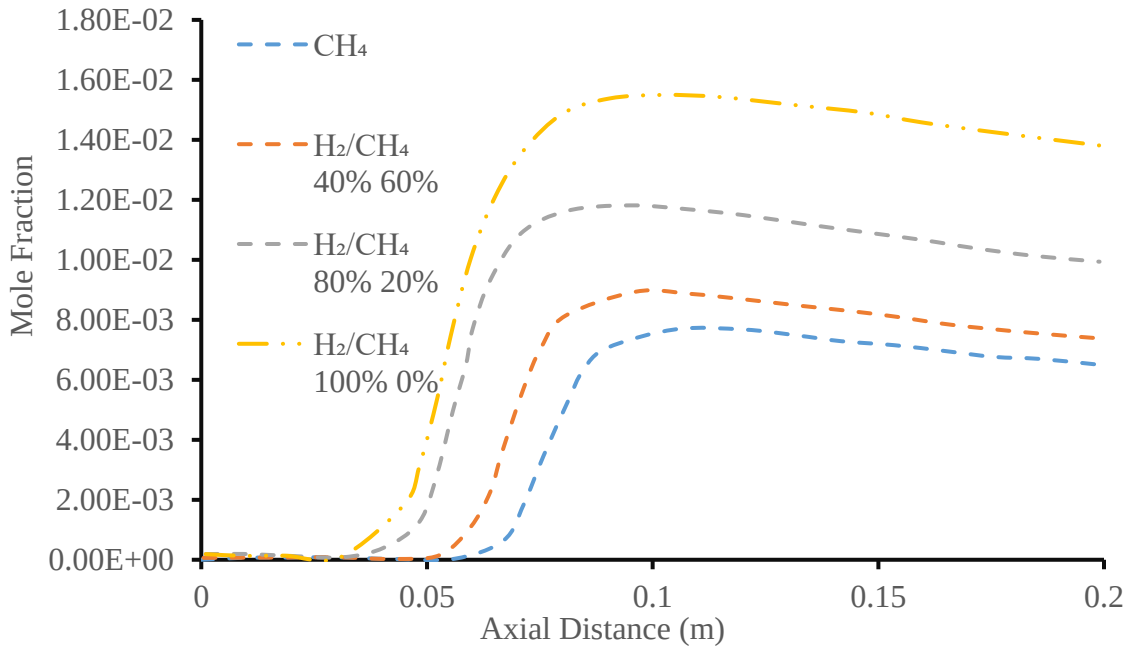


Figure 4-31 Represent changes in OH radical as methane is diluted with hydrogen.

This explanation can be further improved by hydrogen addition as shown in Figures. 4.30 and 4.31. When hydrogen addition is none, maximum concentrations of H and OH are about 0.08 and 0.06 at maximum temperature of 2130 K. As hydrogen addition is increased from 0-40% the peak mole fractions of H and OH radicals shift towards to the inlet. Both temperature and H and OH concentrations are increased. This increase promotes further radical formation in the flames which increase the flame speed as stated by Padley et al [73]. The increase of H and OH trend is not linear, as 40% addition of hydrogen only results 10% increase of radical formation which is very close to the amount of flame speed increased. This determines that the increase of flame speed is related to the increase of radical H and OH in flames. Figure 4.32 displays the change in H and OH at 100% hydrogen addition.

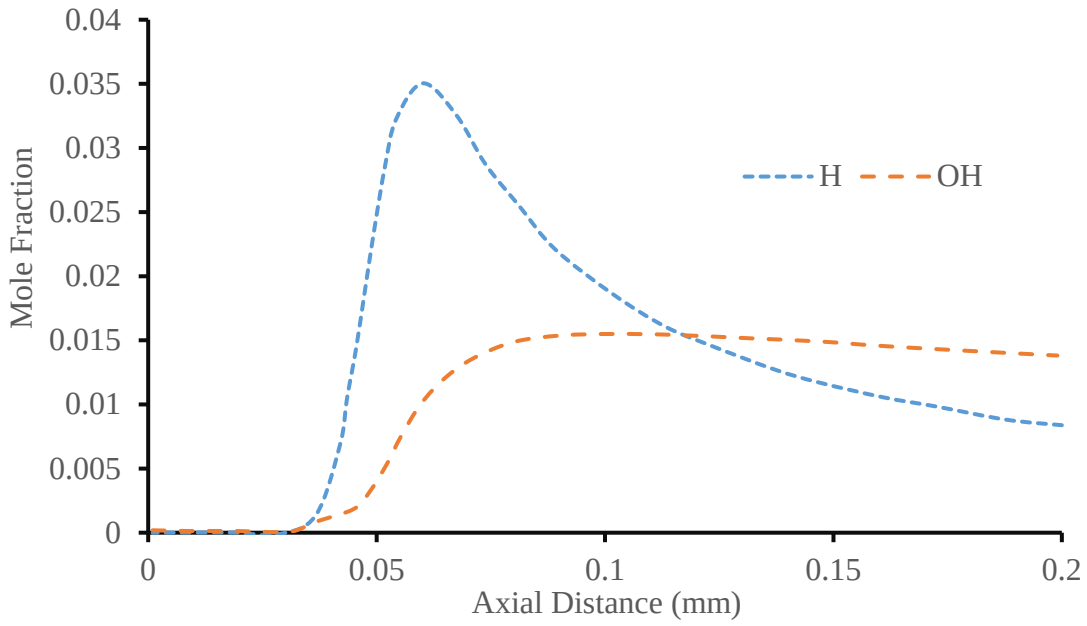


Figure 4-32 Changes in the concentrations of H and OH radicals at 100% hydrogen dilution in methane.

The same trend in flame speed is observed when hydrogen addition is higher than 70 %. There is a large increase in the radical formation, thus increasing the flame speed. This is explained through the production H and OH chain branching. The OH radical is produced in the flame and it reacts with $CH_4$ or CO to produce H radicals. The H radical immediately reacts with oxygen to produce more H and OH radicals, where the O radical keeps increasing in the flame, causing rapid heat release, which increases the reaction rate due to Arrhenius-type temperature dependency. This occurs within a thin reaction zone. The promotion of chain branching is maintained if OH radicals exists, thus increasing flame speed.

In gas turbine development, it is difficult to directly use hydrogen as a fuel even with a high mixing ratio of hydrogen so that in practice small amounts of hydrogen are mixed with hydrocarbon fuels[18]. Furthermore, fuel lean burning can suppress the formation of carbon monoxide, and $NO_x$ formation. By making the combustion lean the temperature is lower so that the production of nitrogen oxides is lower because $NO_x$formation highly depends on the peak flame temperature.

The amount of hydrogen dilution is tested at small amounts up to 40% where Figure 4.31 shows how the temperature increases as hydrogen is added to methane by small increments.

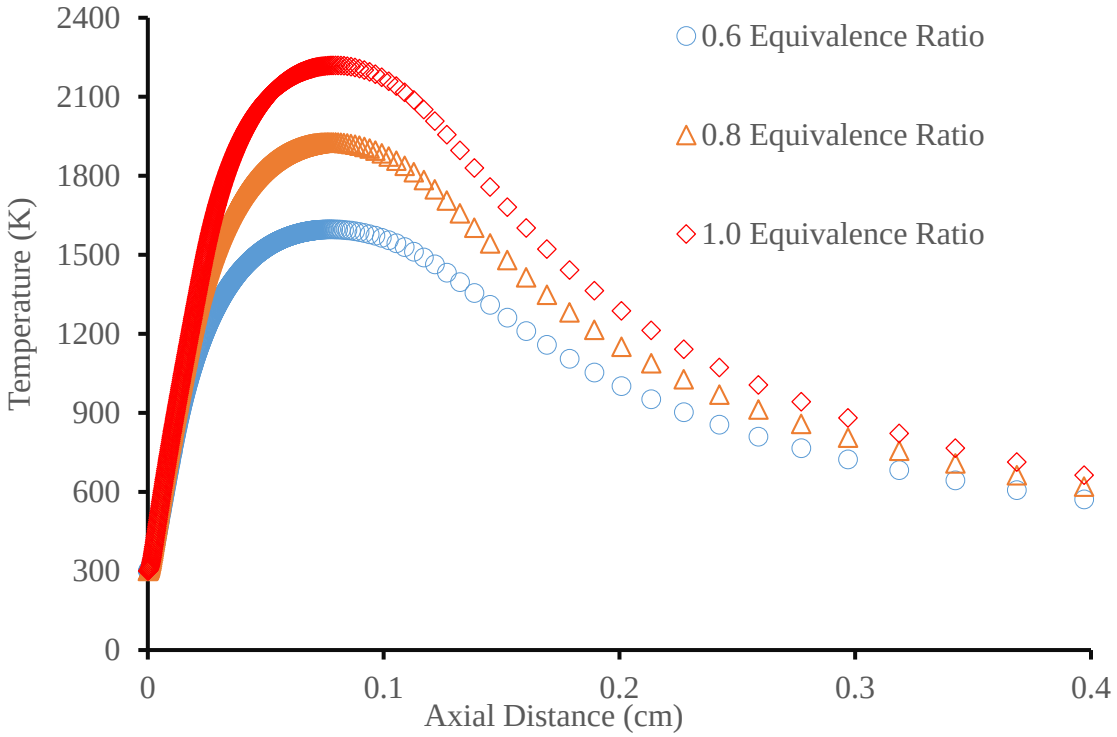


Figure 4-33 Represents Methane-Hydrogen temperature at 30% dilution .

Figure 4.33 shows the temperature distribution of methane-air with 30 % hydrogen from lean to stoichiometry. The flame temperature increases from fuel-lean to the stoichiometry. Furthermore, if compared, flame temperatures slightly increase as the hydrogen is added to methane. The same behavior is displayed for propane. Hydrogen dilution has benefits to achieve combustion and higher flame speeds for lean fuels close to flammability limit that are hard to burn. The calculations for methane-hydrogen flame speed are shown in Figure 4.32 for 0-50% hydrogen additions and in Figure. 4.33 for 0-30% $H_2$ .

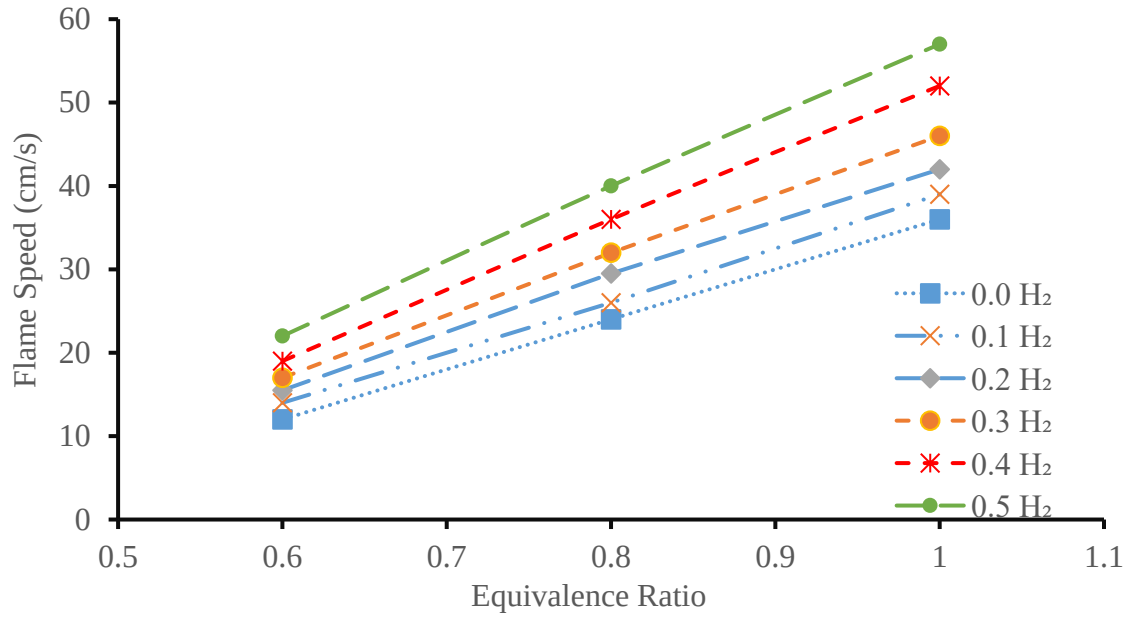


Figure 4-34 Flame speed of methane diluted with hydrogen at 0-50%.

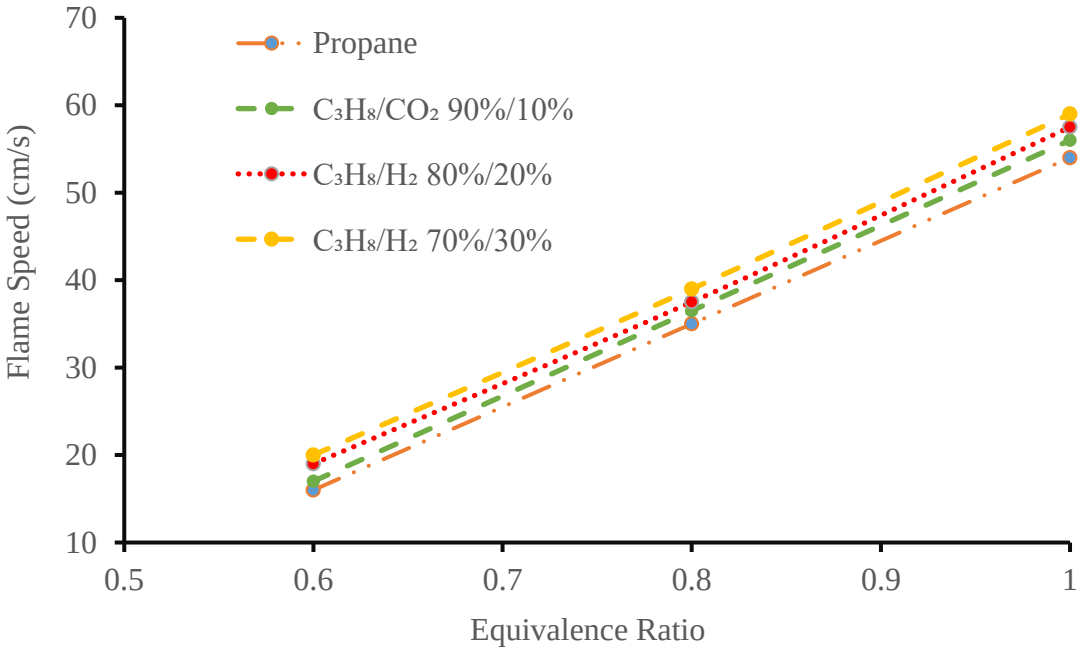


Figure 4-35 Flame speed of propane diluted with hydrogen at 0-30%

It can be seen from Figure 4.34 and Figure 4.35 that the increase of flame speed is preferable when hydrogen is added to methane, however these changes are very linear and

quite small for propane. Furthermore, hydrogen dilutions reduce the emissions of carbon dioxide as illustrated in Figure 4.36 and Figure 4.37

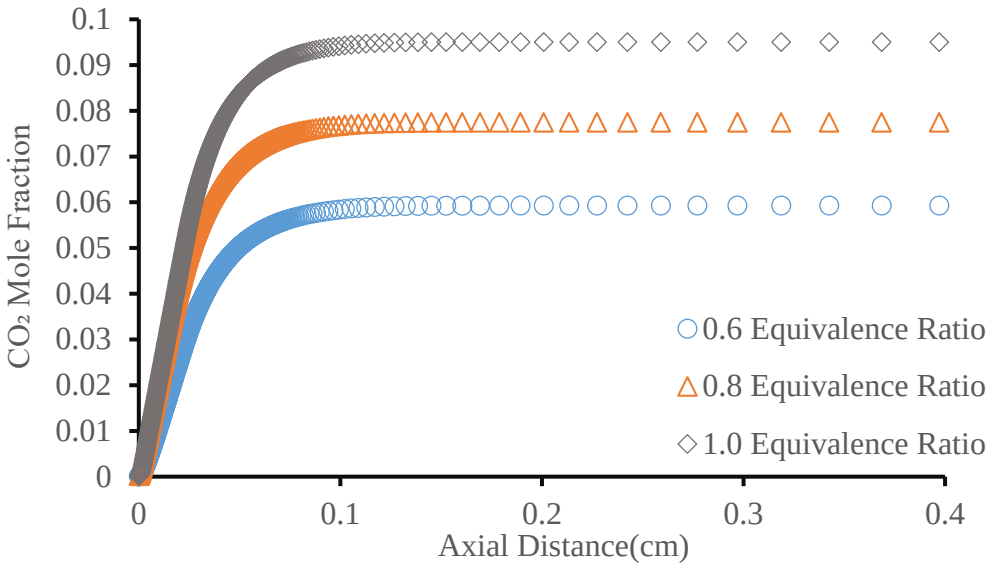


Figure 4-36 $CO_2$ mole fraction for methane-air at lean-stoichiometric.

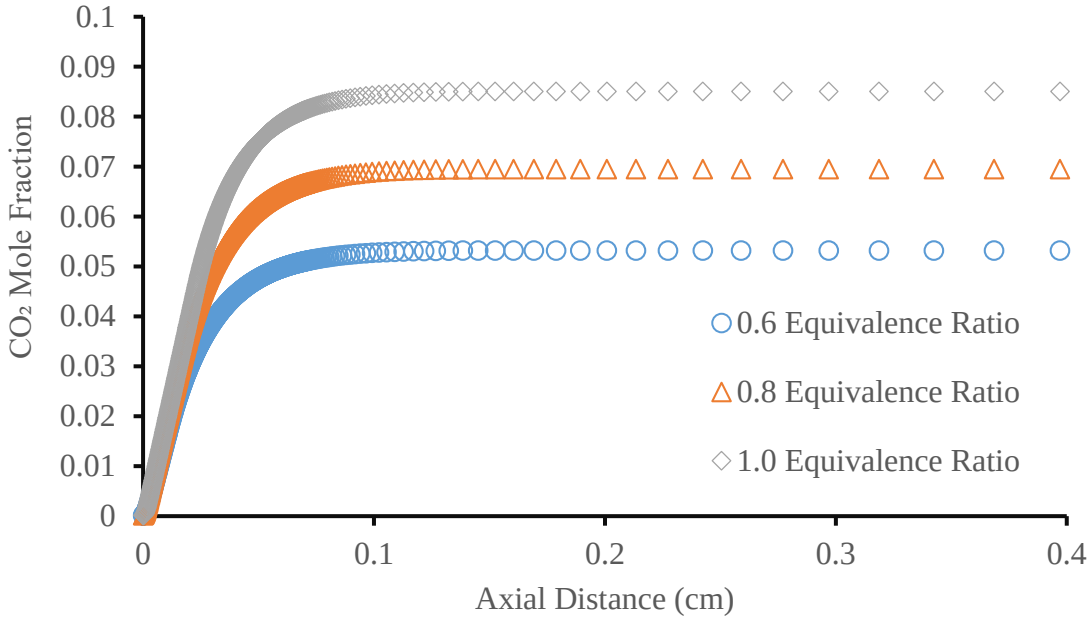


Figure 4-37 $CO_2$ mole fraction for $CH_4$-$H_2$ 0-30% at ambient conditions

The amount of $CO_2$ emissions is reduced, as hydrogen is added to the fuel blend. This reduction is attributed to the fact that carbon in fuel is reduced and replaced with hydrogen that improves the combustion even though the amount of $CO_2$may not be high however, in the long-term usage it could potentially be effective. Similar trend is seen for NO and $N_2O$ in Figure 4.38 and Figure 4.39

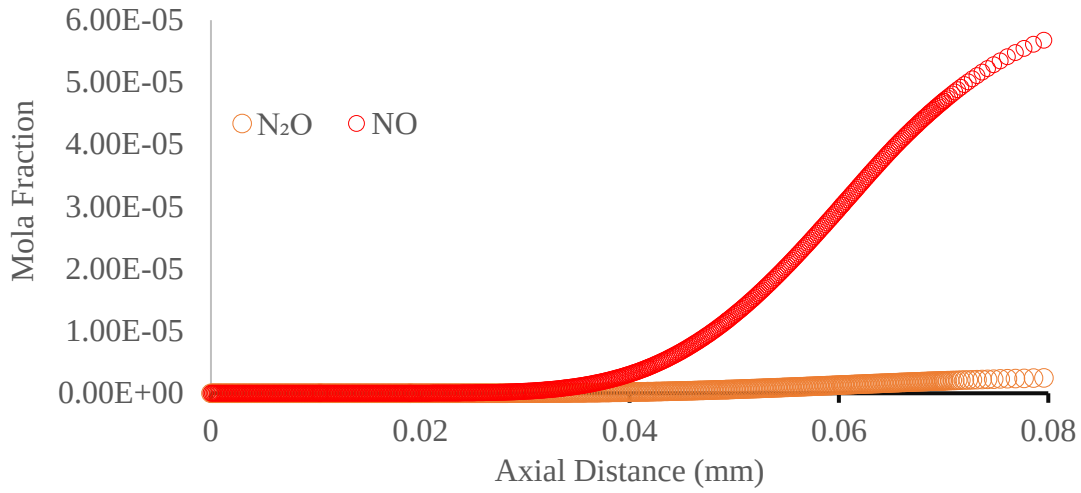


Figure 4-38 The concentration of NO and $N_2O$ for methane-air at stoichiometry.

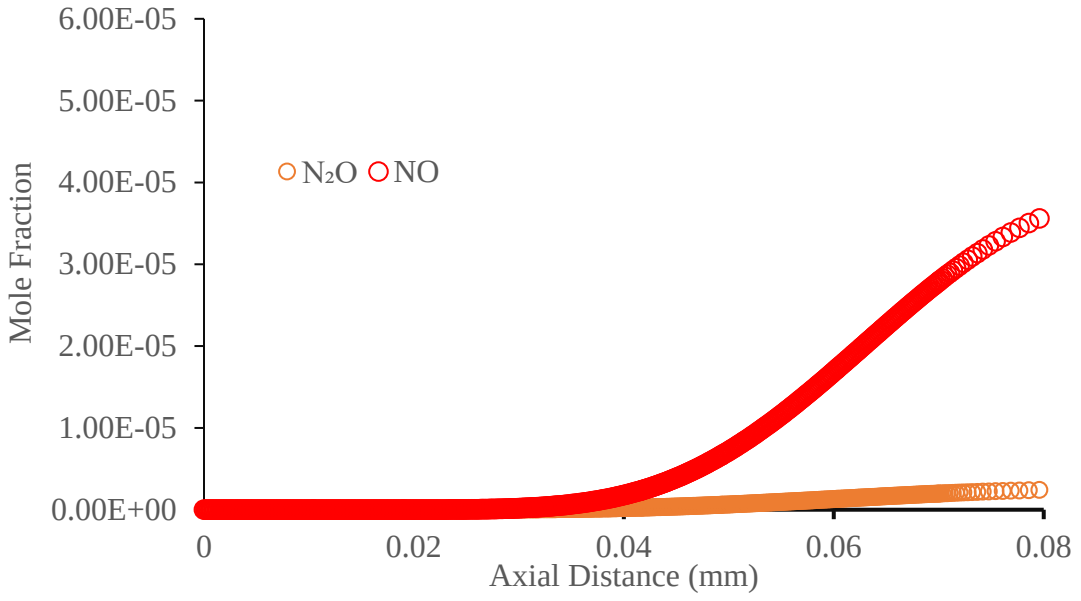


Figure 4-39 The concentration of NO and $N_2O$ methane-air with 30% hydrogen

The amount of NO and $N_2O$ produced from combustion processes are decreased due to $H_2$ addition. With the addition of hydrogen, the fuel mixture can burn in the equivalent ratio that is leaner than the flammable limit of the fuel without hydrogen additive. The method of hydrogen dilution can be a way to counter environmental problems.

### 4.5 Determining Syngas Flame Properties.

Syngas is considered a clean fuel, that could replace dominant fuels used in gas turbines to produce energy, especially in Integrated Gasification Combined Cycle. Studies have shown that the composition of syngas depends on the several factors such as the type of coal, preheat temperatures, and steam-coal ratio. Developments in combustion rely on the use of hydrogen enriched fuels that are safe and efficient [75] In the current project syngas composition will be based upon the gases that were analyzed, such as carbon monoxide, carbon dioxide, hydrogen and water [73]. The contents of syngas depend on the gasification process and raw materials available to produce syngas [76]. Each constituent is added to the gas turbines to improve performance. Combustion characteristics of syngas are studied, through an in-depth understanding of individual components to estimate the behavior of syngas. The results obtained from studying methane and hydrogen blending, makes it possible to determine how syngas or by-product gases will behave. Alvandi found that addition of syngas to methane reduces CO and $NO_x$ emissions [76]. It is important to note that some numerical methods to study syngas, are only applied to certain lean conditions, such USC-Mech II, when tested with different $H_2$/CO blends, GRI 3.0 shows good agreement with experimental data [75]

Experimental and numerical analysis were done to study species profile, and laminar burning velocity for syngas [1, 77-84]. The numerical analysis done for syngas has been compared through GRI-3.0 and San Diego mechanisms at normal temperatures and atmospheric pressure, where the accuracy is accepted for the flame speed. However, errors occur once the preheat temperatures are changed for some test cases. In lean conditions for the combustion of CO-$H_2$ measured flame speed was not in agreement with experimental work using San Diego kinetic mechanism [85]. The current project will try to determine the flame properties using Fluent for a variety of syngas 5% $H_2$ and 95% CO and 50%

$H_2$ 50% CO where the flame speed and radical formation will be tracked for those two cases at different preheat temperatures. The preheat temperatures are used to determine the robustness of the model, meaning will the model able to converge when preheat temperature variable is added. The simulation for each test case is run at fuel lean-rich using the 10-step mechanism. To determine the equilibrium balance of equation the same formula used in Chapter 4 will be used, but this time with the addition carbon monoxide. The following table will summarize the mole fractions for each component used in the test cases studied.

Table 4-10 Summary of the mole fraction for syngas at different compositions and equivalence ratios.

| Equivalence Ratio | Syngas Composition ($H_2$/CO) | Hydrogen | Oxygen | Nitrogen | Carbon Monoxide |
|---|---|---|---|---|---|
| 0.6 | 50%/50% | 0.1007 | 0.1678 | 0.6309 | 0.1007 |
| 0.8 | 50%/50% | 0.1258 | 0.1572 | 0.5911 | 0.1258 |
| 1 | 50%/50% | 0.1479 | 0.1479 | 0.5562 | 0.1479 |
| 0.6 | 5%/95% | 0.0101 | 0.1679 | 0.6309 | 0.1913 |
| 0.8 | 5%/95% | 0.01258 | 0.1572 | 0.5912 | 0.239 |
| 1 | 5%/95% | 0.0148 | 0.1479 | 0.0556 | 0.281 |
| 0.6 | 25%/75% | 0.0503 | 0.1678 | 0.6309 | 0.151 |
| 0.8 | 25%/75% | 0.0629 | 0.1572 | 0.5912 | 0.1887 |
| 1 | 25%/75% | 0.074 | 0.1479 | 0.05562 | 0.2219 |
| 0.6 | 75%/25% | 0.151 | 0.1678 | 0.6309 | 0.0503 |
| 0.8 | 75%/25% | 0.1887 | 0.1572 | 0.5912 | 0.0629 |
| 1 | 75%/25% | 0.2219 | 0.1479 | 0.5562 | 0.074 |

In the previous work done by Langan [54] determinations of flame shape and flame speed for syngas of 5% $H_2$/95% CO and 50% $H_2$ 50% CO did not result in flame stability and convergence, when the premixed model was used in Fluent. The divergence in their studies was due to the lack of developed kinetics, the usage of an older version of the GRI-Mech,

and the equilibrium balance provided by the premixed model in Fluent. Even though 1D simulations can predict the results for those two cases, it is imperative to show the convergence of these cases, using the transport model in Fluent. A comparison will be made between the adiabatic flame temperature obtained through Fluent and GASEQ to determine the accuracy of the model

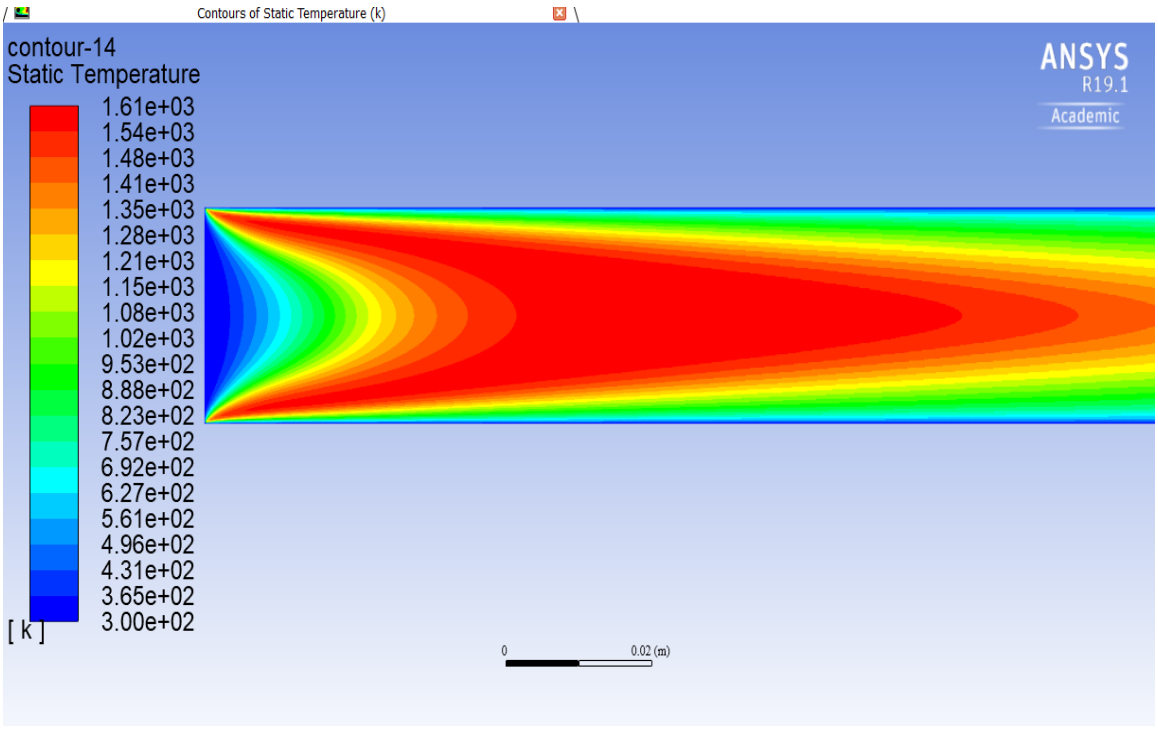


Figure 4-40 Temperature contour for syngas 50/50 $H_2$ $CO_2$ at 0.6 equivalence ratio

Flame stability was obtained for all he cases of syngas at the ratio of 50% hydrogen and 50% carbon monoxide, at varied equivalence ratios of fuel lean to fuel rich

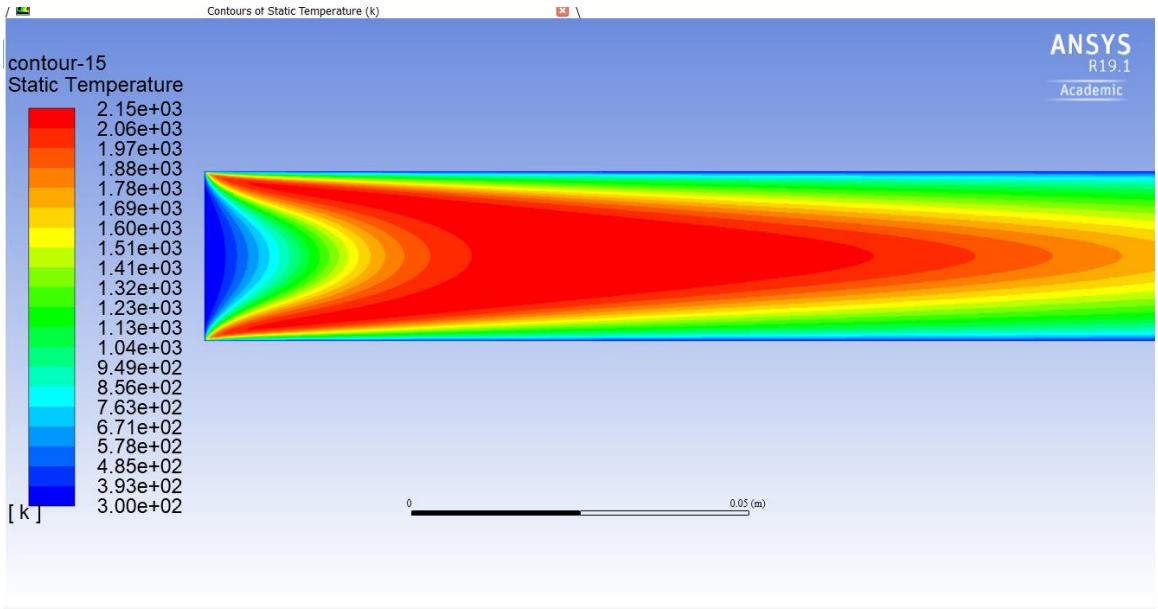


Figure 4-41 Temperature contour for syngas 50/50 $H_2$ $CO_2$at 1 equivalence ratio

The flame structure obtained through fluent data for the stoichiometric condition is shown below in Figure 4.42

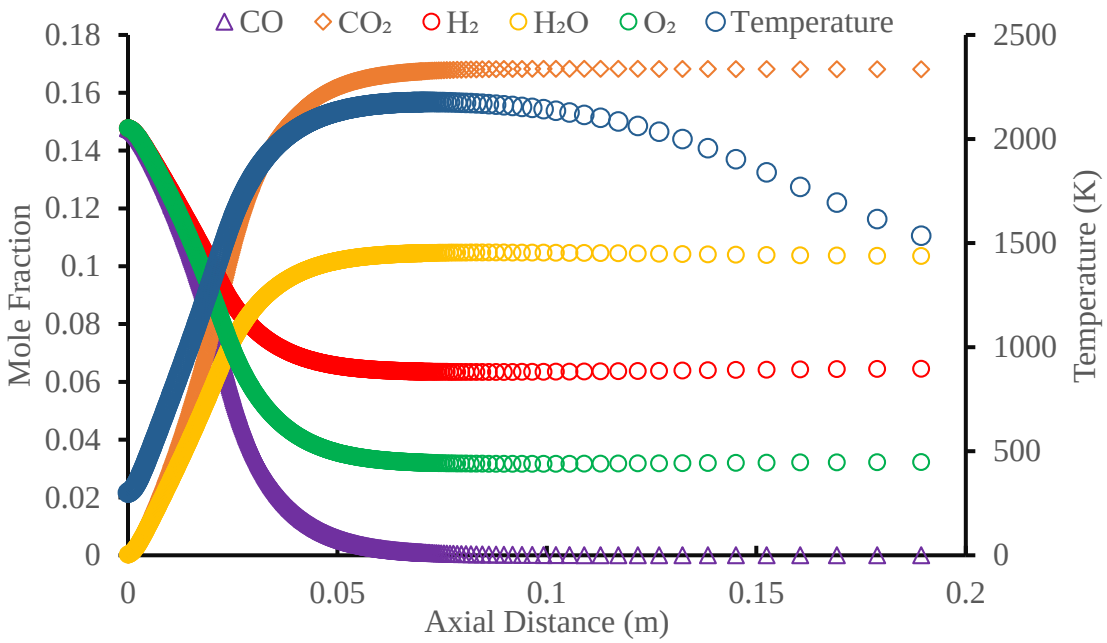


Figure 4-42 Syngas 50/50 flame structure at stoichiometry and ambient conditions.

The combustion of syngas follows a similar trend as methane where the combustion occurs within the first few millimeters and products form throughout the tube. Convergence was

obtained for the case syngas 50/50 using both GRI-MECH 3.0 and 10-step mechanism, the flame shape is conical in both cases and agrees, with the methane-air combustion, however the length of the wave differs and the temperatures. Comparison is made between temperatures obtained through experimental data obtained by Patricia et al [27] and the 10-step mechanism at different equivalence ratios shown in Figure 4.43

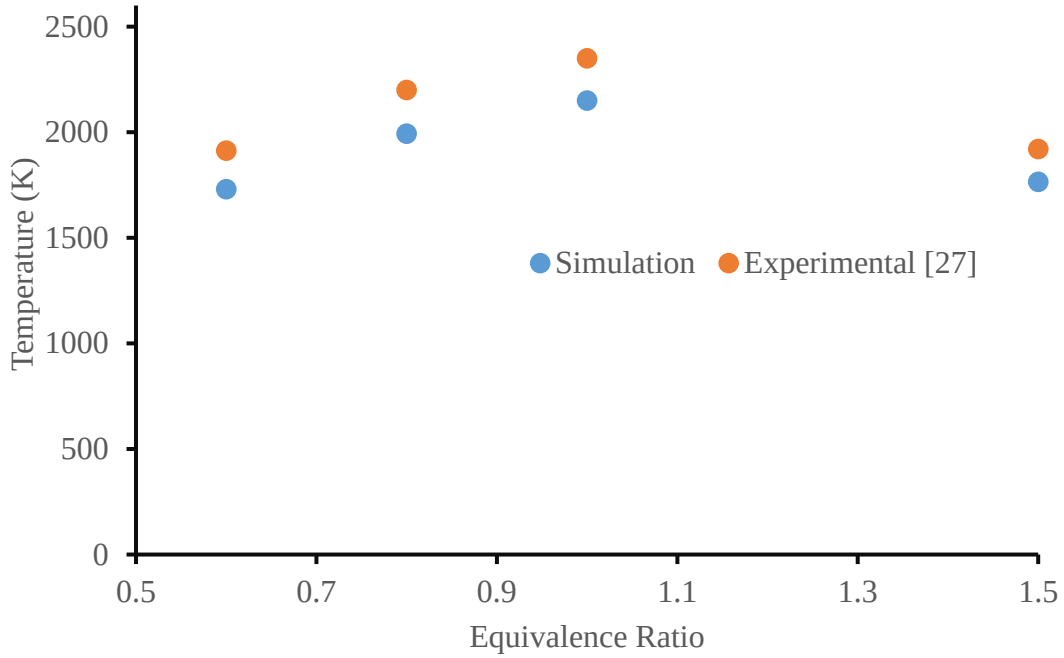


Figure 4-43 Comparison between experimental work and 10 step mechanism adiabatic temperature for syngas 50% hydrogen 50% carbon monoxide [27].

From Figure 4.43 it is noticed that there is a 150 K temperature difference between experimental results and simulation, about 7-10% variation, related to the use of a reduce mechanism. However, this should not affect the flame speed estimation for these fuels. Convergence was also obtained for the case of $H_2$/CO ratio of 5/95 % using similar methods, and results are shown in Figure 4.44 4.45 and Figure 4.46

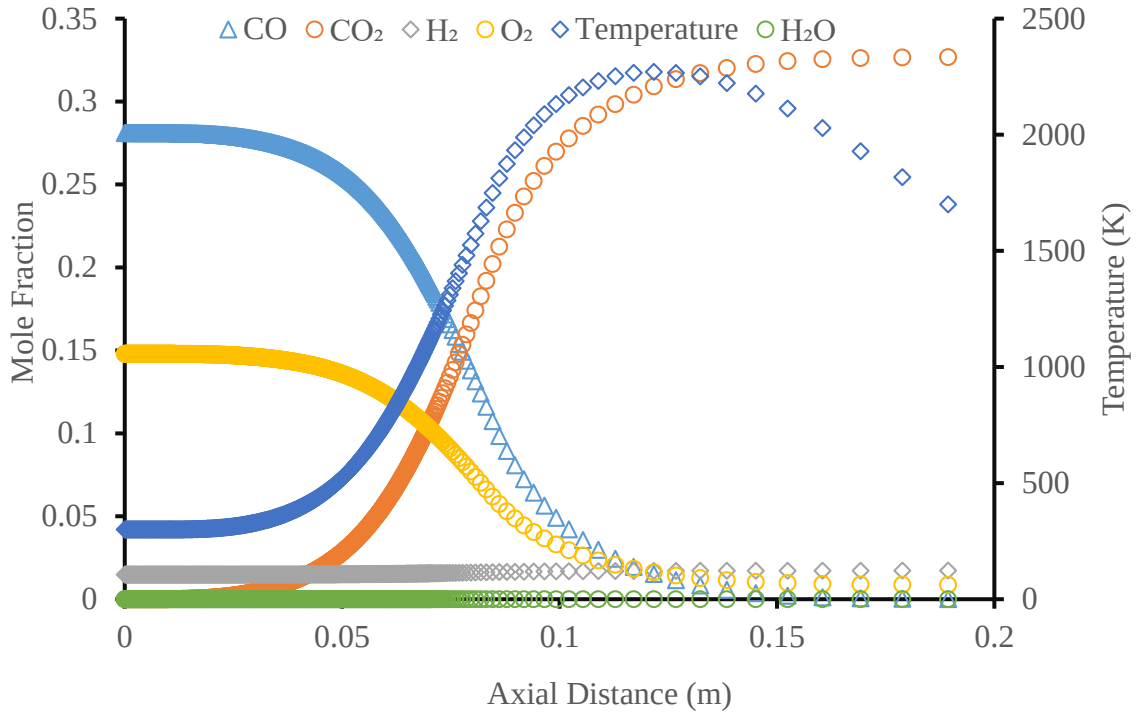


Figure 4-44 Syngas 5/95 $H_2$ CO flame structure at stoichiometry.

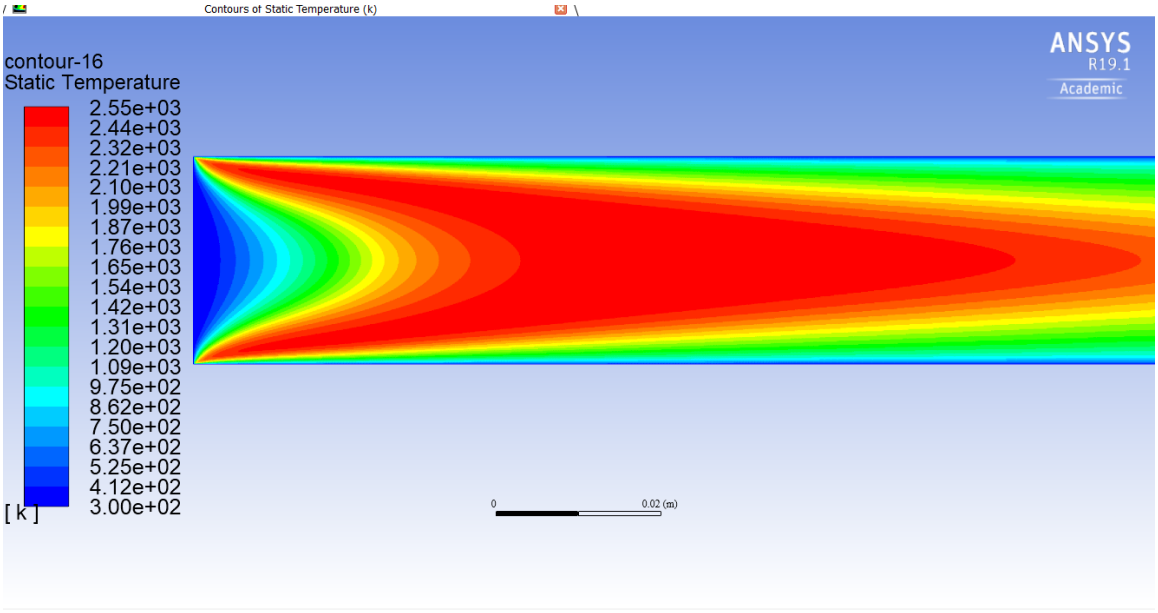


Figure 4-45 Temperature contour for syngas 5/95 $H_2$ CO at 1 equivalence ratio.

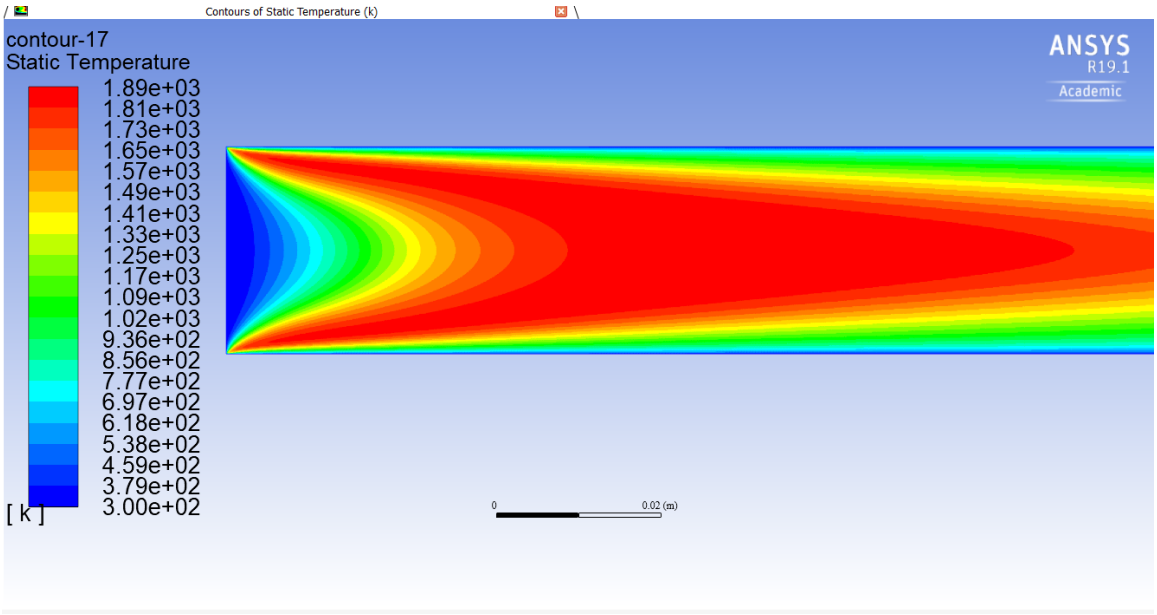


Figure 4-46 Temperature contour for syngas 5/95 $H_2$ CO at 0.6 equivalence ratio

By comparing the results obtained from Figure 4.44 4.45 and 4.46 and the adiabatic flame temperature obtained through GASEQ the result obtained for 5%/95% the accuracy is within 3%, and it is smaller than that of 50/50 ratio shown in Figure 4.44

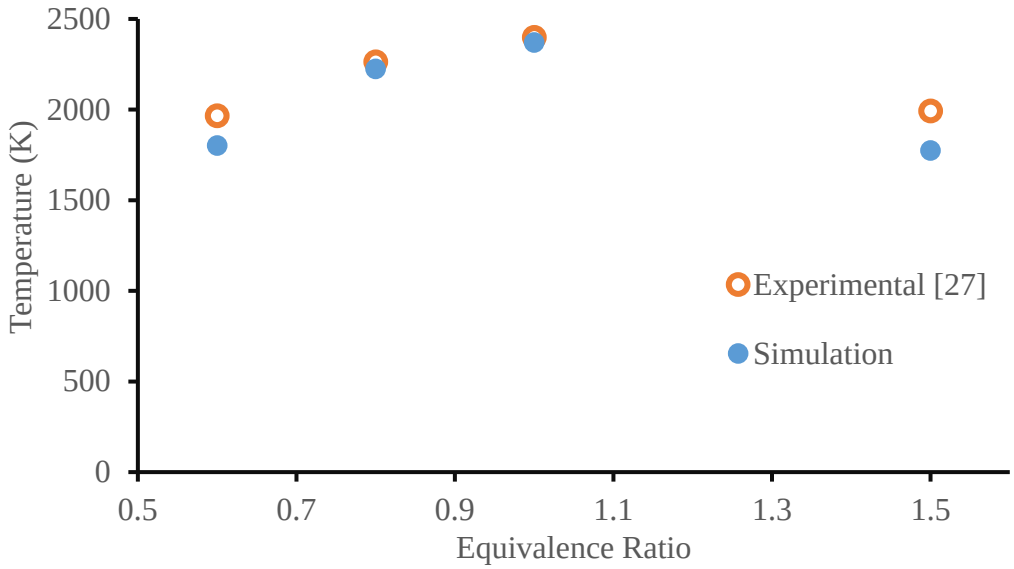


Figure 4-47 Comparison between experimental work and 10 step mechanism adiabatic temperature for 5/95 $H_2$ CO syngas [27, 28].

The flame was calculated using the surface area of the flame method used for methane-hydrogen enrichment, to compare 4 different syngas composition using the 10-step mechanism and GRI-3.0,since GRI-3.0 has been tested extensively with experimental work. Shown in Figure 4.48.

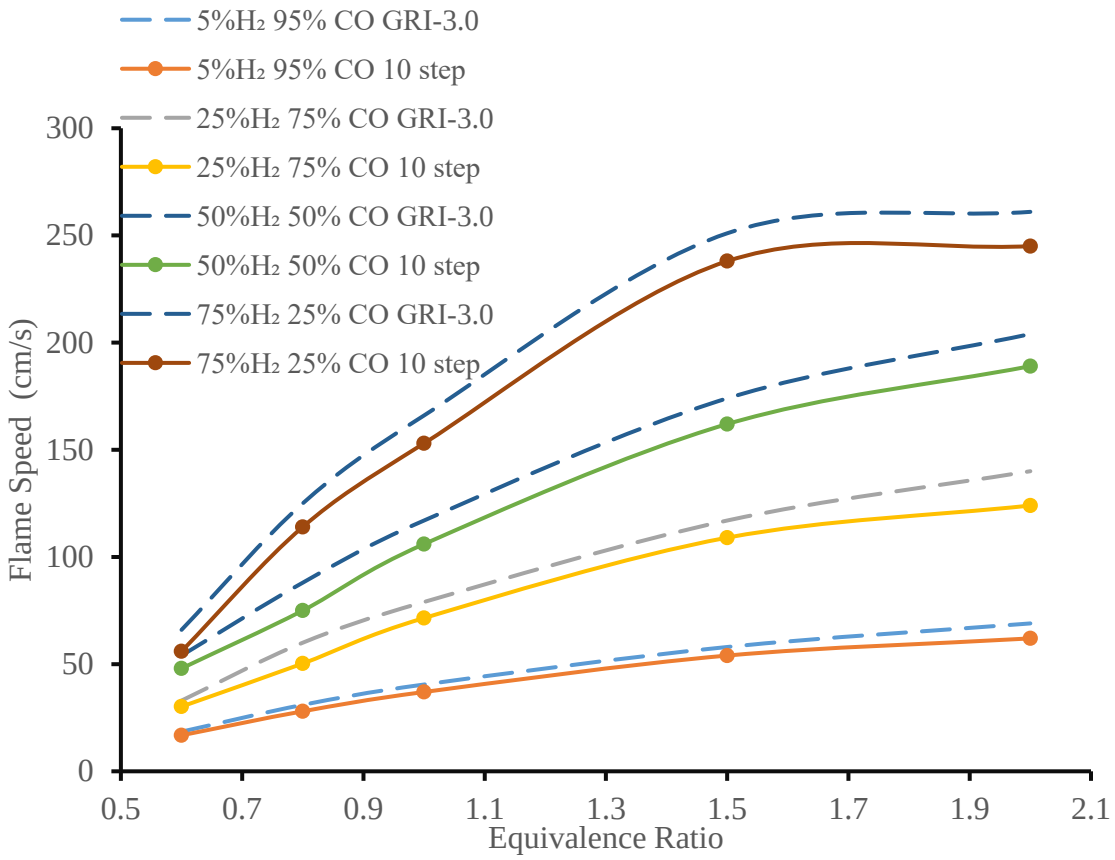


Figure 4-48 Calculated flame speed of different syngas composition and ratios.

It can be seen from Figure 4.48 there is a good agreement with the results obtained through the 10-step mechanism when compared to the GRI-3.0. where the conditions were tested for 5 different equivalence ratios and the line in between the points is used to represent the trend that is obtained, but not the trend of the actual values at different ratios However, upon comparison with experimental data obtained by researchers at 298 K and 1 atm both numerical methods seem to overestimate the actual flame speed [76].

The increase of hydrogen content in the fuel exhibits similar trend when added to methane for all equivalence ratios. The radical formation can be graphed from the data obtained. The cases that were studied are the 5%$H_2$-95% CO and 50%$H_2$-50%CO where the radicals H, O, $H_2O_2$ and OH are obtained shown in Figure 4.49

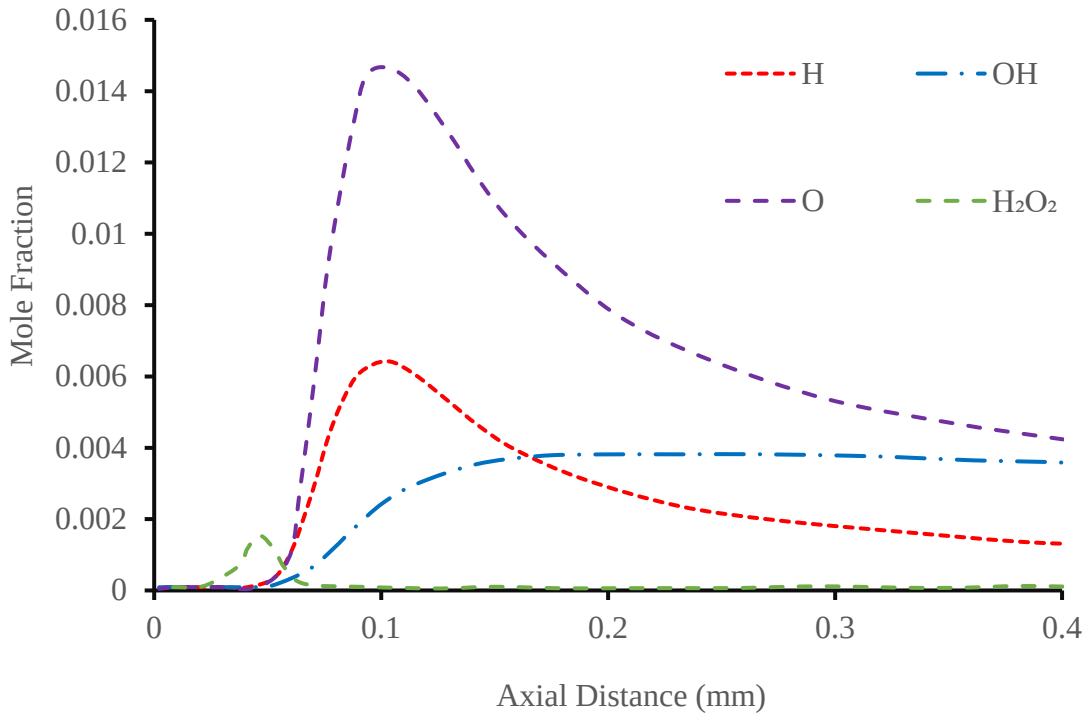


Figure 4-49 The radical formation in the case of 5/95 syngas at stoichiometry.

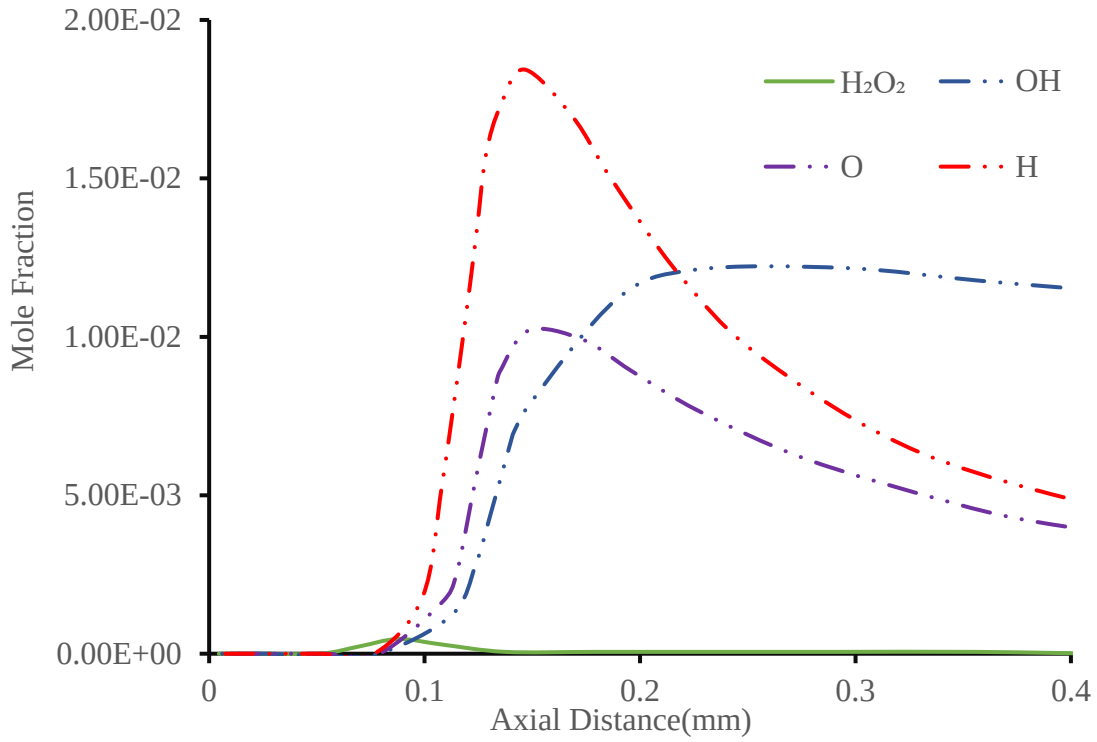


Figure 4-50 The radical formation in the case of 50/50 syngas at stoichiometry.

The effects of hydrogen addition to fuels was previously discussed, showing that the concentrations of the radicals H and OH affected the flame speed. The analysis examined that the correlation between radical formation and syngas particularly occurs within the first few millimeters of the combustion zone [35, 55, 56]. Figure 4.49 and 4.50 show the flame structure for the minor species obtained through fluent for the case of 5% $H_2$and 50% $H_2$ in CO blends at 298 K and 1 atm. If hydrogen is added, there is an increase in the formation of H and OH radicals which control the flame speed, through the increase of reaction rates and a decrease in the O radical. It can be noticed that there exists a nonlinear flame speed relationship that could be seen in the presence of low hydrogen blends in carbon monoxide-air, previous studies by scholte et al [28, 37, 42] investigated the oxidation of CO through the reaction $CO + OH = CO_2 + H$ a comparison is made between 1% 5% and 10% hydrogen/carbon monoxide-air mixtures at 0.6-1.0 equivalence ratio. Is shown in Figure 4.51

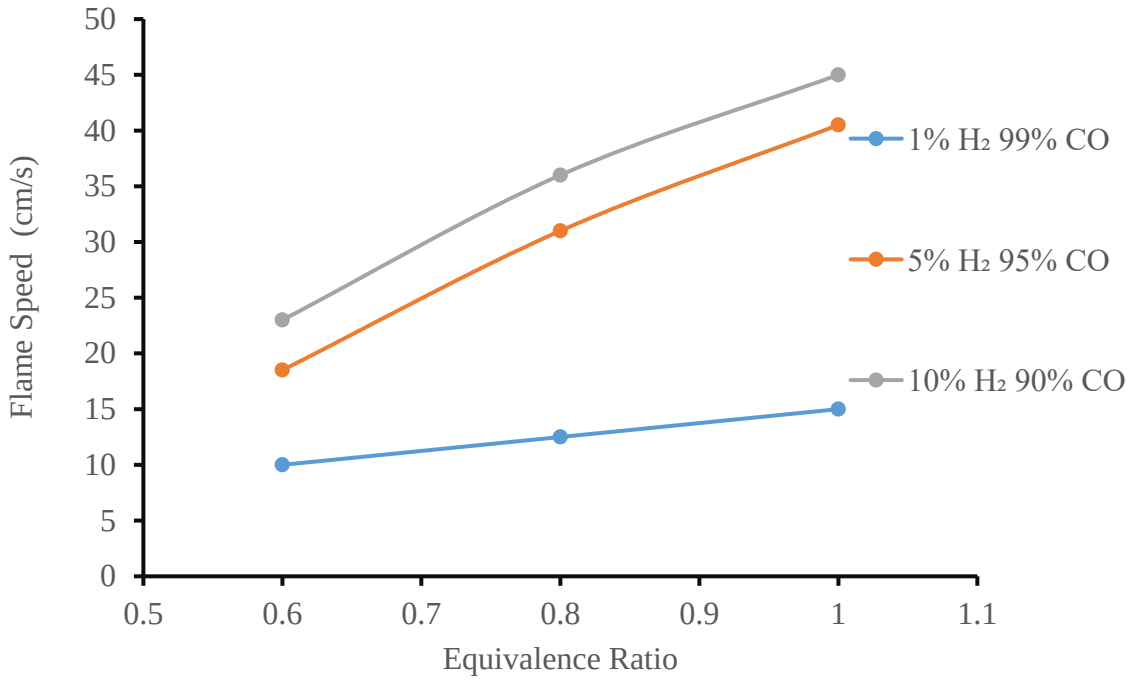


Figure 4-51 Flame speeds obtained for 1% 5% and 10% $H_2$/ CO syngas mixture

It can be seen from Figure. 4.51 the non-linear relationship in terms of hydrogen blending with CO. When the syngas mixture contains 1% $H_2$the flame speed is around 10 cm/s, but at 5% the flame speed at $\phi = 0.6$ it almost doubles reaching 20 cm/s. However, at 10% the increase is very small only about 3 cm/s flame is increased as show in Figure 4.51. It can be understood that flame speed is related to the radical formation which is in turn proportional to the reaction rate and thermal diffusivity as show by Glassman and Yetter [22]

### 4.5.1 Syngas Pre Heat Temperature Effects on Flame Speed

Another method to improve combustion and energy production is done through, increasing preheat temperature to provide better stability of the combustion to maintained throughout the system, Combustion preheat temperature is usually used for systems and processes that require a high temperature, such as steel making, chemical processes, and even sometimes also used in low temperature systems such as steam generation. A study done for liquefied petroleum gas found that changing the preheat temperature by small amounts results in improvements in the efficiency of burners [1] For this project a test case was run for syngas 50% $H_2$ and 50% CO to determine the changes in flame speed based on the changes in

preheat temperatures. The following temperatures of 298 K, 400 K and 500 K were tested and the flame speed obtained for lean and rich fuel, the 10 step mechanism results were compared with GRI-3.0 and experimental work done by Sing et al[76] and results are summarized in the following Figure 4.52

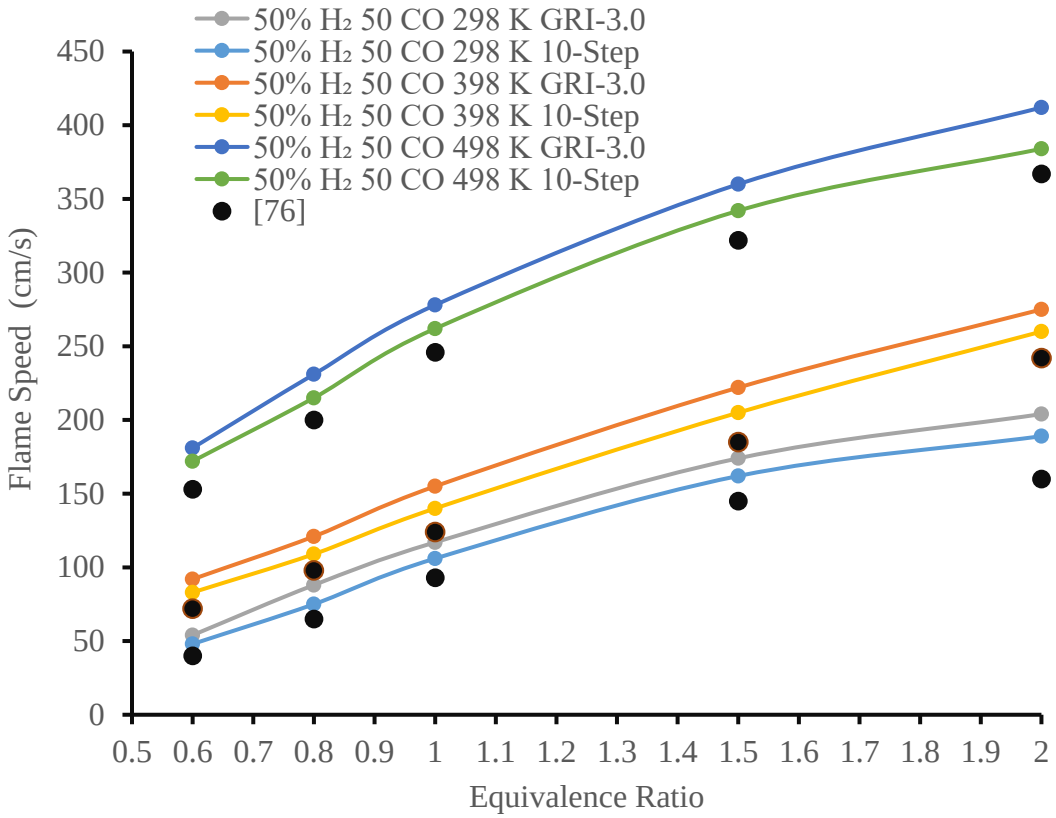


Figure 4-52 Comparison of flame speed at different preheat temperatures for experimental [76], GRI-3.0 and 10 Step

As shown in Figure 4.52 the flame speed for gas increases considerably as the preheat temperature is increased. However, till this day the kinetic mechanism overestimates the flame speed when compared with experimental where similar cases occurred for Natarajan and Singh et all upon the trial of San Diego mechanism and other reduced mechanism [1, 76, 86] the variation in the results appear to be the result of inaccurate determination of reaction rates assumed when higher temperatures are used. The tendency of flame speed increase is explained by Sign et al through sensitivity analysis when temperatures are increased the sensitivity coefficient for reaction $H_2$+O=OH+H and other chain recombination reaction Increases which would explain the increase of flame speed.

## 4.6 Blast Furnace Gas and Coke Oven Gas Results

With understanding of the combustion characteristics of hydrogen, carbon monoxide and methane blend fuels the simulation can apply to two practical syngas, Coke Oven Gas (COG) and Blast Furnace Gas (BFG) to develop better efficiency and performance in steelmaking. These gases are produced from Coke Oven and Blast Furnace where the COG is synthetic gas highly enriched with $H_2$, and BFG is highly diluted with CO and $H_2$, and they are used to convert iron oxides to liquified iron. The composition of the two gases used in this project are listed in Table 4.11

Table 4-11 The composition of BFG and COG studied

| Fuel Component percentage | $CO_2$ | $CH_4$ | CO | $H_2$ | $N_2$ |
|---|---|---|---|---|---|
| COG | 2 | 30 | 4 | 61 | 3 |
| BFG | 21 | 1 | 21 | 3 | 55 |

### 4.6.1 Coke Oven Gas Results

Burning COG can generate energy to supply other process. At the end of coke-production, the left over remains are a mixture of burnable gases which could be reused. For that reason, it is important to understand the properties of COG such as adiabatic flame temperatures and flame speed at different equivalence ratios and preheat temperatures. The COG mainly consists of methane and hydrogen at 1:2 ratio. The mixture at ambient temperature and pressure. The maximum temperature was set around 900 K at which resembles the actual burner in steelmaking factories. The equivalence ratio was set from fuel lean to fuel Trich. The 5-step mechanism was used to simulate both COG and BFG combustion. A sample calculation is shown in Figure 4.53 for COG at stoichiometric ratio and at ambient conditions.

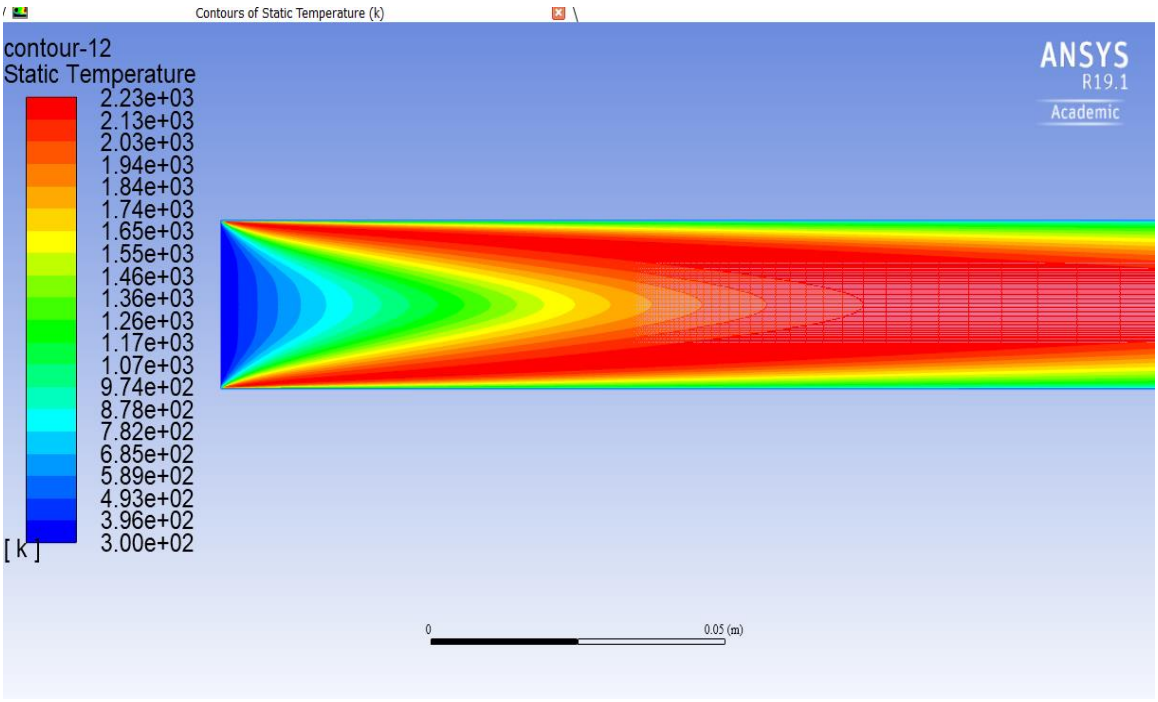


Figure 4-53 COG temperature contour at stoichiometric and ambient conditions

The adiabatic flame temperature for COG reacting with air was calculated at fuel lean to rich conditions with different preheat temperature, and the results are summarized in Figure 4.54

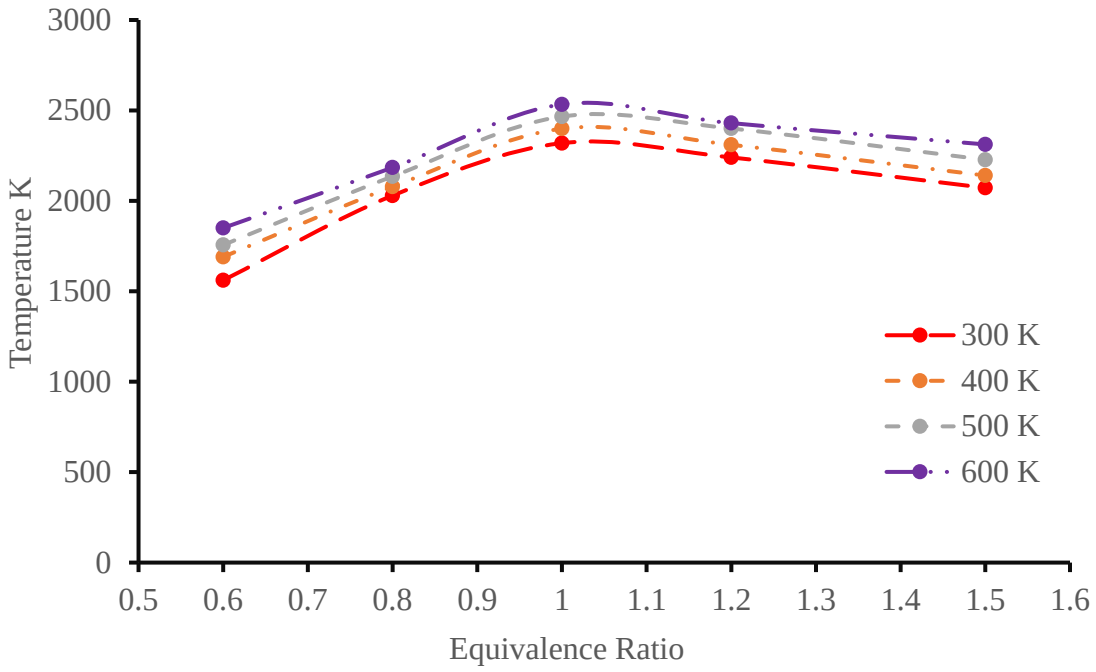


Figure 4-54 COG adiabatic flame temperature at different equivalence ratios and preheat temperatures

It can be noticed that, increasing the preheat temperature affects the adiabatic flame temperature for each tested case as shown in Figure 4.54 the line in between the point is used to show the trend at different equivalence ratios. The highest possible adiabatic flame temperature occurs around 1.05 equivalence ratio. The next step is to determine the effect of preheat temperature on the flame speed. The first tested conditions were applied to stochiometric COG at temperature ranging from 300-900 K shown in Figure 4.55

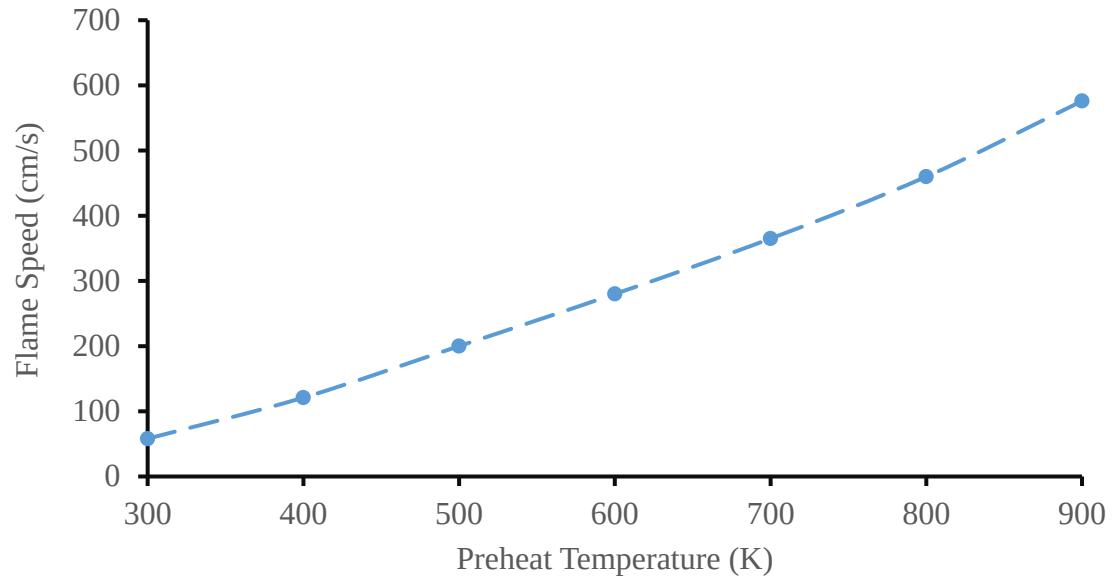


Figure 4-55 Effect of preheat temperature on flame speed at stoichiometric (COG)

by increasing preheat temperature, the flame speed increases drastically. A comparison was further made for COG-air combustion at various equivalence ratio and different preheating. The results are shown in Figure 4.56

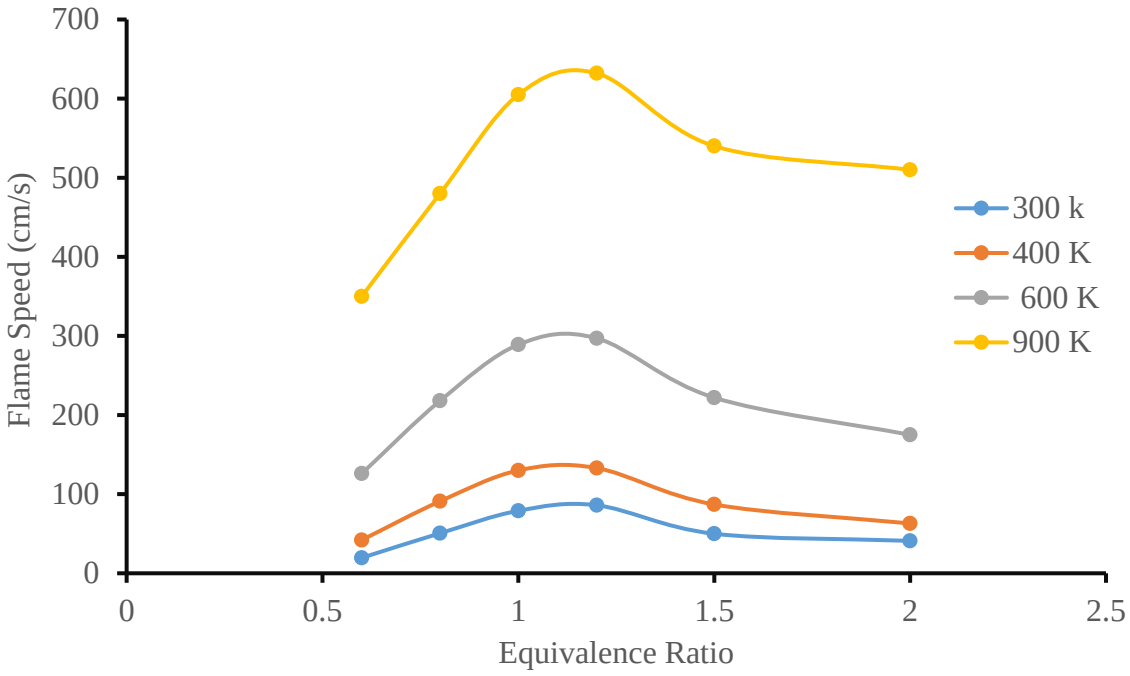


Figure 4-56 COG flame speed at different preheat temperature and ϕ.

As expected, the flame speed peaks at the equivalence ratio around 1.1-1.2. The behavior is like that of methane peaking at 1.1, but not hydrogen which peaks at approximately 1.7. CO-air combustion has the highest flame speed at 2.85 equivalence ratio[87] The flame speed of COG-air combustion is around 83 cm/s, between methane-air and hydrogen-air combustion , while methane-air is 36 cm/s. This suggests that the COG combustion is governed by the methane combustion mechanism in terms of fuel mixing due to having slower reaction rates, leading to lower flame speed than hydrogen-air blends. Furthermore, it was found that the initial temperature is the effective way to enhance the flame speed of mixtures. A comparison is made between the structure of major species for COG at different preheat temperatures and is shown Figure 4.57 and 4.58 where a comparison is made in order to determine the effects of preheat temperatures.

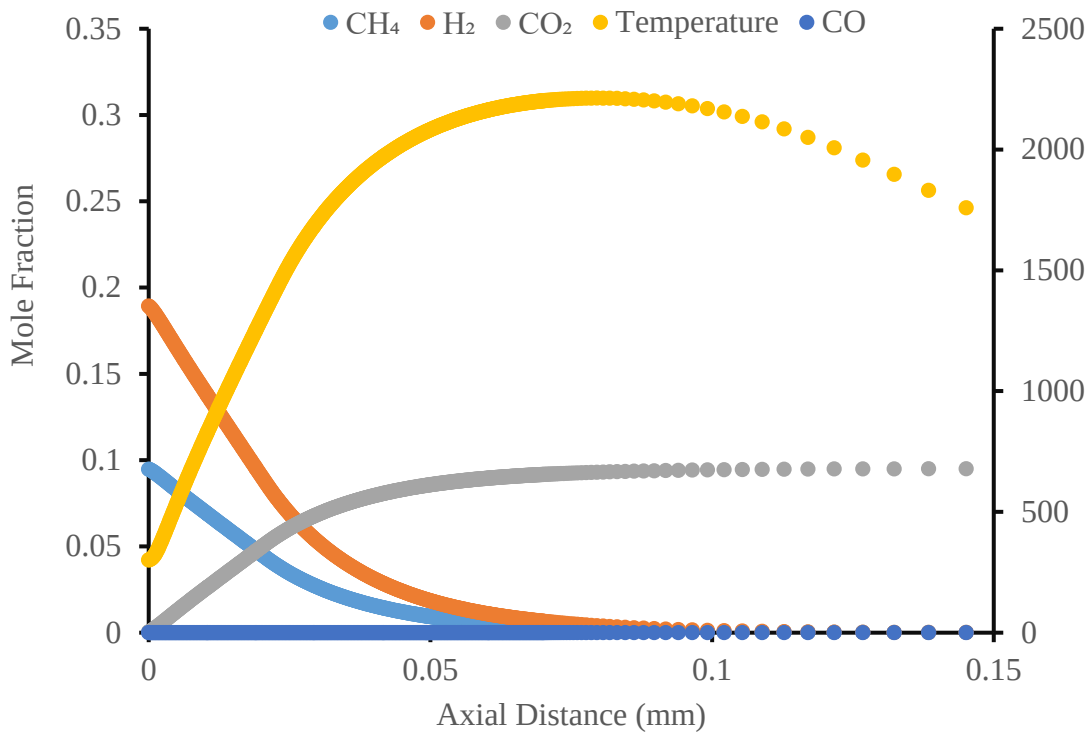


Figure 4-57 Flame structure of COG at ambient conditions.

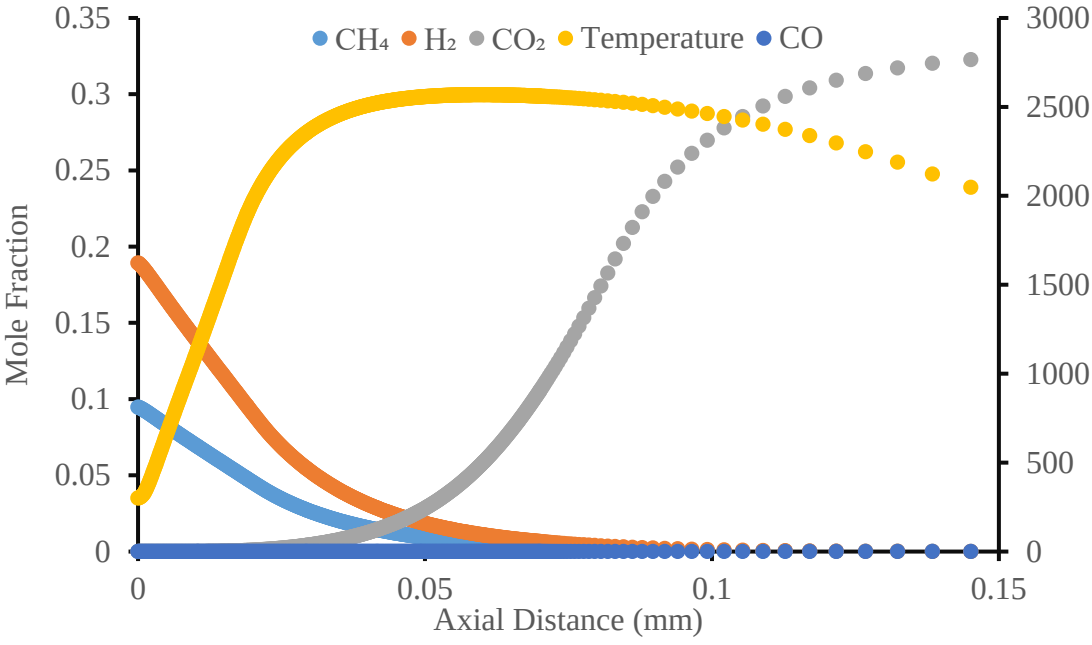


Figure 4-58 Flame structure of COG major species at 900 K preheat temperature

It is seen that both structures seem to be similar that indicates reaction paths unchanging. However, there are differences in the rate of change CO and $CO_2$. This is reasonable because with high preheat temperature the reaction rate for the conversion of CO to $CO_2$ is increased and reaction time is shorter, which shifts the species curves towards the domain input direction. For the light molecule of $H_2$, high temperature promotes it to diffuse upstream generating H and OH radical to convert $H_2$ and CO to the final products.

### 4.6.2 Blast Furnace Gas Results.

BFG is the most available gas for the steelmaking. Its composition depends on the furnace specifications. It contains a large percentage of $CO_2$ and $N_2$ as inert but much less fuels available. A change of hydrogen additive affects the combustion characteristics of flame speed and fuel calorific value. For that reason, the composition provided in Table 4.8 will be the only tested case for BFG in this project. BFG consists mainly of inert gases of $CO_2$ and $N_2$ and of small amounts of fuel gases CO and $H_2$ so that the combustion of BFG has relatively less strength with slow flame speed. The equivalence ratio was varied from lean to rich. The 5-step mechanism was used to simulate the combustion of BFG. A typical calculation is shown in 4.59 for BFG at stoichiometric and ambient conditions.

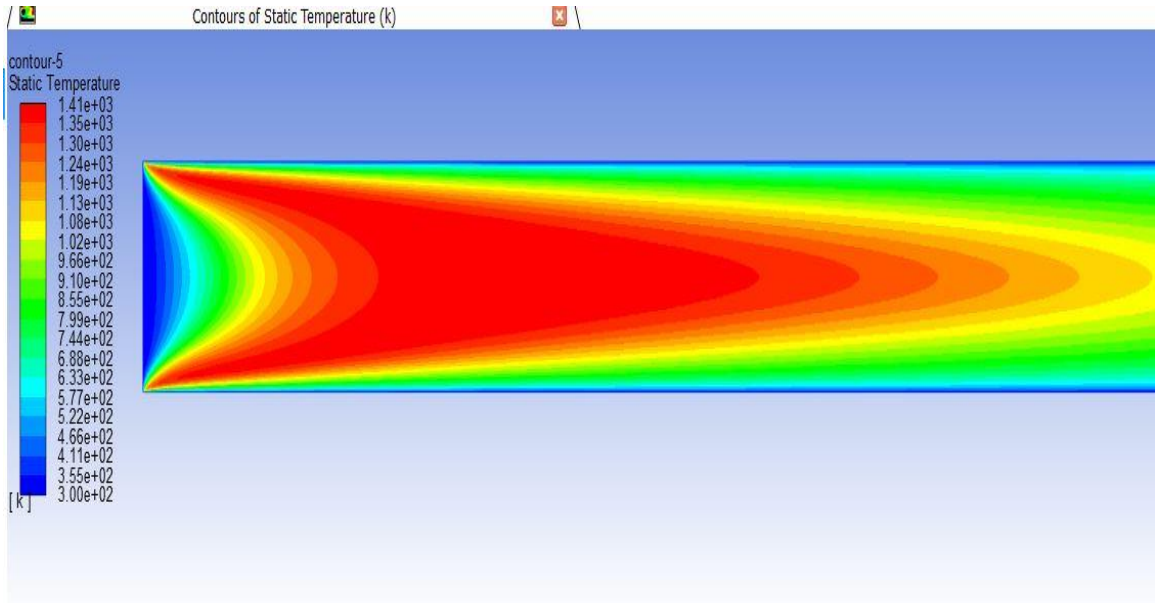


Figure 4-59 BFG temperature contour at stoichiometric and ambient conditions.

It can be noticed in Figure. 4.59 that the adiabatic flame temperature of BFG-air combustion at stoichiometric ratio and ambient conditions is around 1415 K, lower than that of COG-air combustion, because BFG has lower total energy content and higher inert gases. The adiabatic flame temperature of BFG-air combustion with preheating is shown in Figure 4.60, with various equivalent ratios and preheat temperatures.

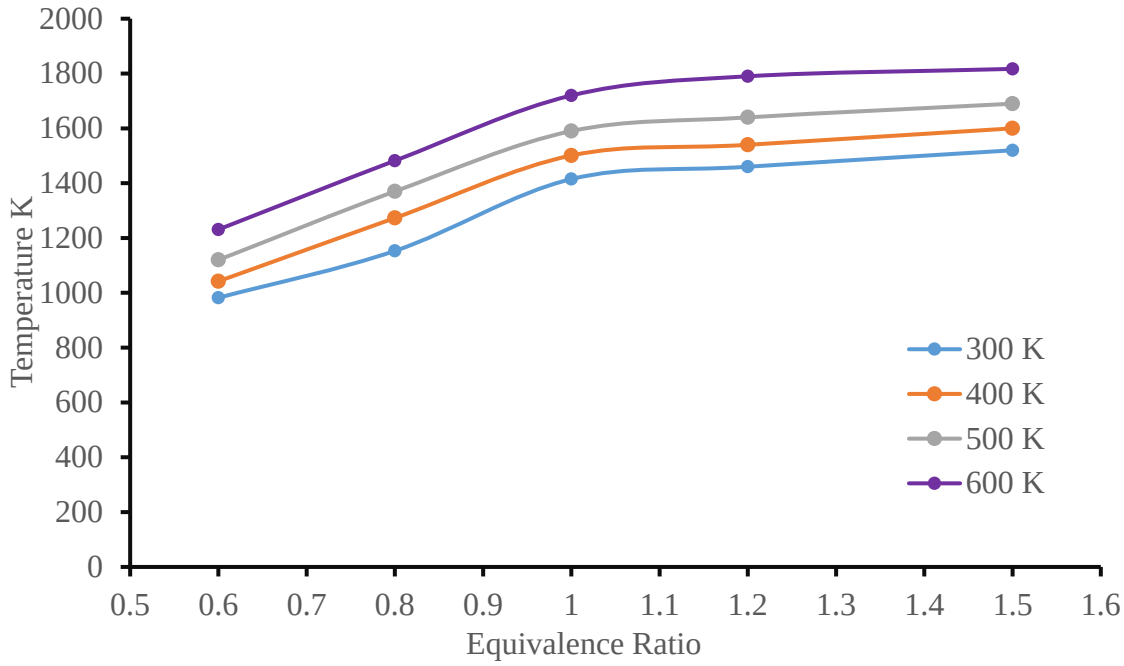


Figure 4-60 BFG adiabatic flame temperature at different equivalence ratios and preheat temperatures.

The adiabatic flame temperature increases as the preheat temperature is increased, and maximum temperatures peaks occur at $\phi = 1.7$, while BFG combustion has higher adiabatic temperatures which peaks at $\phi = 1.1\text{-}1.2$ . This trend is probably due to high content of CO in the BFG gas mixture. Blast Furnace Gas flame speed temperature with preheat temperature changes is summarized in Figure 4.61.

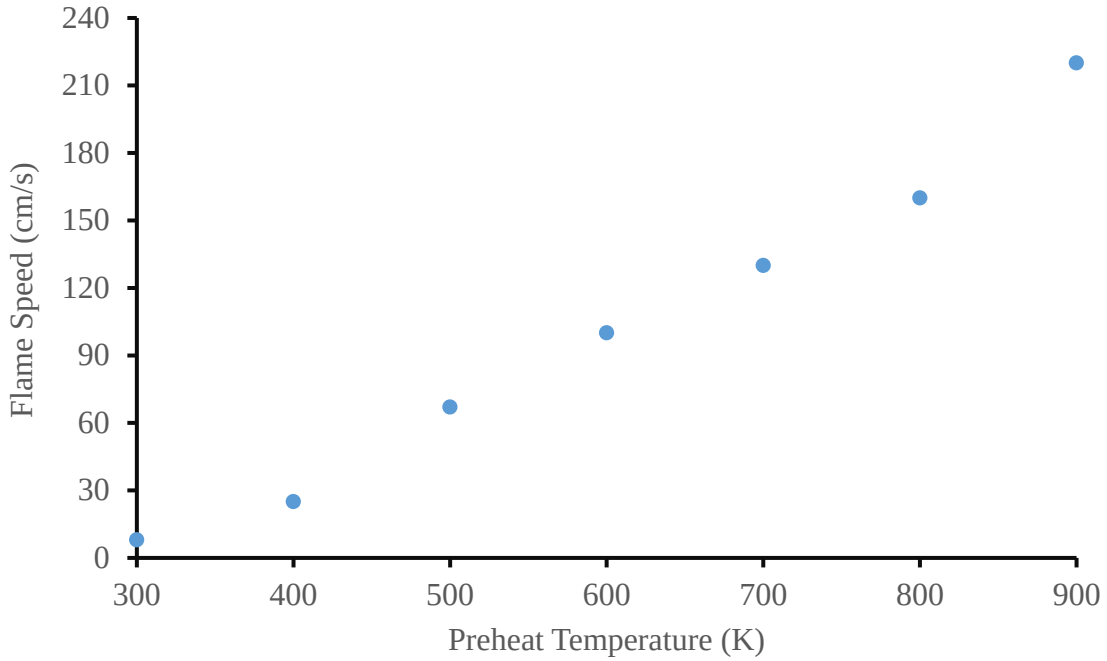


Figure 4-61 Effect of preheat temperature on flame speed at stoichiometric (BFG)

The flame speed using the area method is calculated for BFG at fuel lean-rich conditions. Figure 4.61 represents the dependency of flame speed on the preheat temperature, where the flame speed increases drastically as the preheat temperature is changed.

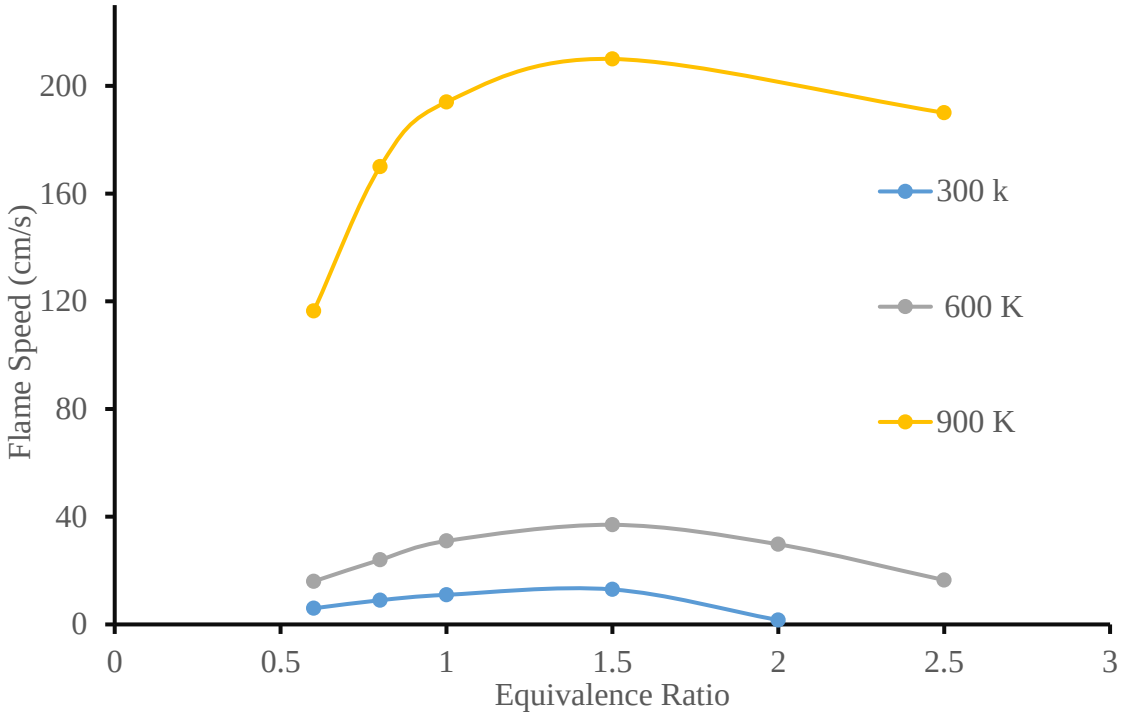


Figure 4-62 BFG flame speed with varying temperatures and equivalence ratios.

From Figure 4.62 it can be noticed that the flame speed for the three different preheating reaches their peaks at fuel rich side around $\phi$ = 1.5-1.6.. Similar to COG the effect of preheating on the increase of flame speed of BFG is not linear. The increase of flame speed of BFG-air is small for the preheat temperature from 300 K to 600 K, while it is much greater when the preheating is from 600 K to 900 K. This combustion characteristics of BFG-air may be caused by its fuel compositions. BFG contains trace amount of $H_2$ and $CH_4$ species. At low temperature the generation of H and OH radicals are slow, causing the rate of CO oxidation with OH and the flame speed of BFG are slow even through BFG is preheated to 600 K. However, when BFG is preheated to 900 K, The H and OH radicals are highly activated such that CO oxidation with OH is accelerated, which produces more H radical and increases the overall flame speed for BFG reaction. Because BFG contains less amounts of $H_2$ and $CH_4$species and relatively large amount of CO, it is expected that if system adds small quantity of water vapor, it will promote the generation of H radical and promote the CO oxidation, thus the overall reaction rate and the flame speed of BFG-air reaction

# Chapter 5 CONCLUSIONS AND FUTURE WORK

Combustion contributes to the major of the energy that supplies, daily lives. However, there is a need to produce cleaner energy that produces less emissions. The goal of the project was to design a model that could simulate premixed flame in 2D, using ANSYS- Fluent and compare the results obtained with GRI-3.0 and available experimental work. The model consisted of a cylindrical tube which was examined in 2D at different conditions, where the first couple centimeters of the model were studied extensively to understand the characteristics and properties of flame. The model was meshed using Finite Element Method, using least number of elements and nodes that could produce results within an acceptable range of accuracy using the shortest time possible.

The project was split in 4 different phases of testing, where in the beginning, a comparison was done with Premixed and Transport models in Fluent to determine the accuracy in finding the adiabatic temperatures, then a detailed study was done to understand the behavior of hydrogen-air and methane-air kinetics based on different fuel lean to rich equivalence ratios. The flame speed was calculated by using the area method through finding the flame surface area which was determined to be the mid-way area in between the beginning and end of a flame wave. It was used to determine the flame speed, different reduced mechanisms (2-5-10 steps) were compared with GRI-3.0 to compare the accuracy of the results where the all represented results were within 3-7% discrepancies. The second phase include the study of hydrocarbon diluted with hydrogen at different equivalence ratios that ranged from fuel lean to fuel rich. The beginning of 2$^{nd}$ phase include simulations done by PREMIX CHEMKIN code where the flame structures and flame speeds for methane-hydrogen air were compared at different levels of blending from 0 to 100% hydrogen. The flame structure for minor species was studied to understand the relationship between radical formation and flame speed. After that, Fluent was used to model the methane- hydrogen enrichment to create a 2D visualization and obtain results that are within an acceptable range with GRI-3.0 and experimental work. The obtained flame speed was within 3-5% for different levels of methane diluted with hydrogen blends. It was shown that there is non-linear relationship between hydrogen blending percentages, where

the flame speed and temperature slowly increase up until 70% hydrogen blending. Values higher than 70% of hydrogen blending resulted in a drastic increase in flame speed. Through studying the radicals H and OH it was determined that increase of hydrogen in the fuel blend resulted in promotion chain branching reactions that results in increasing the H and OH radicals which was correlated to the increase of flame speed and also reduced the $NO_x$ and $CO_2$ emissions.

The third test phase was to understand the behavior of syngas mainly 5% $H_2$ 95% CO and 50% $H_2$ and 50% CO. Three preheat temperatures were applied including 300,400,500 K where the GRI-3.0, experimental work, and 10 step mechanism was used to obtain convergence for the fuel lean to fuel rich equivalence ratios. The flame speed was determined at different blending CO and $H_2$ to compare the different cases of syngas. Furthermore, the sensitivity of hydrogen on CO was studied where within the first couple percentages of $H_2$ added into CO the speed would increase drastically than follow a trend of small increment of flame speed increase after 5% hydrogen is added into CO. The preheat temperatures were applied to the 2 cases of syngas where the results show big discrepancies in flame speed specially at fuel rich conditions at high preheat temperature. It was determined that the error occurs because of an overestimation in the reaction rate when the increased temperature is introduced into the blends. The final case included the study of two variants of syngas and they are BFG and COG where different equivalence ratios and preheat temperatures that are close to industrial work, were tested for each case. The adiabatic flame temperatures of both BFG and COG were calculated where the was an increase in speed, when preheat temperature was increased. It was determined that the COG had similar behavior as methane-air where the highest flame temperature and flame speed were observed at 1.05 equivalence ratio. The preheat temperatures had an apparent effect on CO and $CO_2$ concentrations. The high preheat temperature helps to achieve equilibrium, as the combustion proceeds, the hydrogen decays but it is never consumed to zero even after heat release which pushes the production of intermediate species causing the increase in flame speed. In terms of BFG,the adiabatic flame temperature increases as the preheat temperature increased however, the behavior BFG exhibits is different than the behavior seen in COG in terms of the temperature where the maximum temperature is achieved at

1.6 equivalence ratio resembling hydrogen-air and similar trend is seen for the flame speed. In the case of BFG the methyl radical is not the main factor in heat release and the temperature is not the only factor that determines the flame speed BFG combustion properties are controlled through radical formation only.

The Future work includes, to be able to produce a model that is like the generic combustors that used in actual industrials sectors. Future work could include using alternative fuels such as landfill gases and low calorific value gases that could in reducing the pollutants and provide efficient energy by looking into the emissions of every fuel that was used in the study. Furthermore, recommended work includes the effect of studying different sizes and elements for the model and studying the sources of discrepancies occurring in the results specially in terms of adiabatic temperature and flame speed. In addition to that, results could be expanded by using a reduced mechanism that includes all the important reaction steps for syngas and by-product fuel so that the errors would be less. Other work could include introducing the actual combustor condition into the simulations to obtain more realistic results.

## REFERENCES


[1] L. Aisyah, D. Rulianto, C.S. Wibowo, Analysis of the Effect of Preheating System to Improve Efficiency in LPG-fuelled Small Industrial Burner, Energy Procedia 65 (2015) 180-185.

[2] A. Darwish Ahmad, A. Abubaker, A. Salaimeh, N. Akafuah, Schlieren Visualization of Shaping Air during Operation of an Electrostatic Rotary Bell Sprayer: Impact of Shaping Air on Droplet Atomization and Transport, Coatings 8 (2018) 279.

[3] Y.S. Najjar, A.M. Abubaker, Using novel compressed-air energy storage systems as a green strategy in sustainable power generation–a review, International Journal of Energy Research 40 (2016) 1595-1610.

[4] Y.S. Najjar, A.M. Abubaker, Indirect evaporative combined inlet air cooling with gas turbines for green power technology, international journal of refrigeration 59 (2015) 235-250.

[5] U.S. Energy Information Association, *How the United States uses energy* https://www.eia.gov/totalenergy/data/annual/pecss_diagram.php.

[6] Y. Chen, B.F. Hobbs, J.H. Ellis, C. Crowley, F. Joutz, Impacts of climate change on power sector $NO_x$ emissions: A long-run analysis of the US mid-atlantic region, Energy Policy 84 (2015) 11-21.

[7] U.S.E.I.Association, Carbon dioxide emissions by fuel. https://www.eia.gov/environment/.

[8] P. Tunestål, M. Christensen, P. Einewall, T. Andersson, B. Johansson, O. Jönsson, Hydrogen addition for improved lean burn capability of slow and fast burning natural gas combustion chambers, Report No. 0148-7191, SAE Technical Paper, 2002.

[9] HydrogenTools, Hydrogen Compared with Other Fuels. https://h2tools.org/bestpractices/hydrogen-compared-other-fuels.

[10] R.W. Schefer, D. Wicksall, A. Agrawal, Combustion of hydrogen-enriched methane in a lean premixed swirl-stabilized burner, Proceedings of the combustion institute 29 (2002) 843-851.

[11] L. Jingding, G. Linsong, D. Tianshen, Formation and restraint of toxic emissions in hydrogen-gasoline mixture fueled engines, International journal of hydrogen energy 23 (1998) 971-975.

[12] J. Mackaluso, The use of syngas derived from biomass and waste products to produce ethanol and hydrogen, MMG 445 Basic Biotechnology eJournal 3 (2007) 98-103.

[13] A.K. Das, K. Kumar, C.-J. Sung, Laminar flame speeds of moist syngas mixtures, Combustion and Flame 158 (2011) 345-353.

[14] T. Komori, N. Yamagami, H. Hara, Gas Turbine Engineering Section Power Systems Headquarters Mitsubishi Heavy Industries, Ltd. Industrial Report, 2004.

[15] P. Campbell, J. McMullan, B. Williams, Concept for a competitive coal fired integrated gasification combined cycle power plant, Fuel 79 (2000) 1031-1040.

[16] B. Lewis, G. Von Elbe, Combustion, flames and explosions of gases, Elsevier2012.

[17] K.K. Kuo, Principles of combustion, 2005.

[18] H. KIDO, "Numerical Analysis of Combustion of Hydrocarbon Premixed Mixture added Hydrogen, (2004).

[19] S. Chakravarthy, Realizing high fidelity computational simulations of fluid dynamic phenomena, Computational Fluid Dynamics Journal 16 (2008) 356.

[20] F. Williams, Combustion Theory 2nd ed.,(1985), 434, Addison-Wesley Publishing Company.

[21] A. Linan, F.A. Williams, Fundamental aspects of combustion, (1993).

[22] I. Glassman, R.A. Yetter, N.G. Glumac, Combustion, Academic press2014.

[23] M. C, GASEQ A Chemical Equilibrium Program for Windows http://www.gaseq.co.uk/.

[24] H. Hottel, W. Hawthorne. Diffusion in laminar flame jets. In: editor^editors. Symposium on Combustion and Flame, and Explosion Phenomena; 1948: Elsevier. p. 254-266.

[25] J.N. Bradley, Flame and combustion phenomena, (1969).

[26] C.K. Westbrook, F.L. Dryer, Chemical kinetic modeling of hydrocarbon combustion, Progress in Energy and Combustion Science 10 (1984) 1-57.

[27] V. Zimont, W. Polifke, M. Bettelini, W. Weisenstein, An efficient computational model for premixed turbulent combustion at high Reynolds numbers based on a turbulent flame speed closure, Journal of engineering for gas turbines and power 120 (1998) 526-532.

[28] V.L. Zimont, Gas premixed combustion at high turbulence. Turbulent flame closure combustion model, Experimental thermal and fluid science 21 (2000) 179-186.

[29] A.G. Gaydon, H.G. Wolfhard, Flames, their structure, radiation, and temperature, Halsted Press1979.

[30] B. L'vov, D. Katskov, L. Kruglikova, L. Polzik, Absolute analysis by flame atomic absorption spectroscopy: present status and some problems, Spectrochimica Acta Part B: Atomic Spectroscopy 31 (1976) 49-80.

[31] J. Powling, A new burner method for the determination of low burning velocities and limits of inflammability, Fuel 28 (1949) 25-28.

[32] R. Kee, F. Rupley, J. Miller, M. Coltrin, J. Grcar, E. Meeks, H. Moffat, A. Lutz, G. Dixon-Lewis, M. Smooke, CHEMKIN Release 4.0, Reaction Design, Inc., San Diego, CA, (2004).

[33] R.J. Kee, A Fortran program for modeling steady laminar one-dimensional premixed flames, Sandia Laboratories Report No. SAND 85-8240, (1985).

[34] J. Botha, D.B. Spalding, The laminar flame speed of propane/air mixtures with heat extraction from the flame, Proceedings of the Royal Society of London. Series A. Mathematical and Physical Sciences 225 (1954) 71-96.

[35] Z. Huang, Y. Zhang, K. Zeng, B. Liu, Q. Wang, D. Jiang, Measurements of laminar burning velocities for natural gas–hydrogen–air mixtures, Combustion and Flame 146 (2006) 302-311.

[36] C.J. Rallis, A.M. Garforth, The determination of laminar burning velocity, Progress in Energy and Combustion Science 6 (1980) 303-329.

[37] N. Bouvet, C. Chauveau, I. Gökalp, F. Halter, Experimental studies of the fundamental flame speeds of syngas ($H_2$/CO)/air mixtures, Proceedings of the Combustion Institute 33 (2011) 913-920.

[38] T. Varga, C. Olm, T. Nagy, I.G. Zsély, É. Valkó, R. Pálvölgyi, H.J. Curran, T. Turányi, Development of a joint hydrogen and syngas combustion mechanism based on an optimization approach, International journal of chemical kinetics 48 (2016) 407-422.

[39] A.S. Tomlin, T. Turányi, M.J. Pilling, Mathematical tools for the construction, investigation and reduction of combustion mechanisms, Comprehensive chemical kinetics, Elsevier1997, pp. 293-437.

[40] A.B. Bendtsen, P. Glarborg, K. Dam-Johansen, Visualization methods in analysis of detailed chemical kinetics modelling, Computers & chemistry 25 (2001) 161-170.

[41] N. Peters, B. Rogg, Reduced kinetic mechanisms for applications in combustion systems, Springer Science & Business Media2008.

[42] N. Bouvet, S. Lee, I. Gokalp, R. Santoro. Flame speed characteristics of syngas ($H_2$–CO) with straight burners for laminar premixed flames. In: editor^editors. Third European Combustion Meeting; 2007. p. 1-6.

[43] G. Yu, C. Law, C. Wu, Laminar flame speeds of hydrocarbon+ air mixtures with hydrogen addition, Combustion and Flame 63 (1986) 339-347.

[44] F. Liu, Ö.L. Gülder, Effects of $H_2$ and H preferential diffusion and unity Lewis number on superadiabatic flame temperatures in rich premixed methane flames, Combustion and Flame 143 (2005) 264-281.

[45] Y. Liu, B. Lenze, W. Leuckel, Investigation of the laminar and turbulent burning velocities of premixed lean and rich flames of CH 4-H 2-air mixtures, Dynamics of deflagrations and reactive systems: Flames, (1991) 259-274.

[46] V. Di Sarli, A. Di Benedetto. Study of hydrogen enriched premixed flames. In: editor^editors. First International Conference on Hydrogen Safety, Pisa, Italy; 2005. p. 8-10.

[47] Clarke-energy, Different Gases from Steel Production Processes. Different Gases from Steel Production Processes.

[48] R. ANSYS, Academic Research, Release 15.0, Help System, Ansys Fluent Theory Guide, ANSYS, Inc, Canonsburg, Pennsylvania, USA.

[49] A. FLUENT, 12.0 Theory Guide. Release 12.0. ANSYS, Inc. January 29 (2009).

[50] A. Sayma, Computational fluid dynamics, Bookboon2009.

[51] H.K. Versteeg, W. Malalasekera, An introduction to computational fluid dynamics: the finite volume method, Pearson education2007.

[52] R. Löhner, Applied computational fluid dynamics techniques: an introduction based on finite element methods, John Wiley & Sons2008.

[53] N. Shelil, Flashback studies with premixed swirl combustion, Cardiff University, 2009.

[54] K. Langan, A computational study of two dimensional laminar premixed combustion of methane and some biofuels, (2010).

[55] A. Belcadi, M. Assou, E.H. Affad, E.H. Chatri, $CH_4/NO_x$ reduced mechanisms used for modeling premixed combustion, Energy and Power Engineering 4 (2012) 264.

[56] A. Belcadi, E. Chatri, E. Affad, M. Assou, Reduction of the detailed mechanism GRI-3.0 by using S-STEP algorithm.

[57] C. Bowman, R. Hanson, D. Davidson, W. Gardiner, V. Lissianski, G. Smith, D. Golden, M. Frenklach, M. Goldenberrg, GRI 3.0 Detailed Mechanism, Accessed on, 1999.

[58] A. Patel, S.-C. Kong, R.D. Reitz, Development and validation of a reduced reaction mechanism for HCCI engine simulations, Report No. 0148-7191, SAE Technical Paper, 2004.

[59] H. Soyhan, P. Amnéus, T. Lovas, D. Nilsson, P. Maigaard, F. Mauss, C. Sorusbay, 2000-01-1895 Automatic Reduction of Detailed Chemical Reaction Mechanisms for Autoignition Under SI Engine Conditions, SAE TRANSACTIONS 109 (2000) 1435-1444.

[60] P. Boivin, C. Jiménez, A.L. Sánchez, F.A. Williams, An explicit reduced mechanism for $H_2$–air combustion, Proceedings of the Combustion Institute 33 (2011) 517-523.

[61] T. D'Andrea, P. Henshaw, D.-K. Ting, The addition of hydrogen to a gasoline-fuelled SI engine, International journal of hydrogen energy 29 (2004) 1541-1552.

[62] G. Karim, W. Jones, R. Raine, An examination of the ignition delay period in dual fuel engines, Report No. 0148-7191, SAE Technical Paper, 1989.

[63] N. Slavinskaya, M. Braun-Unkhoff, P. Frank, Reduced reaction mechanisms for methane and syngas combustion in gas turbines, Journal of engineering for gas turbines and power 130 (2008) 021504.

[64] Z.M. Nikolaou, J.-Y. Chen, N. Swaminathan, A 5-step reduced mechanism for combustion of CO/$H_2$/$H_2O$/$CH_4$/$CO_2$ mixtures with low hydrogen/methane and high $H_2O$ content, Combustion and flame 160 (2013) 56-75.

[65] RJ. Blint The relationship of the laminar flame width to flame speed. Combustion Science and Technology. 1;49(1-2) (1986) 79-92.

[66] D.J. Mavriplis, Mesh generation and adaptivity for complex geometries and flows, Handbook of computational fluid mechanics, Elsevier1996, pp. 417-459.

[67] J. Li, Z. Zhao, A. Kazakov, M. Chaos, F.L. Dryer, J.J. Scire Jr, A comprehensive kinetic mechanism for CO, $CH_2O$, and CH3OH combustion, International Journal of Chemical Kinetics 39 (2007) 109-136.

[68] G.P. Smith, D.M. Golden, M. Frenklach, N.W. Moriarty, B. Eiteneer, M. Goldenberg, C.T. Bowman, R.K. Hanson, S. Song, W. Gardiner Jr, GRI-Mech 3.0, 1999, URL http://www.me.berkeley.edu/gri_mech, (2011).

[69] K. Aung, M. Hassan, G. Faeth, Effects of pressure and nitrogen dilution on flame/stretch interactions of laminar premixed $H_2/O_2/N_2$ flames, Combustion and flame 112 (1998) 1-15.

[70] T. Scholte, P. Vaags, Burning velocities of mixtures of hydrogen, carbon monoxide and methane with air, Combustion and Flame 3 (1959) 511-524.

[71] C. Serrano, J. Hernandez, C. Mandilas, C. Sheppard, R. Woolley, Laminar burning behaviour of biomass gasification-derived producer gas, International Journal of Hydrogen Energy 33 (2008) 851-862.

[72] Y. Zhang, J. Wu, S. Ishizuka, Hydrogen addition effect on laminar burning velocity, flame temperature and flame stability of a planar and a curved $CH_4$–$H_2$–air premixed flame, international journal of hydrogen energy 34 (2009) 519-527.

[73] P. Padley, T. Sugden. Chemiluminescence and radical re-combination in hydrogen flames. In: editor^editors. Symposium (International) on Combustion; 1958: Elsevier. p. 235-242.

[74] R.T.E. Hermanns, J. Kortendijk, R. Bastiaans, L. De Goey, Laminar burning velocities of methane-hydrogen-air mixtures, Praca doktorska, Technische Universitat Eindhoven, (2007).

[75] C. Cardona, A. Amell, H. Burbano, Laminar burning velocity of natural gas/syngas-air mixture, Dyna 80 (2013) 136-143.

[76] D. Singh, T. Nishiie, S. Tanvir, L. Qiao, An experimental and kinetic study of syngas/air combustion at elevated temperatures and the effect of water addition, Fuel 94 (2012) 448-456.

[77] M.P. Burke, M. Chaos, F.L. Dryer, Y. Ju, Negative pressure dependence of mass burning rates of $H_2$/CO/$O_2$/diluent flames at low flame temperatures, Combustion and Flame 157 (2010) 618-631.

[78] P. Dagaut, F. Lecomte, J. Mieritz, P. Glarborg, Experimental and kinetic modeling study of the effect of NO and $SO_2$ on the oxidation of CO $H_2$ mixtures, International journal of chemical kinetics 35 (2003) 564-575.

[79] M. Hassan, K. Aung, G. Faeth, Measured and predicted properties of laminar premixed methane/air flames at various pressures, Combustion and Flame 115 (1998) 539-550.

[80] M. Hassan, K. Aung, G. Faeth, Properties of laminar premixed CO/H/air flames at various pressures, Journal of Propulsion and Power 13 (1997) 239-245.

[81] I.C. McLean, D.B. Smith, S.C. Taylor. The use of carbon monoxide/hydrogen burning velocities to examine the rate of the CO+ OH reaction. In: editor^editors. Symposium (international) on combustion; 1994: Elsevier. p. 749-757.

[82] C. Prathap, A. Ray, M. Ravi, Investigation of nitrogen dilution effects on the laminar burning velocity and flame stability of syngas fuel at atmospheric condition, Combustion and Flame 155 (2008) 145-160.

[83] H. Sun, S. Yang, G. Jomaas, C. Law, High-pressure laminar flame speeds and kinetic modeling of carbon monoxide/hydrogen combustion, Proceedings of the Combustion Institute 31 (2007) 439-446.

[84] R. Yetter, F. Dryer, H. Rabitz, A comprehensive reaction mechanism for carbon monoxide/hydrogen/oxygen kinetics, Combustion Science and Technology 79 (1991) 97-128.

[85] S. Alavandi, A. Agrawal, Experimental study of combustion of hydrogen–syngas/methane fuel mixtures in a porous burner, International journal of hydrogen energy 33 (2008) 1407-1415.

[86] J. Natarajan, T. Lieuwen, J. Seitzman, Laminar flame speeds of $H_2$/CO mixtures: effect of $CO_2$ dilution, preheat temperature, and pressure, Combustion and flame 151 (2007) 104-119.

[87] H.-B. He, D.-W. Yao, F. Wu, A reduced and optimized kinetic mechanism for coke oven gas as a clean alternative vehicle fuel, Journal of Zhejiang University-SCIENCE A 18 (2017) 511-530.

## VITA

1. **Place of birth:** Kuwait City, Kuwait
2. **Degree/Education:** B.S Mechanical Engineering, University of Kentucky, Lexington Kentucky, December 2016
3. **Professional positions:** N/A
4. **Professional publications:** N/A
5. **Scholastic and professional honors:** Kuwait's Ministry of Higher Education Scholarship ($52000/year) Based on High Schools GPA
6. **Name:** Essa KH I J Salem